Field Trips Guide

Palaeoseismicity and Active Tectonics during the Quaternary in the Gibraltar Strait (Betic Cordillera, South Spain)

Editors

J. Lario, P.G. Silva, K. Reicherter , C. Grützner and M.A. Rodríguez-Pascua

1st INQUA-IGCP 567 International Workshop on Earthquake Archaeology and Palaeoseismology

7-13 September 2009

Baelo Claudia (Cádiz, Spain)

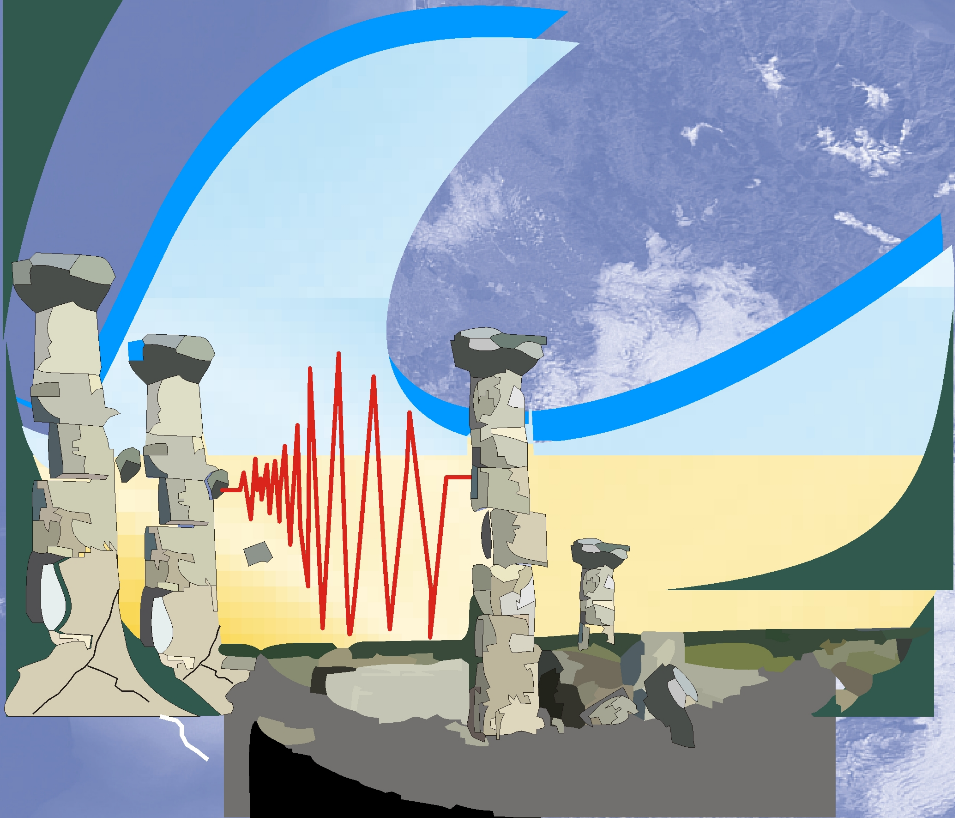

Field Trips Guide

Palaeoseismicity and Active Tectonics during the Quaternary in the Gibraltar Strait (Betic Cordillera, South Spain)

Editors
J. Lario, P.G. Silva, K. Reicherter, C. Grützner and M.A. Rodríguez-Pascua

This **Field trips Guide** has been produced for the **1st INQUA-IGCP 567 International Workshop on Earthquake Archaeology and Palaeoseismology** held in Baelo Claudia Roman ruins (Cádiz, Southern Spain). The event has been organized together by the INQUA Focus Area on Paleoseismology and Active Tectonics and the IGCP-567: Earthquake Archaeology.

This scientific meeting has been supported by the Spanish Research Projects ACI2008-0726, CGL08-03998BTE, CGL08-04000BTE and ACTISIS CGL2006-05001/BTE and UNED grant.

Index

Edited by Instituto Geológico y Minero de España
Deposito Legal: M-27206-2009

FIELD TRIP 1

ARCHAEOSEISMOLOGY OF BAELO CLAUDIA

Stop 1

Brief history of *Baelo Claudia*

A. Muñoz, I. García Jiménez, P.G. Silva and K. Reicherter

Introduction

Different archaeological excavations carried out by the French Institution *La Casa de Velázquez* since 1966, allow a nice insight of the history of an ancient wealthy Roman city in South Spain (Sillières, 1997). The town was settled in the late 2nd Century BC as a strategic site for human and commercial exchange between Europe and North Africa during the Roman times. The ancient Greek geographer Estrabon described *Baelo Claudia* (Belon) as a main harbour for *Mauritania Tingitana* (Fig. 1).

Fig. 1: Model of the ancient Roman City exposed in the *Baelo Claudia* Museum.

The development of the city followed three well differentiated building periods separated by noticeable discontinuities of the archaeological record interpreted as anomalous episodes of city destruction (or demolition) related to earthquake damage by different authors (Menanteau et al., 1983; Sillières, 1995; 1997; Alonso-Villalobos et al. 2003; Silva et al., 2005; 2009). History, archaeological recorded events, and dominant surface process in the configuration of the present archaeological site are summarized in Table 1. The intervening destructive episodes can be relatively dated on the basis of archeological evidence. Some radiocarbon dating is available for the last episodes of ruin of the city.

Archaeological excavations carried out in this site since the beginnings of the 20th Century found, maybe, the best preserved roman urban settlement in the Iberian Peninsula. It is a city of about 13 hectares, delimited by a defensive wall fortified with at least 36 towers. The urban network has a typical N-S/E-W orthogonal pattern, and the excavated zones were focused on the ancient monumental zone of the city (1^{st} Century AD). This monumental zone includes a *Forum*, a religious sector with four ancient *temples* and a *basilica* (presently restored), and a commercial zone constituted by the *macellum* (market) and *tabernae* (shops), as the more relevant buildings. Aside of this ancient city centre the best preserved monuments are the ancient theatre and the thermals. Finally, south of the city and close to the present beach is nicely preserved the ancient industrial sector of the city, constituted by *"garum"* and fish factories, the true economic engine and origin of this ancient roman site.

The excavation of most of the structures and architectural remains presently preserved was conducted during three different stages. In a first stage (1917-1921) the group headed by the French archaeologist Pierre Paris excavated most of the buildings we can observe today. In a second stage (1966-1989) were conducted a total amount of 23 yearly archaeological campaigns under the scientific supervision of *La Casa de Velázquez*, a French school abroad that depends on the French "Ministère de l'éducation nationale, de l'enseignement supérieur et de la recherche". The third stage (1989-Present), developed under the administration of the Junta de Andalucía, has been focused on the conservation, consolidation and restoration of different buildings or city sectors. In this period the cultural and touristy implementation of all the excavated remains gave place to the inauguration of the present *Museo de Baelo Claudia* building in the year 2007. Only few, very specific, archaeological excavations have been conducted during this last stage

First City Period (2nd Century BC – 1st Century AD)

From the end of the 2^{nd} Century BC the fish salting factories of "Garum" were established on the site of *Baelo*, starting a period of increasing commercial activity and urban development until the first half of the 1^{st} Century AD (30-50 AD), when the first Roman settlement is destroyed. This First settlement early becomes an *Oppidum latinum* (category of Roman city). From the second half of the 1^{st} Century BC the city underwent a period of expansion with major urban reforms and the acquisition of the typical N-S/E-W urban orthogonal pattern. During this period were built the ancient *Forum*, *Capitol* and *Temples*. The first City Walls (ca. AD 10-20) and the improvement of the original fish factories and private buildings at the lower coastal sector of the city were also implemented at the end of this period. Remains of this first phase of building are presently scarce because its demolition during the roman period.

This first period of City destruction can be dated in 40-60 AD on the basis of pottery remains beneath collapsed walls, close to the repaired sector of the damaged City Wall (Sillières, 1997). This period is post-dated by the occurrence of an anomalous level of demolition related to ground leveling works on the whole lower sector of the city and reparation works in different severely damaged sectors of the City Wall during 30-50 AD (Sillières, 1995; 1997).

Second City Period (1st Century AD -3rd Century AD)

A second period of the city can be bracketed between the Late 1st Century AD and the Late 3rd Century AD (ca. AD 260-290). The initiation of this period of expansion and prosperity starts at ca 48-50 AD when the city acquired the imperial Label of *"Claudia"*. Early during this period took place the building of the monumental zone of *Baelo Claudia* including the *Basilica, Temples, Forum, Curia, Capitol, Macellum* and *Theatre*, which remains can be presently observed. These monuments display clear signals of recycling of previous architectural elements, and former foundations were partially reutilized (Sillières, 1995). City development also included the reparation, reinforcement and thickening of the damaged 1st Century City Wall, the Improvement of the harbor south of the city, the implementation of three large aqueducts and a redesign of the urban pattern, including all the pavements of the *Forum* and streets we can see today (E-W *Decumanus* and N-S *Cardos*).

This Monumental City was rebuilt on a “demolition horizon” for ground levelling artificially cemented on surface by *opus cementum*. Public works involved the creation of an artificial terrace (500 m2) for the building of the new capitol and Isis temple North of the Forum, and the excavation of the clayey substratum for terracing the Theatre site (Sillières, 1997). Both excavations were carried out at the toe of a suspect Late Pleistocene Paleocliff (Silva et al., 2005) separating the lower and upper sector of the city. This period of prosperity finished by an anomalous episode of abrupt ruin and depopulation of the city accompanied by a relevant commercial decay revealed by numismatic anomalies from the 260-290AD (Bost et al., 1987; Sillières, 1997). This abrupt destruction of the city is illustrated by many archaeological and architectural evidences today (Menateau et al., 1983; Sillières, 1995; Silva et al., 2005; 2009) which have been related to strong earthquake damage. However the city was not completely abandoned and a reconstruction of the damaged city took place, however the monumental zone of the city was never restored again (Fig. 2).

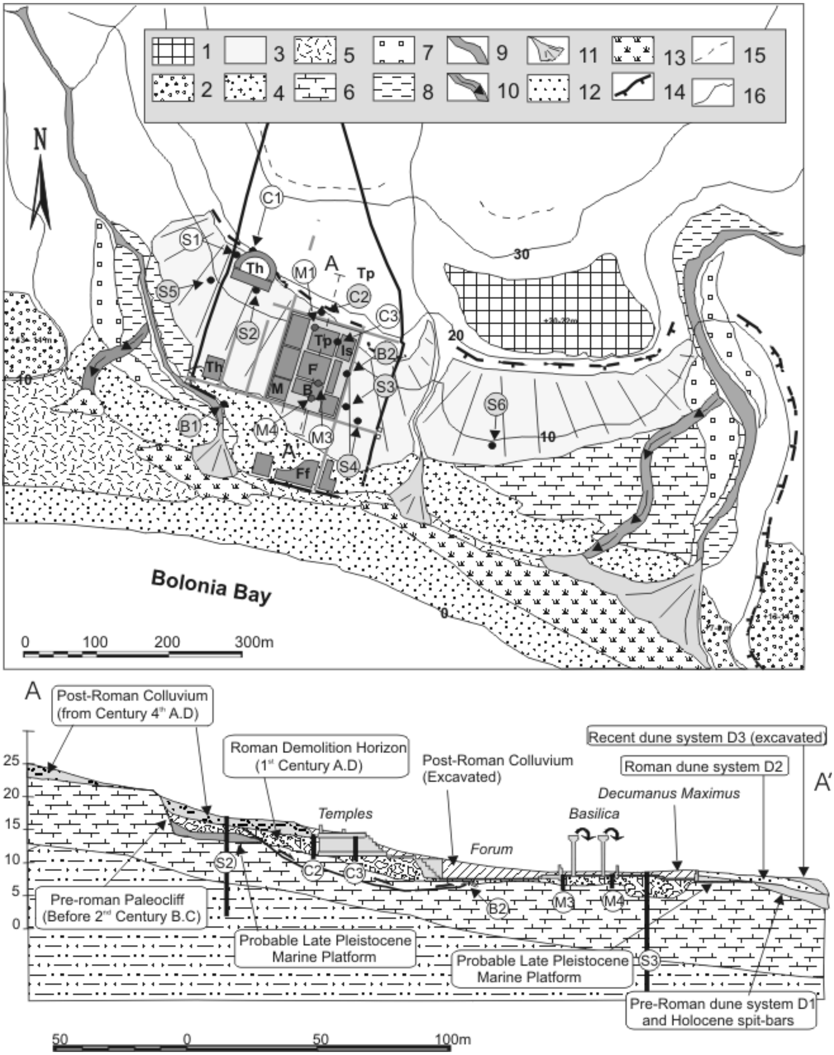

Fig. 2: Geomorphological map of the ancient urban area of *Baelo Claudia.* (Th) *Theatre*; (Tp) *Temples*; (F) *Forum*; (B) *Basilica*; (M) *Macellum*; (Ff) Fish factories; (Tr) Roman Baths. Legend: (1) Marine abrasion platform; (2) Late Pleistocene Marine terraces; (3) Betic substratum; (4) Holocene spit-bar system including D1 and D2 dune system of South Spain; (5) Recent D3 dune system; (6)lagoon deposits; (7) Fluvial terraces; (8) Flood plains; (9) channel beds; (10) abandoned channels; (11) terminal river systems; (12) Beach deposits; (13) marshes; (14) Paleocliff; (15) bedrock scarps; (16) contour levels (modified from Silva et al., 2005).

This second episode of city destruction (as logically the previous one) was strongly influence by unstable ground conditions, favoring landslide events, liquefaction and differential settlement (Borja et al., 1993; Silva et al., 2005; 2009). Secondary effects largely amplified the damage at the monumental zone of the city.

Third City Period (3rd Century AD – Late 4th Century AD)

The third eventual period of the city developed between the Late 3rd Century AD and de Late 4th Century AD (ca 395 AD). Damaged structures are artificially leveled and new poor quality buildings are constructed over the ruins following a different urban pattern. Only the partially damaged remains of the *Macellum, Basilica, Isis Temple* and *Theatre* survived. Fish factories and some sectors of the Theatre were used as houses. The City Wall was never again restored or reinforced (Sillières, 1997).

This period is coeval with the eventual progressive collapse of the damaged ruins (*Basilica*, *Temples*, etc.). The period of main destruction of the City Walls and *Macellum* (Market) can be bracketed at 350-370 AD from pottery evidences (Didierjean et al., 1978). This period of decadence and increased ruin culminates with the total lack of coins (roman or other) from ca 395 AD (Menanteau et al., 1983; Bost et al., 1987). These data indicate a nearly total breakdown of the commercial activity in the City, although a reduced activity is recorded during until the early 8th Century. In this late period small Paleo-Christian to Visigothic settlements occupied and reutilized the ruins of monumental zone for housing. Definitive abandonment of this city took place shortly before the 711 AD Muslim conquest of the Iberian Peninsula.

The Archaeoseismological dates

Based on the set of archaeological findings and data updated until the end of the 70's Decade, Menanteau et al., (1983) proposed the time interval AD 350-395 as the bracketed age for the probable causative earthquake. This author fairly suggests the relation of recorded archeoseismic damage and anomalies with the well known 365 AD Crete Earthquake-Tsunami Event. The work of Sillières (1995) for first time suggest the occurrence of a previous earthquake event during the first half of the 1st Century AD in the basis of reutilization and "bricolage" of architectural elements for the construction of the Monumental zone of the city during the second building period.

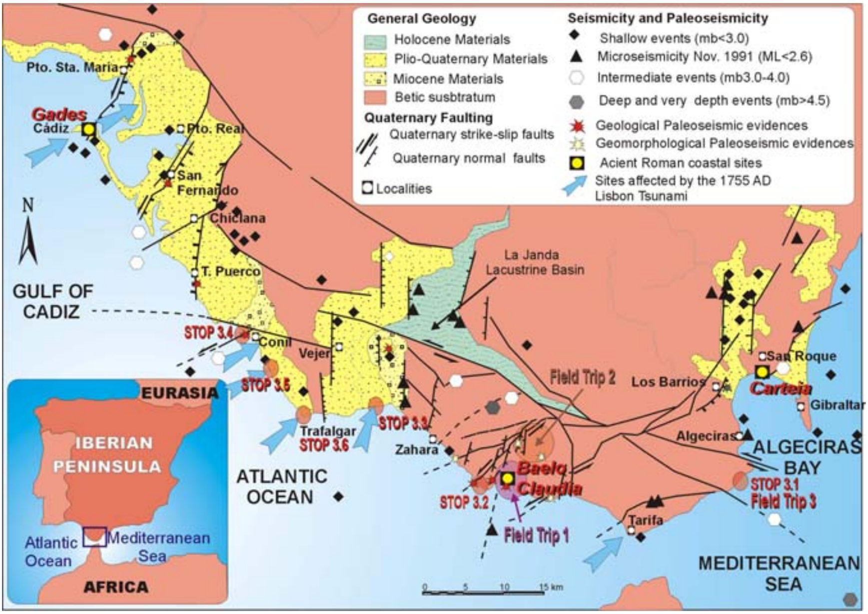

Fig. 3: Overall geology, main Quaternary faults and seismic activity in the Gibraltar Strait zone illustrating the zones of Field trips 1, 2 and 3, and stops of Field trip 3 around the Spanish coast of the Gibraltar Strait (After Silva et al., 2009)

Alonso-Villalobos et al. (2003) document a high-energy littoral event (probable Tsunami) in a little fluvial outlet east to *Baelo* at cal. 2150-1825 BP (ca. 75-200 AD). Archeological excavations in the ancient roman city of *Carteia*, located in the Algeciras Bay about 40 km east of Baelo Claudia document another high-energy littoral event sealing pottery factory remains of the second half of the 1st Century AD (Arteaga and Gonzalez Martín, 2004). Silva et al. (2005) underwent the first archeoseismological analysis of the present ruins, linking the two periods of city destruction with the occurrence of ground shacking by near-field events related to nearby NE-SW strike-slip faults (i.e. Cabo de Gracia Fault). No evidence of tsunami damage and remains were found by these last authors in *Baelo Claudia* and propose de dates of 40-60 AD and 360-395 AD for the intervening paleoearthquakes affecting to the archaeological site.

Eventually continuous archaeoseismological and paleoseismological research conducted by Klaus Reicherter (RWTH Aachen University, Germany) and Pablo G. Silva (Universidad de Salamanca, Spain) since the year 2004 allowed a finer analysis of dates and deformations related with probable earthquake damage in *Baelo Claudia* (Silva et al., 2009). In this last work, last earthquake damage visible in the present roman remains is bracketed between 260-290 AD, whilst the date of 360-390 AD is considered to be the eventual episode of overall ruin and abandonment of the ancient roman city. Silva et al. (2009) enlarge the list of suspect faults probably related with these destructive events, including Normal N-S normal faults (Fig. 3) subject to present moderate instrumental seismicity around the Gibraltar Strait area (Goy et al., 1994; Silva et al., 2006) and detected by seismic profiling offshore in the Bolonia Bay (Hüschber et al., 2007). Documented tsunami-type events for this period include vague descriptions of strong events occurred at 33 AD, 346 AD and 386 AD in the SW Portuguese coast around the Gulf of Cadiz (Galbis, 1932; Campos, 1992). These are classically associated to the presumed epicentral area of the well known 1755 AD Lisbon Earthquake-Tsunami, which caused damage and flooding in the cities of Conil and Tarifa, west and east respectively of *Baelo Claudia*. Therefore the nature of the observed deformations and the type of causative event is still an open debate: *"The Baelo Claudia Earthquake Problem".*

Stop 2

Archaeoseismological records at *Baelo Claudia*

P.G. Silva, K. Reicherter, J. Lario, C. Grützner, M.A. Rodríguez-Pascua, R. Pérez López, J.L. Giner-Robles, T. Bardají, J.L. Goy, C. Zazo, I. García Jiménez and A. Muñoz

Introduction

The building damage preserved in the ancient city of *Baelo Claudia* can be classified in two main groups (Silva et al., 2009): (a) deformation structures and wall collapse horizons preserved within the ground excavated by archeological probe trenches; and (b) deformation structures and architectural disruptions presently at surface in the excavated sectors of the city.

The deformation structures preserved within the ground are mainly associated with the Roman geoarcheological horizon and can be related to the first episode of city destruction (40-60 AD). Most of them are linked to collapse horizons around the eastern sector of the city-wall at the base of the Roman level. These collapse horizons are constituted by large blocks (0.5 x 0.3 m) of the first city wall. Actually there is little evidence outcropping at this archaeological site. The deformation structures presently preserved at surface are affecting the archeological remains belonging to the second period of the city (after its first destruction in the 1st Century AD) and can be related to the second event of city destruction (260-290 AD) and eventual abandonment (365-390 AD).

Most of these architectural disturbances were described in an earlier paper by Silva et al. (2005), comprising, faulted and westward tilted city-walls, directional southwest collapse of the columns of the Basilica, and pervasive pop up-like arrays in the pavements of the Forum and *Decumanus Maximus*. Silva et al (2009) carefully mapped all these structures performing a detailed measurement of the orientations of the pop up-like arrays, directional tilting of walls, pavement joints, and corner break-outs of the pavement flagstones quantifying and characterizing the directionality of deformation.

The Monumental sector of the *Temples, Forum* and *Macellum*

The recent work of Silva et al (2009) indicates that most of the structural and architectural damage observed in this zone is the result of a secondary ground effect: a landslide in the NE corner of the ancient Forum affecting to the zone of the Isis Temple (Fig. 4B). Here, walls are offset between several decimeters to more than one meter, and most parts of the city wall are anomalously tilted towards the S and N (Figs. 5B and C). The area of the Isis Temple is only partly excavated. Some of the best examples of building deformation are observable in the Isis temple. Rests of fallen columns (SW-directed) and wall and pillar collapses are also directed in S to SW direction, but also scarp and slope parallel (Fig. 5B and C). A crude stratigraphy based on Roman pottery suggested its abandonment and destruction during the 4th Century AD (Silva et al., 2009). However ^{14}C dating for the colluvial deposits beneath the fallen columns and walls (Fig. 5A) indicate that the collapse of the temple can be related with the firs episode of city destruction (2020±27 BP - 1930±27 BP) during the 1st Century AD (Grüztner *et al.*, in press). The Isis Temple was constructed on a small topographic scarp and shows also other deformation features, like offsets, tilting and bending of walls and foundations (Fig. 5B).

Below the artificial topographic step, this was carved to build the *Forum*, all houses situated in the E show severe distortion and bending (Figs. 4A-C and 5D). E-W directed up-thrusting and folding as well as the pop up-like structures affecting the pavement of the forum (Figs. 4D and 6F) are interpreted to be induced by discrete landslide, which affected to pavements and early foundations (Fig. 5D).

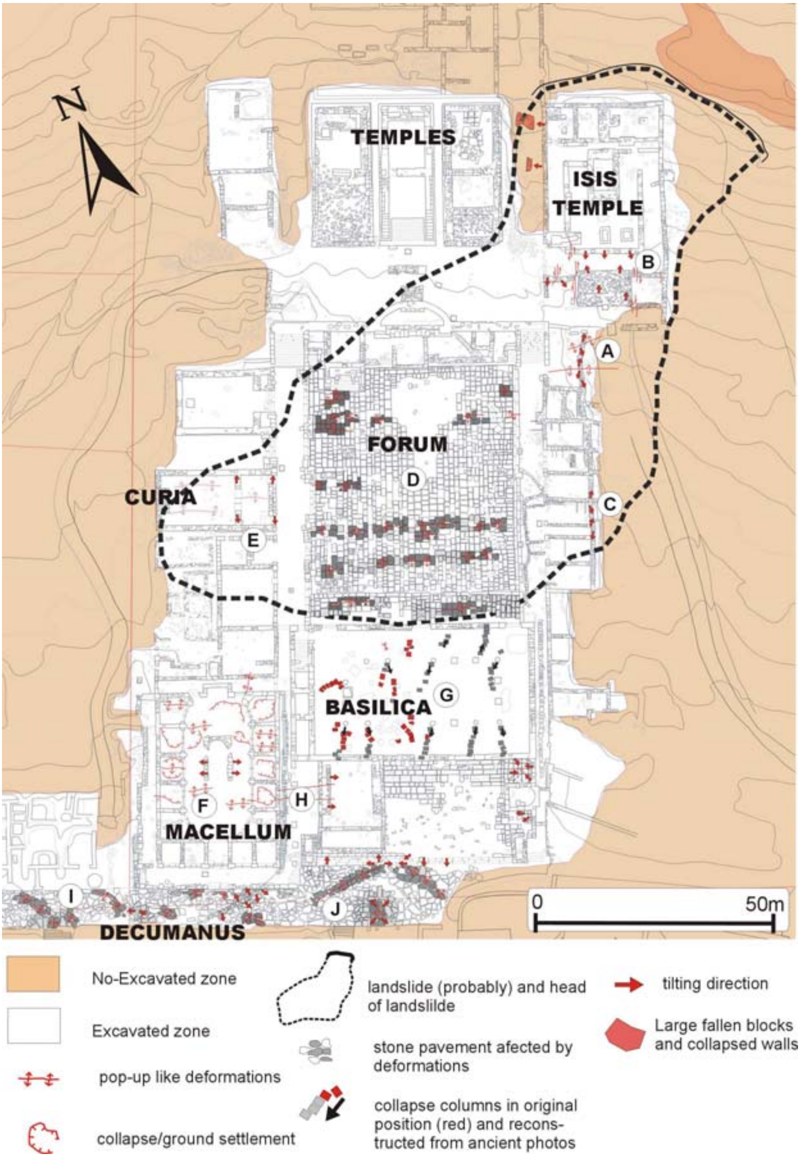

Fig. 4: Detailed map of surface deformations and architectural disruptions observable in the lower sector of the ancient Roman City of *Baelo Claudia*. All the mapped disruptions belong to the second period of city destruction (260-290 AD). Letters A-J locations of sites discussed in thefield-guide (modified from Silva et al., 2009).

E-W-trending low amplitude folds are clearly deforming the stairs, basement of house walls and the *opus dominum* (Roman mortar) of the ancient *Curia* at the western zone of the Forum (Fig. 4E) and the ancient *Macellum* (market) located immediately SW of the forum (Fig. 4F). These architectural disruptions may as well be related to the landslide event as a consequence of limited earth flow at the landslide toe as illustrated in the cross section of Fig. 2.

Fig. 5: Deformations recorded around the *Isis Temple*. A: Collapsed wall onto the ruins and debris of the western side of the *Isis Temple* displaying the stratigraphy of destruction horizons. B: Close-up view of northward tilting and offsets in the *Isis Temple*; white arrows indicate the tilting direction. C: General view of northwards tilting on foundations, pavements and walls of the *Isis Temple* (see Fig. 5B for location); white arrows indicate the tilting direction. D. General view of severely bended walls along the eastern side of the Forum down slope the Isis Temple (see Fig. 4 A-C for location).

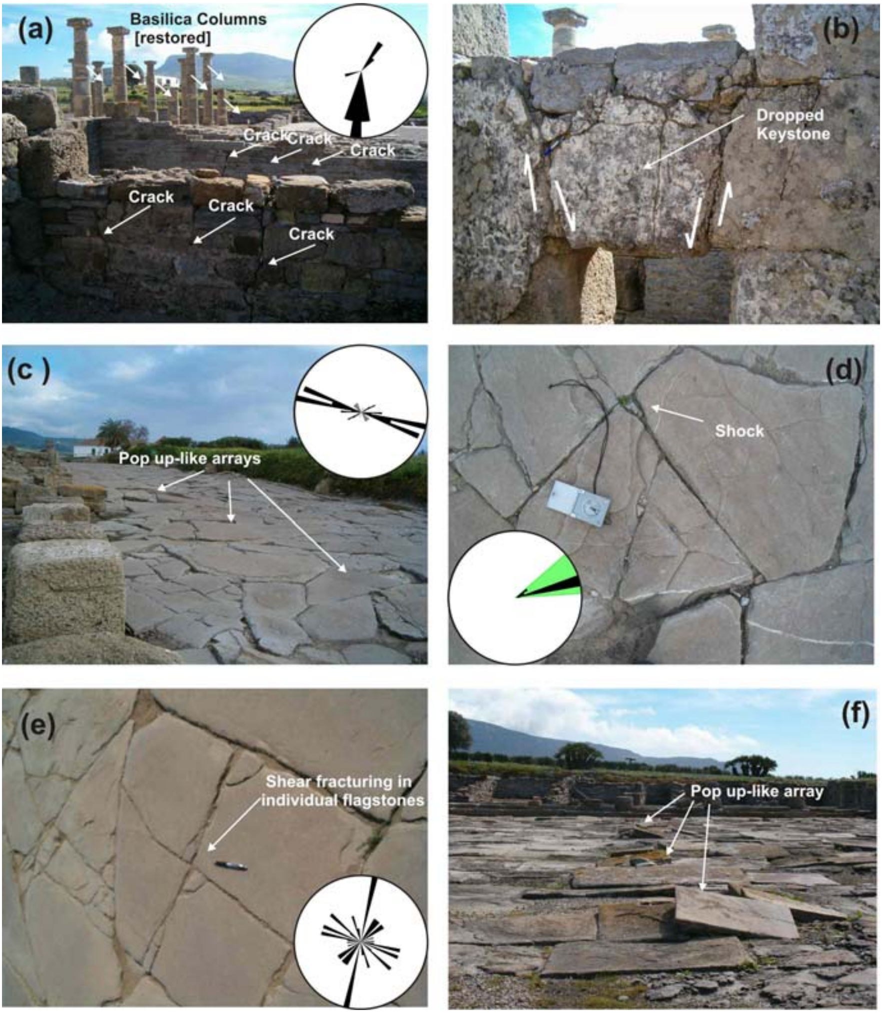

Fig. 6: Main structural deformations observed on the pavements and walls of *Baelo Claudia*. A: Propagation of Cracks in the walls of the ancient *Basilica* and adjacent *Macellum* with indication of the collapse orientations of the columns (and relative rose diagram for column collapse). B: Dropped Keystone in the western wall of the *Basilica*. C: Pop-up like arrays affecting the eastern sector of the *Decumanus maximum* and rose diagram of preferred orientations for these structures. D: Shocks developed in the corners of individual flagstones and rose diagram of measured orientations. E: Fractures (i.e. shear joints) in individual flagstones and rose diagram of measured orientations. F: Pop-up like deformation affecting to multiple flagstones in the *Forum* (from Silva et al. , 2009)

In the Forum flagstone couplets of the pavement are deformed showing pop up-like alignments. They are arranged in at least six well preserved lineaments crossing the entire pavement zone with consistent N110E orientations (Fig. 4D). These lineaments show a spacing ranging from 7.35 to 6.25 m, but in the southern sector there are some less developed intermediate lineaments with spacing of 2.5-3.7 m (Silva et al., 2005). In most of the cases, the flagstone couplets spur against each other, or even are partially upthrusted, displaying maximum vertical displacements of 4-6 cm and overlapped sections of 3-2cm. Only in two isolated cases pop-up like deformation is produced by rupture of individual flagstones. In any case, pop-up trends are strongly conditioned by the orthogonal disposition of the forum pavement, and difficult its use for the determination of ground movement (Silva et al., 2005).

In any case, the deformation structures observed close to and within the *Macellum* area are unidirectional. Numismatic and pottery findings indicate that the *Macellum* had a very limited activity of use by the Romans after the earthquake from ca. 260 AD to 395 AD, when commercial activity eventually terminated (Menanteaú et al. 1983; Sillières 1997). Summarizing, most of the observed structures in this area of the city are compatible with a SSW-directed and E-W trending complex landslide (Fig. 4; Silva et al., 2009).

The *Basilica*

The remains of the ancient *Basilica* are one of the most outstanding examples of earthquake architectural deformations before is restoration, as occurring in many places of historical seismic shaking in the eastern Mediterranean region (Ambraseys 1971, 2006; Stiros 1996).

Most of the columns collapsed towards the SW and SSW, with the column drums in a domino-style (Figs. 4G and 7). Drum impacts in the ancient floor of this building are numerous and there was no debris-layer between the columns drums and the ancient floor (Sillières 1997), indicating the sharp and sudden character of the collapse event (Silva et al. 2005). The directional collapse of the columns is incompatible with the intervening SSW directed landslide event, and hence indicates a ground movement directed towards the NE to NNE (if the *Basilica* columns were destroyed by seismic waves).

Fig. 7: Ancient photography of early excavations of the *Basilica* displaying the domino-style of the columns collapse (modified from Sillières, 1997).

Additionally, in the western N-S wall of an annexed building of the *Basilica* there are some fractures cutting through two or more adjacent blocks (Fig. 6A). Those affect most of the preserved wall and can be continued to the eastern wall of the building and to the adjacent western wall of the *Macellum* stores (Fig. 4H). One of these fractures is also associated with the subsidence of a keystone of an arch-window located in the western wall of the edifice annexed to the *Basilica* (Fig. 6B). Such kinds of fractures have been associated with minimum earthquake intensities of VIII MSK by Korjenkov & Mazor (1999) and Hinzen (2005).

Pop up-like arrays at the *Decumanus maximus*

South of the *Basilica*, the *Decumanus Maximus* (main E-W trending street) displays a wide variety of pop up-like arrays of flagstones (Figs. 4J-I and 6C) such as synclinal and anticline structures (Fig. 4J). The detailed mapping carried out for this work (flagstone by flagstone) lead to distinguish among those deformations due to ancient subsurface canalizations and post-burial differential settlement from others resulting from horizontal ground acceleration. Aside from the more spectacular deformations induced by the presence of subsurface roman structures, the rest of the pop up-like arrays are arranged following a main N130-125E orientation and a secondary N50-60E one (Figs. 4 and 6C). Vertical displacements of up to 30 cm and flagstone up-thrusting are common (Fig. 6F). A wide variety of joints and corner break-outs due to horizontal shocks densely fracture the set of flagstones. Structural data measured for pop up structures, joints and shocks directions from flagstone break-outs indicate very congruent orientations. The break-outs are mostly found along the NE edges of the flagstones. Orientation of these indicators is systematically distributed, pointing to a shock from the SW, and folding in NW-SE direction (Fig. 6). At the end of the *Decumanus Maximus*, just to the south of the Basilica a semi-circular dome-like structure with a radius of about 6 meters affect to the entire ancient pavement suggesting severe ground subsidence (Fig. 4J) including liquefaction.

Fig. 8: Remains of the Northern bastion of the Eastern City Wall tilted to the west and affected by different fractures and cracks.

The City Wall and the Eastern Aqueduct

The city wall surrounds the village and was built for representative and not defensive purposes. At the end of the *Decumanus Maximum* it has two main gates, the *Gades* Gate (Cádiz) in the west, and the eastern *Carteia* Gate (Fig. 4). The wall is equipped with several watchtowers. Generally, the city walls are in a very bad condition. Parts are not excavated or are collapsed, others are missing, because of later quarry-use. The eastern wall and its towers are preserved and excavated in parts up to the groundings. A detailed mapping of titling orientations, fractures and associated displacements can be consulted in Silva et al. (2009)

During the excavation older rests of a former city wall have been encountered, this wall is topped by a "demolition horizon" with big blocks of wall boulders. This horizon may correspond to the 40-60 AD earthquake outlined by Silva et al. (2005). Major damage is also well observed along the eastern city wall, which is mainly tilted to the WSW between 15° to 20º, but in some case up to 25º (Fig. 8). Tilting is accompanied by intense fracturing and rotation of individual segments against each other, often in an anti-clockwise sense. Some of those cracks in the Northern Bastion and close to it display offsets on the order of centimeters to meters, but commonly they are smaller than 20 cm. partly, the cracks were already restored by Romans (Menanteau et al. 1983). Evident signal of westwards tilting, destruction and fracturing are displayed in the preserved remains of the western sector of the City Wall near the Theatre zone (Fig. 9).

Fig. 9: Remains of the Western segment of the City Wall with differential tilting to the West and affected by different fractures and collapsed sectors. Note recent reparation works between the tilted segments.

The eastern aqueduct outside the city walls crosses a little creek, the western part of the aqueduct collapsed downhill, and now forms seven slided parts. The entrance through the city walls is almost perpendicular and has been excavated in 2007. Some of the arcs show rotational displacement around a horizontal axis, this might be interpreted as a slow deformational feature (low energy) originating probably from small creek-parallel landslides.

Fig.10: Deformations observed in the recently excavated eastern aqueduct of the city. Note displacement of the ancient canal in the western slope of the creek.

The Roman *Theatre*

In the upper sector of the City the main archeological remain is the theatre of the 1st Century AD (Fig. 4) built during the first phase of the city and directly founded in the clayey substratum. It displays not only earthquake or landsliding deformation, but also a lot of restoration. The Muslims started to build a watchtower in the right part of the theatre, also the theatre served as living place for many people in post-Roman times. Therefore it is quite difficult to assign some of the observed deformations to true earthquake damage because its multiple uses, burial and quarrying activity. Presently, the entire inner part is completely restored and filled with concrete, however, the collapsed stairway to the loggia is still in-situ, and directed towards the south (Fig. 9).

On the other hand, open cracks in the walls and inclined walls are interpreted as generated by slow deformation. On the other hand, big fallen blocks of the tiers are attributed to coseismic damage. A lot of triangle-shaped cracks and break-outs are found at pillar bases of the building, which are probably related to rapid deformation.

Fig. 11: Southward collapsed staircases in the northern *loggia* (Fondo Norte) of the *Theatre*

The Fish factories and the Lower coastal sector of the city

On the contrary, in the lower coastal sector of the city, south to the *Decumanus maximus*, the fish factories zone shows almost no destruction due to sudden seismic shocks or landsliding (only minor cracks). Fish factories are founded in a different substratum than the rest of the city of sandy nature, and completely buried by dunes after its abandonment. However this zone was restored after the last destruction event of the city (260-290 AD) and fish factories were reutilized as well as factories or houses. Many evidences of reutilization of column drums, decorated blocks, etc prove the poor quality of the city restoration after 260-290 AD.

Fig. 12: Lower sector of the city. Restoration and reutilization of recycled architectural elements

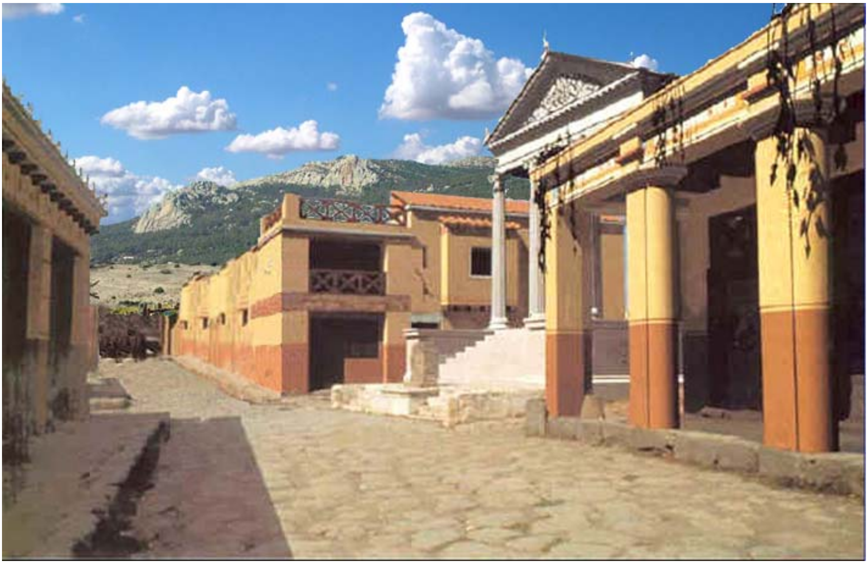

Fig. 13: Idealized reconstruction of The *Baelo Claudia* Building. View of the *Decumanus Maximus* to the West, Sierra de La Plata

DATES	HISTORICAL FEATURES	ARCHEOLOGICAL MILESTONES	GEOMORPHIC AND HUMAN PROCESSES
Before Late 2nd Century BC	No urban settlement in the zone	Neolithic tombs on the cliff of Cape Camarinal	Colluvial slopes partially bury staircase marine terraces. Dune system development (D_1) on the Holocene spit-bar system.
Late 2nd Century BC	First Roman settlement	First "fish" factories; increasing commercial activity with Africa.	Scarce human modification (or not documented). Local incorporation of archeological artifacts to surface formations
Late 2nd Century BC to Middle 1st Century AD	First Building phase (lower coastal sector). First settlement becomes *Oppidum latinum* (category of Roman city). Major urban reforms.	Construction of the Ancient Square or *Forum*, Ancient Capitol, Temples and first City Walls (ca. AD 10-20). Amplification and improvement of first fish factories and private buildings Urban orthogonal pattern.	Major landscape reworking. Ground digging; generation of artificial talus on colluvial slopes N of the Forum square; Soil beheading and alteration of surface hydrology.
Middle 1st Century AD (ca. AD 40-60) <u>PROBABLE EARTHQUAKE</u>	Demolition and/or Collapse of private and public buildings. Damage of City Walls inducing tilting a collapse levels	Demolition horizon overlays clayey substratum, folded roman pavement and house foundations in the lower sector of the city. Ancient temples leveled up to a meter above the ancient ground surface.	Probable localized landslide event NE of the Forum. Overall ground leveling; artificial silty and clayey filling with incorporation of large architectural elements.
Late 1st Century AD to Early 2nd Century AD	Second Building phase Maximum extension and prosperity of the city, which acquires the imperial Label of "*Claudia*" at ca. AD 48 -50. Improvement of the harbor south of the city.	Development of the monumental zone (*Basilica*, Temples, *Forum*, *Curia, Capitol*, *Macellum* and *Theatre*). Recycling of previous architectural elements, and partial use of former foundations. Ancient forum square shortened North and South. Reparation, reinforcement and thickening of the 1st Century City Wall. New urban orthogonal pattern, including all the pavements of the forum and streets (E-W *Decumanus* and N-S *Cardos*)	Rebuilding of the city on the "demolition horizon", artificially cemented on surface by *opus cementum*. Creation of an artificial terrace (500 m^2) for the building of the new capitol and Isis temple North of the *Forum*.
Late 3rd Century AD (ca. AD 260-290) <u>PROBABLE EARTHQUAKE</u>	Abrupt ruin and urban depopulation. The damaged city was never fully abandoned, but the monumental buildings were never restored or rebuilt.	Pop-up like deformations in *Forum* and *Decumanus maximus*. Collapse of Basilica column drums and *Macellum* roofs. Isis Temple partially collapsed. Westwards tilting of most house walls and city walls. Harbor and fish factories presumably abandoned	Probable localized and reactivated landslide event (ca. 5000 m^2) affecting to the artificial terrace NE of the Forum. Severe ground settlement and subsidence affecting the south side of the Basilica. Liquefaction?

DATES	HISTORICAL FEATURES	ARCHEOLOGICAL MILESTONES	GEOMORPHIC AND HUMAN PROCESSES
Late 3rd Century AD to Middle 4th Century AD	**Third Building phase.** Poor quality buildings are constructed over the ruins following a different urban pattern	Damaged structures are artificially leveled and new poor quality buildings are constructed over the ruins. Only the partially damaged remains of the *Macellum* and *Basilica*, *Isis Temple* and *Theatre* survived. Fish factories and some sectors of the Theatre were used as houses. The City Wall was never restored or reinforced.	Intervening horizon of ruins leveling some of the damaged urban structures for city rebuilding.
Late 4th Century AD (ca. 350 – 395 AD) EVENTUAL RUIN OF THE ROMAN CITY	**Eventual ruin** of remains of *Isis Temple*, *Macellum* and *Basilica* and definitive abandonment of the Ancient Roman city.	Severely damaged remains of the *Isis Temple*, *Macellum*, *Basilica*, and Southern sector of the *Theatre* progressively collapsed on the intervening horizon of ruins.	Roman and post-Roman colluvial formations bury the damaged remains of the city. Coastward shifting due to development of Dune system D_2.
Late 4th Century AD to ca 8th Century AD.	**Late Urban Development.** Small Paleo-Christian to Visigothic settlements on former monumental zone, with a very different urban pattern.	For first time graves and tombs are carved within the ancient Monumental zone of the city. Definitive abandonment shortly before the AD 711 Moors conquest of the Iberian Peninsula.	Colluvial burying of the destroyed roman city. Soil swelling and slope creeping amplify and magnify pavement damage. Burying of lowermost sector of the city by dunes.
Late 8th Century AD to 1292 AD.	**Military garrison of the Moors.** Small military sentinel and watchtower built on the ruins of the Theatre	In 1292 the reconquista of Tarifa by the Spanish 1870-1907 AD First archaeological findings. 1917-1921 AD First archaeological excavations	Slope wash sediments containing Roman rubbish (bones, teeth of animals, e.g. pigs, and seashells) and ceramics and glass.

Table 1: Periods, events and geological processes related to the organization of the Roman archeological site of Baelo Claudia (modified from Silva et al., 2009).

References

Arteaga, C. & González Martín, J.A. 2004. Presencia de materiales marinos y dunares sobre un alfar romano en la Bahía de Algeciras (Cádiz, Sur de España). Actas de la VII Reunión Nacional de Geomorfología, Toledo, España, 393-399.

Alonso-Villalobos, F.J., Gracia-Prieto, F.J., Ménanteau, L., Ojeda, R. Benavente, J. & Martínez, J.A. 2003. Paléogeographie de l'anse de Bolonia (Tarifa, Espagne) à l'époque romaine. In: The Mediterranean World Environment and History. Elsevier S.A.S. Amsterdam, 407 -417.

Ambraseys, N. N. 1971. Value of historical records of earthquakes, Nature, 232, 375-379.

Ambraseys, N. N. 2006. Earthquakes and Archaeology. Journal of Archaeological Science, 20, 1-9.

Becker-Heidmann, P. Reicherter, K. & Silva, P.G. 2007. 14C dated charcoal and sediment drilling cores as first evidence of Holocene tsunami at the Southern Spanish coast. Radiocarbon, 49, 2, 827-835.

Borja, F., Martínez, A. & Troya, A. 1993. El proceso histórico de destrucción de la ciudad Romana de Baelo Claudia (SW Cádiz): Caracterización geotécnica y análisis de formaciones superficiales. Arqueología Espacial 16/17, 297-308.

Bost, J.P., Chaves, F., Defeyrot, G., Hiernard, J., Richard, J.C., 1987. Belo IV: Les monnaines. Pub. Casa de Velazquez, Serie Archeologie 6. Ed. Broccard, París.

Campos, M.J. 1991. Tsunami hazard in Spanish coast of the Iberian Peninsula. Science of Tsunami Hazards, 9 (1), 83-90

Didierjean, F., Lunais, S. & Paulian, A., 1978. La douzième campagne de foullies de la Casa de Velazquez à Belo en 1977 (Bolonia, Cadix). Chro. Mél. Casa de Velazquez 14, 433-464.

Galbis, R.J. 1932. Catálogo sísmico de la zona comprendida entre los meridianos 5º E y 20ºW de Greenwich y los paralelos 45º y 25º N. Dirección General del Instituto Geográfico, Catastral y de Estadística, Madrid.

Goy, J.L., Zazo, Mörner, N.A., C. Hoyos, M., Somoza, L., Lario, J., Bardají, T., Silva, P.G. & Dabrio, J.C. 1994, Pop up-like deformation of a Roman floor and liquefaction structures in SW Spain as possible paleoseismic indicators. Bulletin of the INQUA Neotectonics Comisión, 17, 42-44.

Goy, J.L., Zazo, C., Silva, P.G., Lario, J., Bardají, T. & Somoza, L. 1995. Evaluación geomorfológica del comportamiento neotectónico del Estrecho de Gibraltar durante el Cuaternario. In: Esteras, M. (ed), El Enlace Fijo del Estrecho de Gibraltar, SECEGSA, Madrid. Vol., 2. 51-69.

Gracia, F.J., Rodríguez Vidal, J., Benavente, J., Cáceres, L. & López Aguayo, F. 1999. Tectónica Cuaternaria en la Bahia de Cádiz. In: Pallí, L., Roqué, C. (eds), Avances en el estudio del Cuaternario español. AEQUA-UdG, Girona, España, 67-74.

Grützner, Ch., Reicherter, K. & Silva P.G. (submitted). Comparing semiquantitative logic trees for archeoseismology and paleoseismology:the Baelo Claudia (southern Spain) case study. In: M. Sintubin, I.S. Stewart, T. Niemi & E. Altunel (eds.), Ancient Earthquakes. Geological Society of America Spec. Vol.

Guerrieri, L. & Vittori, E. 2007. Intensity Scale ESI 2007. Memoria Descritiva de la Carta Geologica d'Italia, 74. Servizio Geologico d'Italia, APAT, Rome. 41 pp. http://www.apat.gov.it/site/en-GB/Projects/INQUA_Scale

Hinzen, K.G. 2005. The use of engineering seismological models to interpret archaeoseismological findings in Tolbiacum, Germany: A case study. Bulletin of the Seismological Society of America, 95 (2), 521 – 539.

Hübscher, C., Betzler, C. Reicherter, K. & Lüdmann, T. 2007. The Meteor M69/1 cruise report, CARBMED, unpublished report, University of Hamburg.

Korjenkov A.M. & Mazor, E. 1999. Earthquake characteristics reconstructed from archaeological damage patterns: Shivita, the Negev Desert, Israel. Natural Hazards, 18, 193-226.

Luque, L., Lario, J., Zazo, C., Goy, J. L., Dabrio, C. J. & Silva, P. G. 2001. Tsunami deposits as palaeoseismic indicators: examples from the Spanish coast. Acta Geológica Hispanica, 36, 197-211.

Luque, L., Lario, J., Civis, J., Silva, P.G., Goy, J.L., Zazo, C. & Dabrio, C.J. 2002. Sedimentary record of a tsunami during Roman times, Bay of Cadiz, Spain. Journal of Quaternary Science, 17, 623 – 631.

Mártinez Solares, J.M. 2001. Los efectos en España del Terremoto de Lisboa (1 de Noviembre de 1755). Monografía nº 19, Instituto Geográfico Nacional (IGN). Madrid, Spain.

Martínez Solares, J.M. & Mezcua, J. 2002. Catálogo Sísmico de la Península Ibérica (880 AC – 1900). Monografía nº 18, Instituto Geográfico Nacional (IGN). Madrid, Spain.

Menanteau, L., Vanney, J.R. & Zazo, C. 1983. Belo II : Belo et son environment (Detroit de Gibraltar), Etude physique d'un site antique. Pub. Casa de Velazquez, Serie Archeologie 4., Ed. Broccard, París.

Silva, P.G., Borja, F., Zazo, C., Goy, J.L., T. Bardají, T., De Luque, & L., Lario, J. 2005. Archaeoseismic record at the ancient roman city of Baelo Claudia (Cádiz, South Spain). Tectonophysics, 408, 129-146.

Silva, P.G., Goy, J.L., Zazo, C., T. Bardají, T., Lario, J., Somoza, L., De Luque, L., & González-Hernández, F.M. 2006. Neotectonic fault mapping at the Gibraltar Strait Tunel area, Bolonia Bay (South Spain). Engineering Geology, 84, 31-47.

Silva, P.G., Reicherter, K. Grüztner, Bardají, T. Lario, J., Goy, J.L., Zazo, C., & Becker-Heidmann, P 2009. Surface and subsurface paleoseismic records at the ancient Roman City of Baelo Claudia and the Bolonia Bay area, Cádiz (South Spain). In: (K. Reicherter, M. Michetti & P.G. Silva, Eds.) Paleoseismology: Historical and prehistorical records of earthquake ground effects for seismic hazard assessment. Geological Society of London Spec. Vol.316, 93-121.

Sillières, P., 1995. Le Capitole de Baelo Claudia: Un cas d'incohérence de datations archéologique et stylistique et un exemple de solution. Annas 7/8, 285-298.

Sillières, P. 1997. Baelo Claudia: Una ciudad Romana de la Bética. Junta de Andalucía - Casa de Velázquez, Madrid.

Stiros, S. 1996. Identification of earthquakes from archaeological data: methodology, criteria and limitations. In: Stiros, S., Jones R.E. (eds), Archaeoseismology Ocassional paper nº 7 of the Fitch Laboratory, Bristish School at Athens, Athens, 129-152.

Zazo, C., Silva, P.G., Goy, J.L., Hillaire-Marcel, C. Lario, J. Bardají, T. & González, A. 1999. Coastal uplift in continental collision plate boundaries: Data from the Last interglacial marine terraces of the Gibraltar Strait area (South Spain). Tectonophysics, 301, 95-119.

FIELD TRIP 2

LANDSLIDES AND TECTONIC SCARPS IN THE BOLONIA BAY

Landslides and Tectonic Scarps in the Bolonia Bay

T.M. Fernández-Steeger, C. Grützner and K. Reicherter

Introduction

The excursion area is situated in the western Mediterranean and belongs to the Betic Cordillera. Together with the Rif Cordillera they form an arc-shaped mountain belt joining across the Straits of Gibraltar bordering the Alborán Sea. The Bolonia Bay is situated within the southernmost part of the Betic Cordillera in the Campo the Gibraltar Flysch units. The neotectonic setting (Fig. 1) of the area is influenced by the highly active tectonic setting of the convergent plate margin between Africa and Eurasia and therefore regularly affected by minor to moderate earthquake events. The geological environment of the Bolonia Bay with steeply dipping Eocene to Aquitanian sandstones of the Sierra de la Plata and San Bartolomé mountain ranges and subordinate claystone-rich Flysch units provides an ideal study area to investigate both seismic and gravitational/hydrological triggered mass movements. Intensive geotechnical investigations were carried out on the different rocks and mostly clayey soils. These investigations were accompanied by ground penetrating radar (georadar, GPR) measurements and empirical as well as numerical simulations to estimate the landslide susceptibility and triggering conditions.

Geology

The Bedrock geology in the Bolonia Bay is dominated by the Gibraltar Flysch, consisting of highly tectonized turbiditic units such as the Eocene to Aquitanian Aljibe (quartzsandstones, clays and caolinites) and Bolonia (sandstones, pelites and fine turbidites) units (Fig. 2). These units are intensely folded and thrust over the plastic Cretaceous to Eocene turbiditic sandy and clayey sediments of the Facinas and Almarchal units. During the Alpine orogeny, from Burdigalian to Late Tortonian, they have been overthrusted by turbiditic sediments of Cretaceous to Eocene age (Sanz de Galdeano 1990; Weijermars 1991; Silva et al. 2006). Sections of the fragmented nappes such as the San Bartolomé and parts of the Sierra de la Plata rotated clockwise and dextral displacement took place. This processes and the individualization of detached blocks lead to the present day topography.

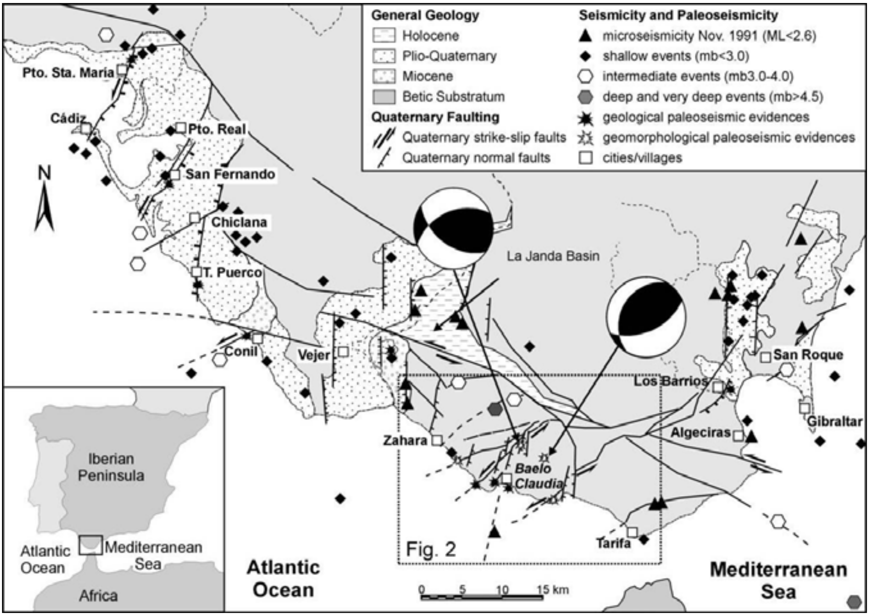

Fig. 1: Main Quaternary faults and seismic activity in the Gibraltar Strait. Data compiled from Benkhelil (1977), Goy et al. (1994), Gracia et al. (1999) and Zazo et al. (1999). Seismic data from the IGN DATA BASE (IGN, 1994) updated with data available in the IGN web site. Microseismic data from Makris et al. (1993). Stress distribution from structural measurements on Plio-Quaternary materials in La Laja and San Bartolome ranges (from Silva et al. 2009).

The Facinas and Almarchal formations (Fig. 2) of the flysch complex are made up of very plastic clayey and sandy layers, which are the main cause for the large number of mass movements that have been observed in the bay area (Fig. 6). From post-Messinian times on large landslides on-shore, but also off-shore take place on the upthrusted as well as the backthrusted topographic fronts such as the Sierra de la Plata littoral part. These events have proven to be a relevant process shaping the landscape of the Gibraltar Strait region.

Geotechnical investigations show that many of the residual soils from these units are highly active and show activity coefficients up to 4.4. The clay mineralogy shows smectite contents of up to 40%. The effective friction angels are between 5° and 15° and the effective cohesions between 25 and 44 [kN/m^3]. The Bay is surrounded by three steep mountain ranges of Aquitanian sandstone, the Cabo de Gracia and La Laja mountain range in the west and the

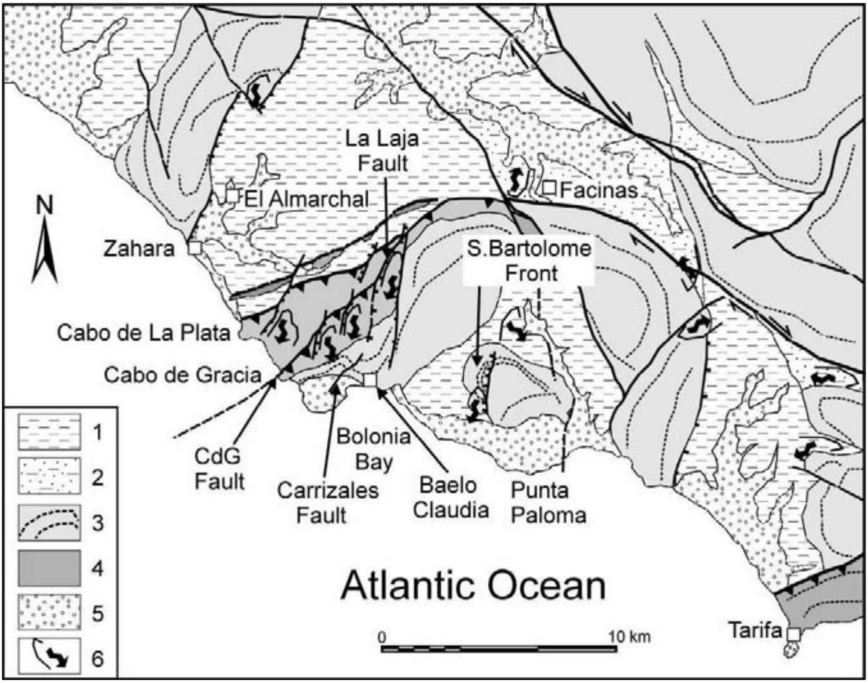

Fig. 2: Regional map of neotectonic structures and Flysch units of the Gibraltar Arc in the surveyed zone. 1) El Almarchal Unit (plastic clays); 2) Facinas Unit (plastic clays); 3) El Aljibe Flysch nappe (mainly sandstones): dotted lines = trace of Betic of uprighted stratification planes; 4) Flysch-slabs activated during the neotectonic period (Bolonia and Tarifa); 5) Post-collisional Pliocene and Quaternary deposits; 6) landslide units (from Silva et al. 2009, for location see Fig. 1).

San Bartolomé in the east (Fig. 3 and 4). Especially the western and northern mountain front of the San Bartolomé shows intensive jointing and detachment of large blocks (Fig. 5). Rock fall debris and blocks cover the slopes at the foot of the mountain range. The prominent La Laja (Fig. 6) and Cabo de Gracia mountain fronts form kilometer-scaled lineaments and are most likely related to neotectonic activity (Silva et al. 2009). Numerous studies describe the tectonic setting (e.g. Zazo et al. 1999; Silva et al. 2006), the paleoseismological and archeoseismological records at the Roman ruins and adjacent areas (Goy et al. 1994; Sillières 1997; Alonso-Villalobos et al. 2003; Silva et al. 2005, 2006, 2009).

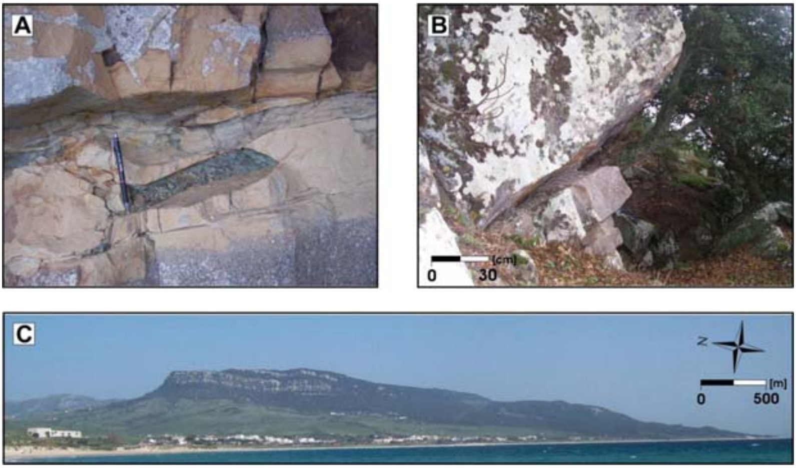

Fig. 3: A: Turbiditic sandstones of the San Bartolomé: the clay-lens is evidence for the high energetic environment in which sedimentation took place. (Pencil for scale, line of sight: west) B: Aljibe-Sandstone units San Bartolomé: alternating thickness of beds. (Line of sight: west) C: East view of the detached part of the Aljibe Flysch nappe forming the mountain range of San Bartolomé (from Müller, 2008).

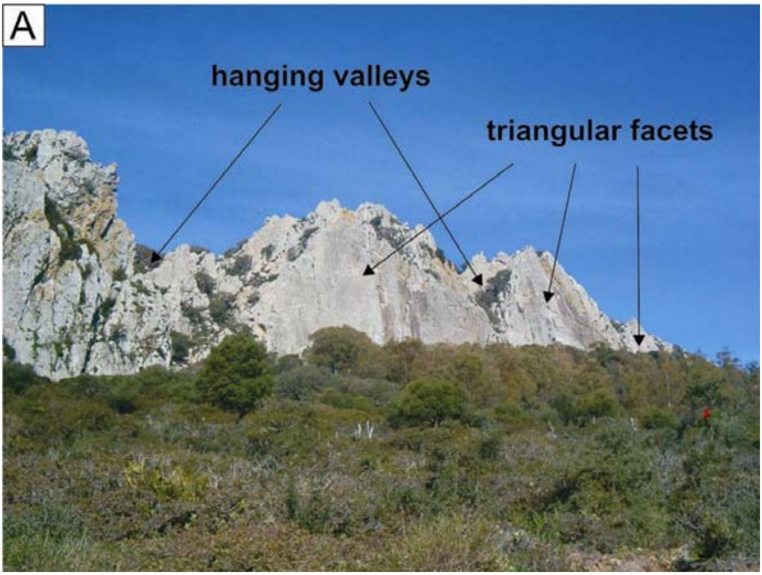

Fig. 4: La Laja Range Front; (A) Geomorphology of La Laja Range with well-developed triangular facets and hanging valleys in near vertical bedding Aljibe Sandstone Formation (from Silva et al., 2009).

The La Laja Range shows additionally geomorphological evidences of recent activity such as well-developed triangular facets, hanging valleys, as well as other minor markers of tectonic activity. Large mass-wasting processes are accommodated by normal faults along the nearly vertical dipping, bedding parallel topographic fronts (Fig. 4).

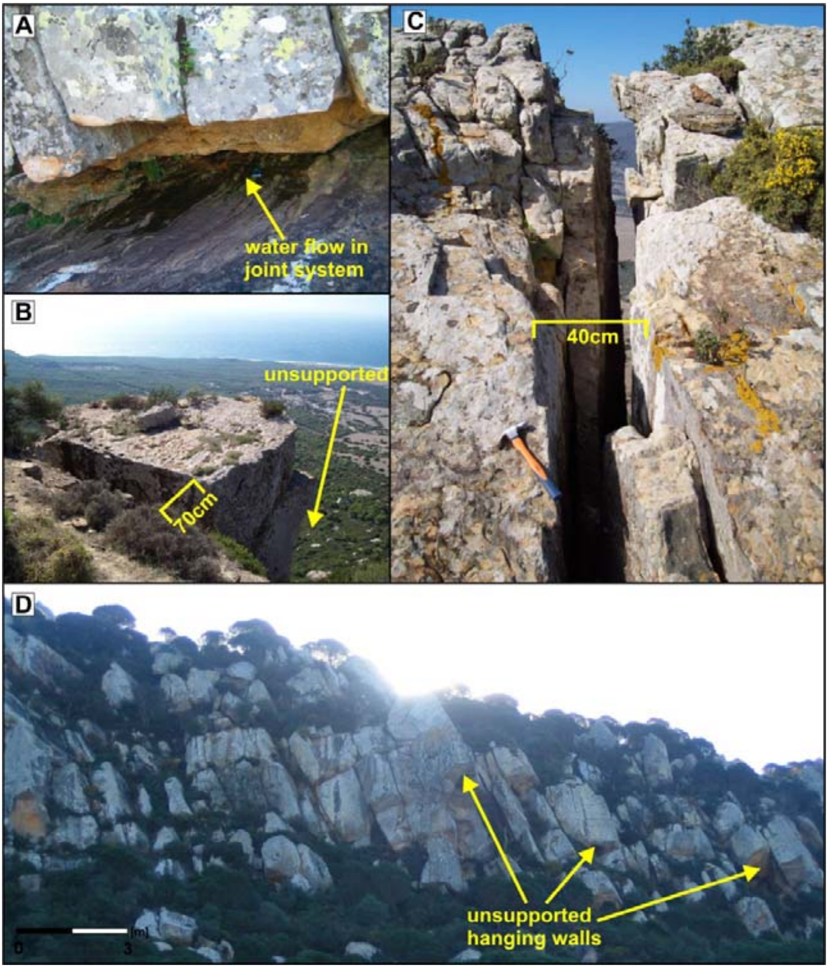

Fig. 5: Intensively joint and fragmented mountain front of San Bartolomé showing the nearly ideal perpendicular joint and bedding system. A and D show some unsupported blocks in the western rock face of the mountain ridge. Some of the bedding planes and joints act as periodic springs, draining the rock face. B and C show the wide joint opening at the top of the mountain, indicating like in B the danger of rock toppling (from Müller, 2008).

Landslides

The neotectonic environment and the landslide prone lithology led to the theory of earthquake triggered or amplified rock falls and landslides. Extensive field campaigns took place from 2006 to 2008. The aim was to gain knowledge about the mass movement mechanisms in the area and to check whether rock fall and landslide events coincide with the earthquakes that are held responsible for the destruction of the Roman city of Baelo Claudia. Comparison of investigations at the archeological site with the phenomena of the surrounding slopes in the bay should clarify, which of the damages observed are due to slow deformation and if possible to separate them from earthquake effects.

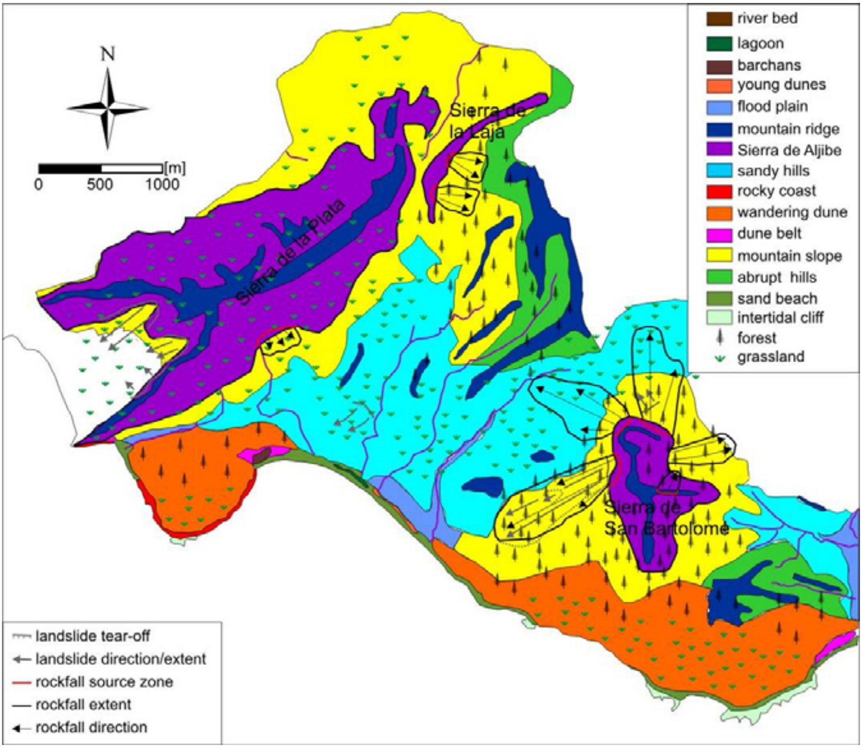

Figure 6: Geomorphological map of the Bolonia Bay area. Only the important and well developed rock fall deposits and landslides are displayed (from Müller, 2008).

For this reason, the rock falls at the La Laja and San Bartolomé mountain ranges were object to detailed field mapping (Fig. 6 and 7). Run-out distances of big blocks were described as well as erosion effects and even the orientations of Visigoth and Neolithic tombs that seem to show subsequently rotation due to post depositional movements. Debris mapping and comparison with aerial photographs from the 1950s and the 1990s should give an idea of the amount of re-deposited and moved material. Detailed investigation including excavation of single, prominent blocks was taken out in order to date the events. The erosional features of the weathered sandstone units have been investigated in situ. Jointing, bedding, and inclination of sometimes unsupported rocks have been mapped. The clay layers that are assumed to act as sliding layers have been sampled at different locations. Additionally, samples of charcoal and soil were taken for 14C-dating from several sites.

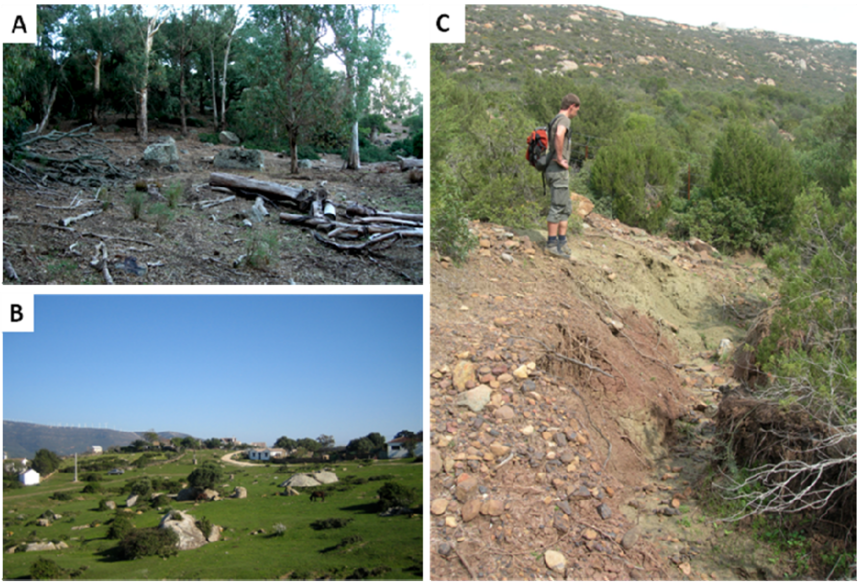

Fig. 7: Rock fall and landslide processes in the Bolonia area. A shows rock fall blocks at the foot of the La Laja ridge. B shows a rock block field at the northern flank of the San Bartolomé in Bethis. Picture C shows a small scarp ahead of Atlanterra at the north western flank of the Sierra de la Plata mountain ridge.

This broad investigation is of relevance as the identification and evaluation of triggering mechanism and dating of landslides may assist the hazard and risk evaluation. Especially in situations where an overlapping of different geological processes may lead to similar damage symptoms and landscape modifications, a good process understanding is essential to identify the triggering processes. This is even more important as the results from landslide investigations are relevant not only for landslide hazard identification but may also support earthquake risk evaluation and paleoseismological investigations. For example the new Environment Intensity Scale - ESI 2007 initiated by the INQUA also uses secondary effects like landslides and rock falls to rate earthquake intensities (Guerrieri & Vittori, 2007).

Fig. 8: Rockfall dating and identification of post-depositional movements using the changes of orientation of the strictly east orientated Visigoth tombs.

Stop 1

Rockfalls and Landslides at the San Bartolomé

For rockfall investigations and simulations, competitive data sets and case studies are important to develop a good process understanding (especially regarding the triggers) and to set up reliable models. For empirical or data driven stochastic modelling the quality of the reference data sets has a major impact on model skills and knowledge discovery. Therefore, rockfalls in the Bolonia Bay were mapped. At the San Bartolomé the siliciclastic Miocene rocks are intensively joined and disaggregated by a perpendicular joint system (Fig. 9). Although bedding supports stability as the dip is not directed towards the rock face, the deposits indicate a continuous process of material loss from the 80 m high cliff of the mountain front by single large rock falls. At the NE flank of the San Bartolomé in the upper overthrusted part of the nappe, a larger event which may be described as a rock avalanche (Fig. 10) can be seen. At the western mountain front, the shape of the rock face, fields of rock boulders and a large landslide support the idea of a large rockfall event by a collapse of parts of the mountain front, leading to an undrained loading and triggering subsequently a large landslide (Fig. 10).

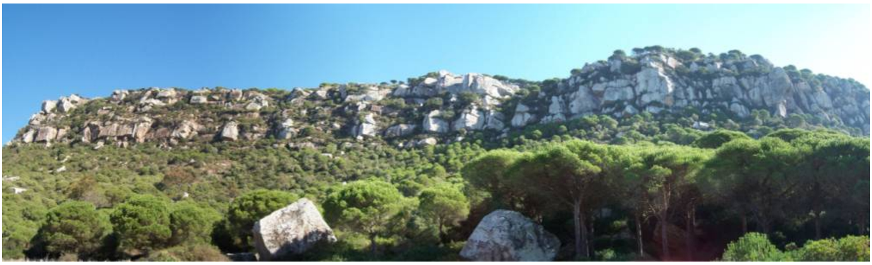

Fig. 9: The siliciclastic Miocene rocks at the northwestern flank of the San Bartolomé are intensively joined by a perpendicular joint system and are highly disaggregated. The rock boulders in the foreground have a volume of more than 15 m^3.

For the rockfall investigations more than 300 blocks were mapped and their size, shape, type of rock, and location were determined. The work concentrated on rockfall blocks with a volume of more than 2 m^3 and up to 350 m^3 (Fig. 11). Occasionally, very long runout distances of up to 2 km have been observed, leading to the idea of a post-depositional reactivation and transport. For all major source areas and deposits, runout analysis using empirical models and a numerical trajectorian model has been performed.

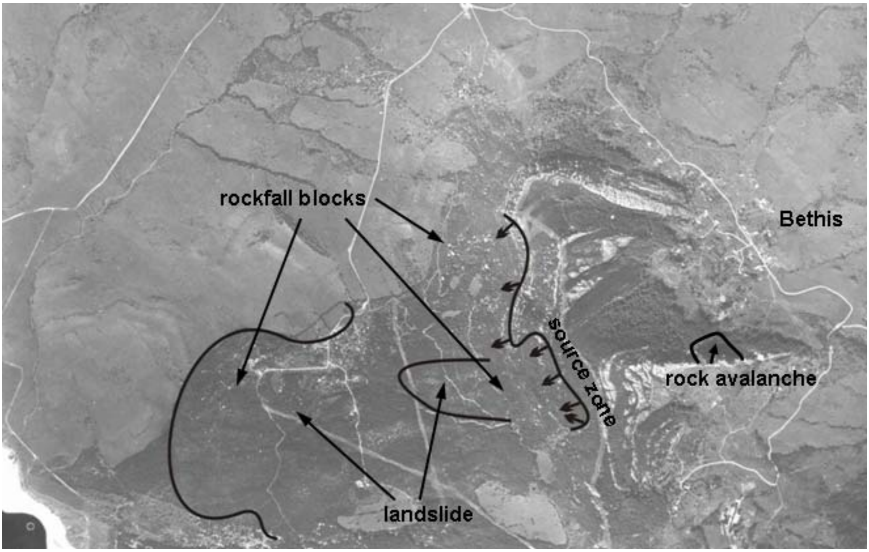

Fig. 10: At the NE flank of the San Bartolomé in the upper overthrusted part of the nappe, a rock avalanche is located. At the western mountain front the shape of the rock face, fields of rock boulders with runouts of up to 2,000 m indicate a large event with subsequent landslide activation.

Empirical and numerical models were used to investigate if these runout distances are reliable or additional forces or processes are involved. Most empirical models are based upon the relation between fall height and travel distance. Beside the “Fahrböschung” from Heim (1932) the “shadow angle” introduced by Evans and Hungr (1993) is most common today. However, studies from different sites show a wide variance of the angle relations (Dorren 2003, Corominas 1996). The reasons for that might be different environments and trigger mechanisms, or varying secondary effects such as post-depositional movement. Today, “semi” numerical approaches based on trajectorian models are quite common to evaluate the rockfall energy and the runout distance for protection measures and risk evaluations. The results of the models highly depend on the quality of the input parameters. One problem here might be that some of the parameters, especially the dynamic ones, are not easy to determine and the quality of the digital elevation model has a large impact on energy estimations and travel paths. At the western flank of the San Bartolomé the model of “shadow angel”, “Fahrböschung” and a numerical simulation using “Rockfall 6.2” (Spang & Sonser 1995) have been applied to the mapped rockfall deposits.

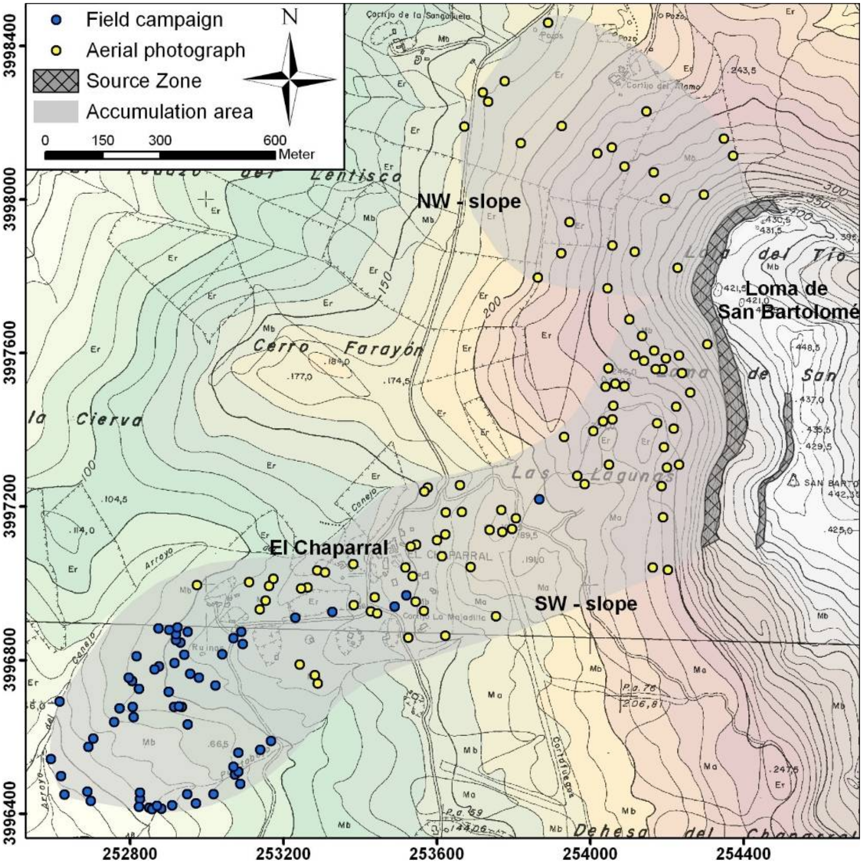

Fig. 11: Location of the source zone of the rockfalls at the western mountain front of the San Bartolomé and the distribution of larger rockfall blocks (> $2m^3$). Some of the blocks especially in the south show a runout length of nearly 2 km (from Braun, 2008).

The results revealed a good coherence of all three modelling attempts in some cases. Especially for deposition areas where many single rockfall events could be identified as young all models performed well and showed nearly identical results. In other areas with large deposits and long travel distances, the model predictions vary strongly and the shadow angles do not fit the usual ranges at all. Here, post-depositional transport by surface-near landslides in a piggy-back style is postulated. Medium- and large-scaled landslides and creep in soils are proven in the whole bay. Landslide bodies can be observed in the deposition areas and were proved with GPR. Additionally, the weathered marls and clays of the Flysch deposits below the rock face are highly active and likely to be subject to sliding after heavy rainfalls. Another reason for the extraordinary long runout distances might be seismic triggering. This trigger mechanism was simulated for various blocks, but did not lead in any case to the expected results. Strong winds have also to be considered as an additionally trigger mechanism for rockfalls by leverage as wind forces > 5 Bft are present in the forested study area more than 300 days per year. The results show that simple stochastic analysis using large data sets without taking triggering mechanism and geological environment in consideration may lead to more general models. More data sets and comparative studies are necessary to evaluate the threshold values for the empirical models like the shadow angle. Anyhow the results from the described investigation show that on a screening and planning level the results of the empirical methods are quite good.

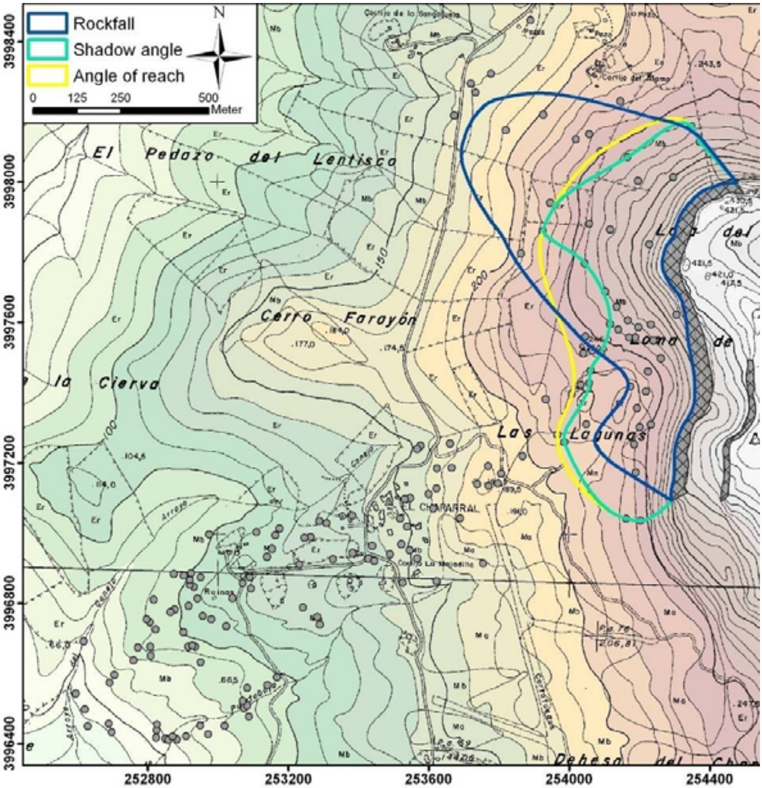

Fig. 12: Comparison of the run-out distances determined by the three models. For the most areas the model results match quite well. The results of the trajectorian model Rockfall 6.2 show more deviations than the other models due to the consideration of the local topography of the travel path and dynamic ground parameters.

Fig. 13 shows an example of a shallow-seated landslide at the slopes below the San Bartolomé mountain ridge. Between 63 and 82 meters, a clear change in reflection amplitudes occurs. Furthermore, continuous reflectors mark the slide plane. The high amplitudes are interpreted as due to the change in humidity in the landslide unit, while the reflection pattern directly images the slide's geometry. In this area, hyper-plastic clays are responsible for the mass movement. The slide imaged in figure 13 has a length of around 20 meters and a maximum depth of 20 ns TWT (approx. 1 m).

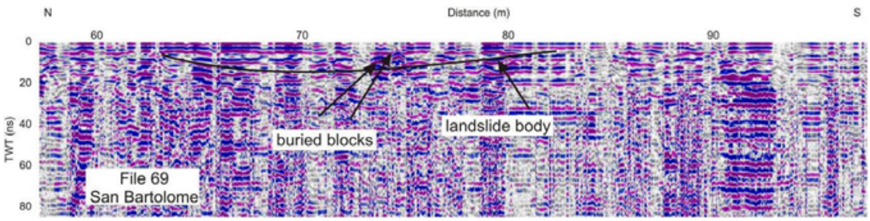

Fig. 13: 270 MHz GPR profile starts at the base of the San Bartolomé the north and range about 42m down the slope on foliage-covered underground. Several small landslide units and buried rockfall blocks are visible in the data (Grützner et. al., 2008).

Buried blocks with diameters from 0.5 to 2m form reflection hyperbolae. In the whole area, these blocks can be observed in the field. Some of them are partly buried due to earlier events and post-event sedimentation. The depth of the debris varies over the whole profile and is 0.5 m in the section of figure 13. As shown in profile 69, some of the rockfall blocks are embedded within a landslide body. This effect can be observed at various places in the San Bartolomé area. In some locations a gap between debris accumulation zones and the rock falls source can be observed. The GPR measurements support the idea that a post-rock fall piggy-back transport of the blocks is possible, caused by the hyper-plastic clays that act as a slide plane. This theory would both explain the long run-out distances and the gap observed in the field.

Stop 2

Rockfalls and Landslides at the La Laja mountain range

Consisting of Aquitanian sandstone, the nearly vertical La Laja mountain front (Fig. 14 and 4) is dominated by four hanging valleys. Debris cones have formed at the bases of these structures, showing coarse-grained sediments and numerous big blocks. As they show no or only sparse grass vegetation, it is clear that erosion and sedimentation rates are very high in this area. Hundreds of large boulders at the base of the mountain front give an expression of the rock fall activity. Eucalyptus trees growing in the area show damages from rock impacts, which allow a preliminary dating of single events.

Fig. 14: South view of the La Laja mountain ridge. Due to the upright bedding the rock faces at the front represent the bedding plane. The highest peak of the Sierra de la Plata, the Silla de Papa in the background is separated by a steep valley in between.

The 270 MHz profile presented in figure 15 was recorded on a debris cone in order to determine the sediment thickness and to identify large boulders. The rock surface marked in file 4 is part of a system of eroded beds, which have been in front of the mountain range that forms La Laja today. The eroded beds are still visible in the field, are almost vertical and show a slight inclination towards the bedding-parallel La Laja wall. Therefore, these beds form sediment traps and are responsible for the variations in the debris cone thickness. At the uppermost part, the sediment cover is only about 1 m (20 ns TWT), while the thickest part of the cone forms in the middle of profile 4 with about 3.5 meters

(70 ns TWT). Reflection hyperbolae indicate the occurrence of big blocks. The unevenly distribution of these buried boulders shows that they accumulate at the base of the debris cone. As adjacent profiles reveal the same or at least similar patterns, it is possible to draw conclusions on the geometry of the cone and to estimate the total amount of debris, which is in the order of 1.000 m³ in this case.

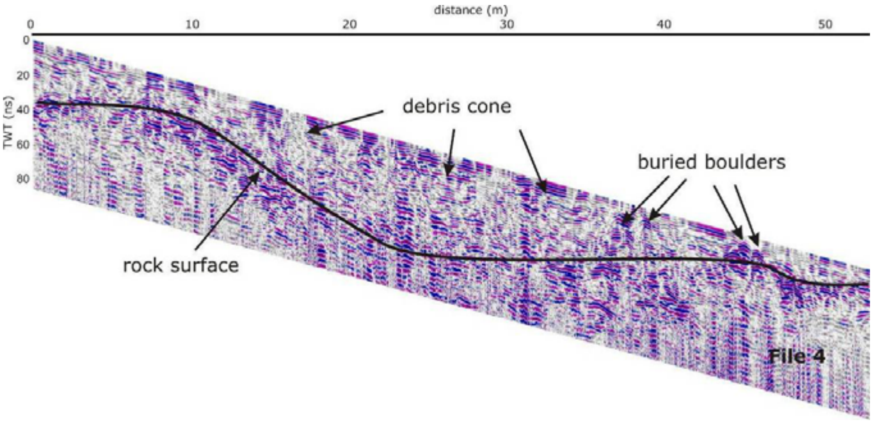

Fig. 15: 270 MHz profile from the La Laja mountain range. The profile was recorded on a debris cone at the base of a hanging valley. GPR data clearly reveal the thickness of the sediments and show the staircase structure of the underlying rock surface. 20 ns TWT represent ~ 1 m depth.

In case of the La Laja, rockfall simulations proved the observations made in the field in most cases (Fig. 16). The joint system of the mountain range was mapped, showing a clear E-W orientation (Vollmert, 2008) almost perpendicular to the NNE-SSW bedding (see Fig. 17). Dipping is in the order of 70°. Two different ways of block movement occur at the La Laja: Wedge sliding seems to be the main mechanism that leads to the formation of the hanging valleys. Toppling and buckling can be observed in a number of places, where large parts of the yet disaggregated banks are being pushed out of the wall by sediments that accumulate in the bedding gaps.

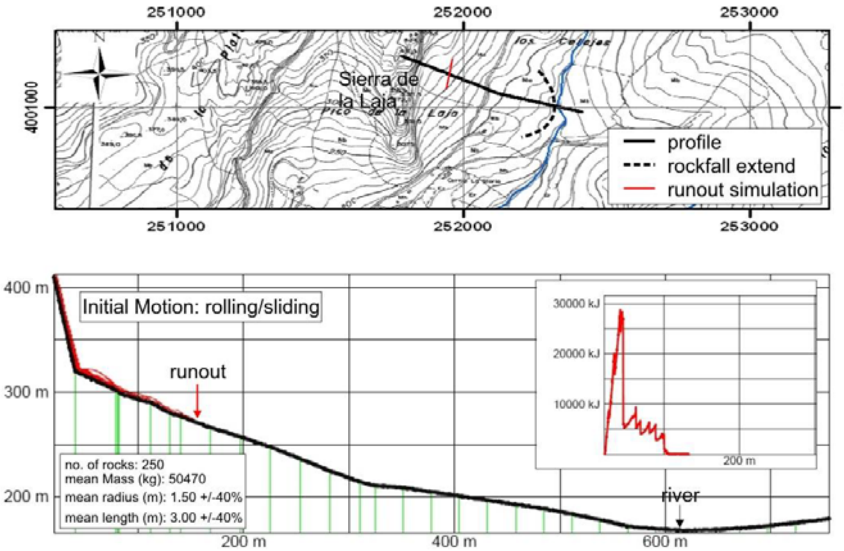

Fig. 16: Rockfall simulation using Rockfall 6.2. The upper figure shows the location of the profile and maximum run-out, while the lower shows the block motion, terrain profile and the kinetic energy (from Müller, 2008).

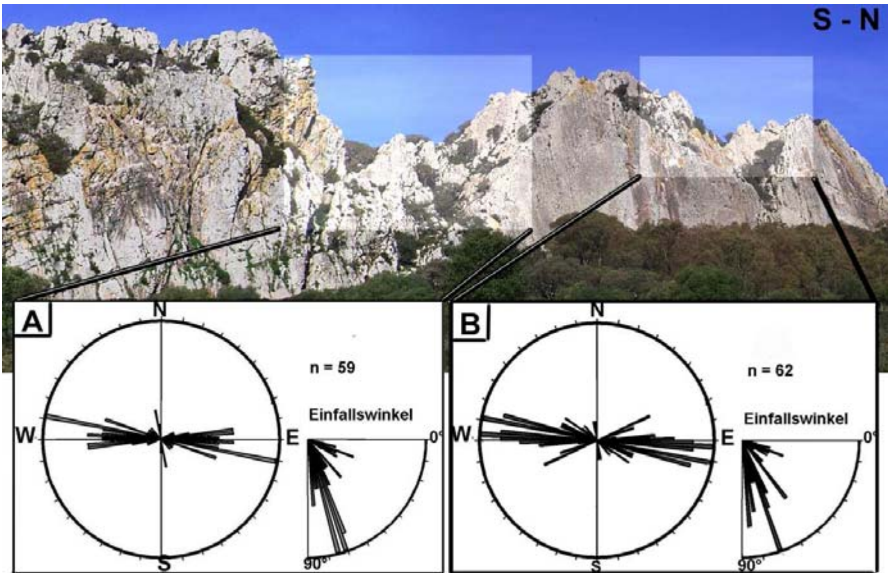

Fig. 17: Joint mapping at the la Laja shows a clear east-west trending joint system in the two southernmost hanging valleys (from Vollmert, 2008).

At various places indications for past but also recent sliding processes in the Flysch units may be observed (Fig. 18). Especially the weathered Almarchal units are very sensitive on rising water contents, showing a high plasticity and low shear angels. All this gives evidence of landslides triggered by intense precipitation periods. Anyhow, simulations show (Fig. 19) that shallow landslides like the one in figure 13 will only occur under the condition of considerably reduced cohesion. Deep seated landslides, especially under saturated conditions, may occur at the slopes below the surrounding mountain ranges, which may explain the secondary transport of big rock boulders. For seismically triggered landslides, only first simulations using the critical acceleration and Newmark Displacement (Jibson et. al., 2000) for different earthquake sources and magnitudes were computed. The results show also that the slopes below the mountain ranges are mainly affected. Anyhow, it should be mentioned that the additionally affected areas are quite small and investigations in other areas show that the Newmark displacement does not work very well for deep seated landslides.

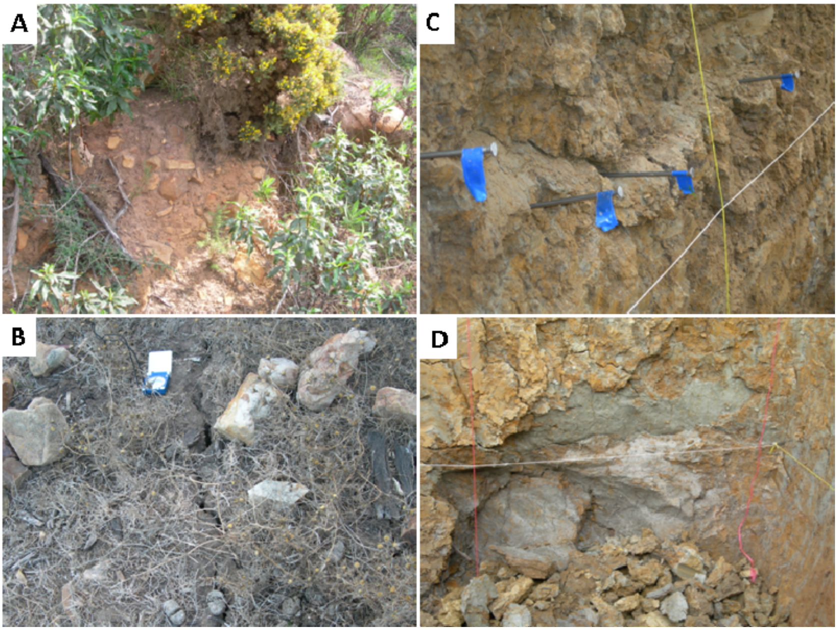

Fig. 18: Examples for active landslide processes at the Sierra de la Plata and La Laja mountain range. A: Young scarp NW of Atlanterra. B: Slope parallel extension cracks at the La Laja. C and D: sliding planes in a trench close to the Capo de Gracia Fault. C: shallow but long extended slope parallel sliding plane. D: Deep (> 2m) and more upright convoluted sliding planes.

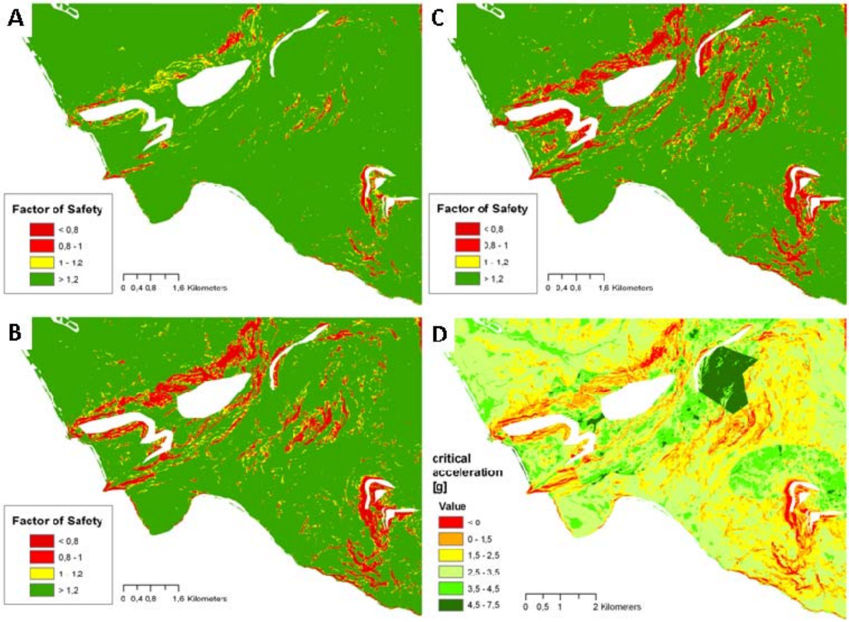

Fig. 19: A - C: Distribution of the factor of safety (FS) in the Bolonia Bay. D: Critical acceleration after Newmark (1965) for a 3m deep landslide. A, B: FS for saturated conditions and 3 m (A) and 5m (B) deep sliding plane. C: FS for a shallow (1m) landslide under unsaturated conditions neglecting the cohesion due to weathering and alteration effects. Comparing the results from parameter variation and considering the geotechnical soil parameters, this indicates that landslides occurrence is definitely coupled to precipitation and weathering states.

References

Alonso-Villalobos, F.J., Gracia-Prieto, F.J., Ménanteau, L., Ojeda, R. Benavente, J. & Martínez, J.A. 2003. Paléogeographie de l'anse de Bolonia (Tarifa, Espagne) à l'époque romaine. In: The Mediterranean World Environment and History. Elsevier S.A.S. Amsterdam, 407 -417.

Benkhelil, J., 1977. Etude néotectonique de la terminaison occidentale des Cordilléres Bétiques (Espagne). Thése d'Etat, Univ. Nice, France.

Braun, a. (2008): Felssturzanalyse und Risikokartierung in der Bucht von bolonia (sierra Bartolomé), Südspanien. Unpubl. BSc thesis, RWTH Aachen University, pp. 56.

Corominas, J. 1996. The angle of reach as a mobility index for small and large landslides. Canadian Geotechnical Journal, 33, 260 – 271.

Dorren, L.K. 2003. A review of rockfall mechanics and modeling approaches. Progress in

Physical Geography, 27 (1), 69 – 87.

Evans, S. & Hungr, O. 1993. The assessment of rockfall hazard at the base of talus slopes. Canadian Geotechnical Journal, 30, 620 – 636.

Goy, J.L., Zazo, C., Mörner, N.A., Hoyos, M., Somoza, L., Lario, J., Bardají, T., Silva, P.G. & Dabrio, J.C. 1994. Pop up-like deformation of a Roman floor and liquefaction structures in SW Spain as possible paleoseismic indicators. Bulletin of the INQUA Neotectonics Comisión, 17, 42-44.

Gracia, F.J., Rodríguez Vidal, J., Benavente, J., Cáceres, L., López Aguayo, F., 1999. Tectánica Cuaternaria en la Bahia de Cádiz. In: Palli, L., Roqué, C. (Eds.), Avances en el estudio del Cuaternario español. AEQUA-UdG, Girona, España, pp. 67– 74.

Grützner, C., Fernández-Steeger, T.M., Reicherter, K., Müller, D., Rodríguez Bouzo, L., Silva, P.G., 2008. Historic and prehistoric landslides and rock falls in the Bolonia Bay region/SW Spain. EGU General Assembly 2008, Vienna, EGU2008-A-06099

Guerrieri, L. & Vittori, E. 2007. Intensity Scale ESI 2007. Memoria Descritiva de la Carta Geologica d'Italia, 74. Servizio Geologico d'Italia, APAT, Rome. 41 pp. http://www.apat.gov.it/site/en-GB/Projects/INQUA_Scale

Heim, A. 1932. Bergsturz und Menschenleben. Vjschr. d. Naturforsch Ges. Zürich, 216 pp.

IGN, 1994. Banco de Datos Sísmicos, Servicio Nacional de Sismología. Instituto Geográfico Nacional (IGN), Madrid. Petición de datos n8 94/0001 (Data file).

Jibson, R.W., Harp, E.L., Michael, J.A. (2000): A method for producing digital probabilistic seismic landslide hazard maps, Engineering Geology, 58, 271–289

Makris, J., Egloff, E., 1993. Seismic and seismicity study of the Gibraltar Strait. Unpublished Report. SECEGSA-SNED Gibraltar Strait Project. Unv. Hamburg, Germany

Müller, D. (2008): geotechnical and Geophysical Investigations on Mass Movements in the Bolonia Bay, Southern Spain. Unpubl. Diploma thesis, RWTH Aachen University, pp. 89.

Newmark, N.M. (1965): Effects of earthquakes on dams and embankments. Geotechnique, 15, 1139 – 160.

Sanz de Galdeano, C. 1990. Geologic evolution of the Betic Cordilleras in the Western Mediterranean, Miocene to present. Tectonophysics, 172, 107-119.

Sillières, P. 1997. Baelo Claudia: Una ciudad Romana de la Bética. Junta de Andalucía - Casa de Velázquez, Madrid.

Silva, P.G., Borja, F., Zazo, C., Goy, J.L., Bardají, T., Luque, L., Lario, J. & Dabrio, C.J. 2005. Archaeoseismic record at the ancient Roman city of Baelo Claudia (Cádiz, South Spain). Tectonophysics, 408: 129-146.

Silva, P.G., Goy, J.L., Zazo, C., Bardají, T., Lario, J., Somoza, L., Luque, L., & González Hernández, F.M. 2006. Neotectonic fault mapping at the Gibraltar Strait Tunel area, Bolonia Bay (South Spain). Engineering Geology, 84: 31-47.

Silva, P.G., Reicherter, K., Grützner, C., Bardají, T., Lario, J., Goy, J.L., Zazo, C., Becker-Heidmann, P., 2009. Surface and subsurface paleoseismic records at the ancient Roman city of Baelo Claudia and the Bolonia Bay area, Cádiz (South Spain). In:

Historical and Prehistorical Records of earthquake Ground effects for Seismic Hazard Assessment (edited by Reicherter, K., Michetti, A.M. & Silva, P.G.) J. Geol. Soc. London, Spec. Publ., 316, 93-121.

Spang, R. M. & Sonser, Th. 1995. Optimized rockfall protection by “ROCKFALL”. Proc 8th Int Congress Rock Mechanics, 3, 1233–1242.

Stich, D., Serpelloni, E., Mancilla, F. L. & Morales, J. 2006. Kinematics of the Iberia—Maghreb plate contact from seismic moment tensors and GPS observations. Tectonophysics 426, 295-317.

Vollmert, A. 2008. Felsstürze und hängende Täler entlang des La Laja Escarpments, Tarifa, Südspanien. Unpubl. BSc. thesis, RWTH Aachen University, Germany

Weijermars, R. 1991. Geology and tectonics of the Betic Zone, SE Spain. Earth Science Reviews, 31, 153-236.

Zazo, C., Silva, P.G., Goy, J.L., Hillaire-Marcel, C., Lario, J., Bardají, T. & González, A. 1999. Coastal uplift in continental collision plate boundaries: Data from the Last interglacial marine terraces of the Gibraltar Strait area (South Spain). Tectonophysics, 301, 95-119.

FIELD TRIP 3

QUATERNARY TECTONICS IN THE GIBRALTAR STRAIT AREA

Stops

1. Mirador del Estrecho
2. Cabo de la Plata Fault
3. Barbate tsunami deposits
4. Hotel Flamingo Fault
5. Cape Trafalgar
6. Conilete Tower tsunami deposits

Stop 1

Mirador del Estrecho (Tarifa): Introduction to Tectonics and Geology

P.G. Silva and K. Reicherter

Introduction

The Gibraltar Strait connects the Atlantic with the Mediterranean, above the convergent Africa-Eurasia plate boundary in the westernmost area of the Betic Cordilleras (S Spain) and the Moroccan Rif (NW Africa). In this area, the Africa-Eurasian plate boundary is rather undefined as manifested by scattering of earthquake foci. The continental collision zone promotes westwards by the displacement of nappes of the Betic Internal Zone. The stacking and thrusting mainly occurred during the early Miocene, including large scale folding and back-thrusts in the Gibraltar Arc (Leblanc 1990; Sanz de Galdeano 1990, Weijermars 1991). Late Neogene post-collisional convergence resulted in the development of a diffuse plate boundary of more than 700 km width, in which the Africa-Eurasia convergence was distributed through a wide range of interactive NW and SE trending transpressive and transtensive structures linked to the broad NW-SE plate convergence (Weijermars 1991; Vázquez & Vegas 2000).

The aforementioned tectonic regime is consistent with regional studies for this zone of the Betic Cordillera (Galindo Zaldivar et al. 1993; Reicherter & Peters 2005) and the entire Iberian Peninsula (Herraiz et al. 2000). SHmax trajectories, based on Plio-Quaternary deformations, borehole breakouts, focal and moment tensor solutions (Herraiz et al. 2000; Jiménez-Munt et al. 2001; Stich et al. 2003), indicate NNW-SSE-directed horizontal compressive stresses in the Gibraltar Strait area.

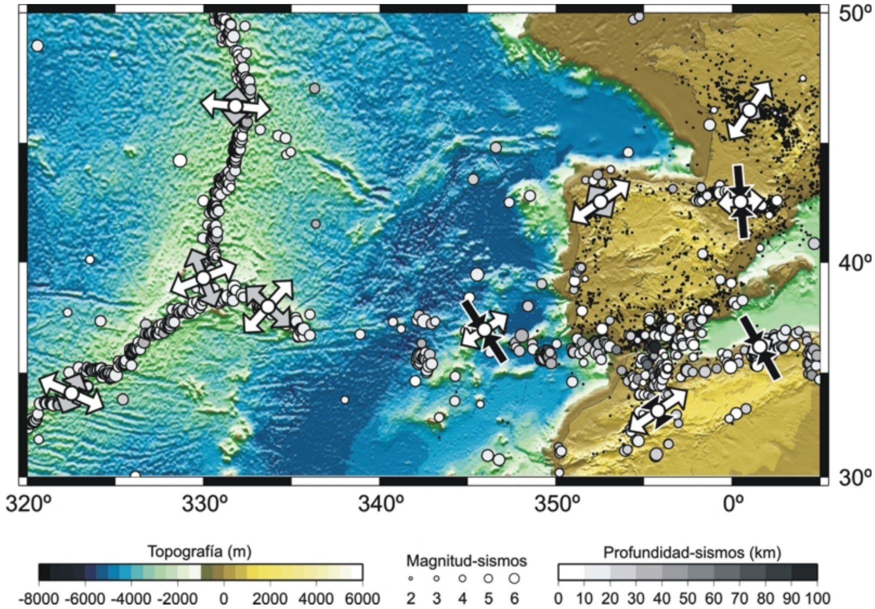

Fig. 1: Map showing the records of instrumental seismicity and broad stress orientation at the Africa-Eurasia Plate Boundary between the Mid Atlantic oceanic rise and the western Mediterranean (reprinted from Vera et al., 2003)

The Late Neogene to present Geodynamic Setting

This compressive NNW-SSE-directed stress field induces mainly a "transpressive" setting in the Gibraltar Strait Area. This is defined by the development of conjugate master strike-slip faults, trending NE-SW and NW-SE with a variety of left-lateral to right-lateral sense of displacement; Fig. 1.1). This geodynamic framework is characteristic for the whole emerged northern sector of the Gibraltar Strait (Benkehelil 1977; Goy et al. 1995; Gracia, et al. 1999), but has been also described from the African coast of Morocco (Akil et al. 1995), and deduced from the submarine sector of the Strait (Sandoval et al. 1996).

An obvious discrepancy between present plate convergence rates of 4-5 mm/yr (Noomen et al. 1993) up to 5.6 mm/yr (Jolivet et al. 1999) and estimated maximum uplift rates of 0.15 mm/yr in this zone during the late Quaternary seems to indicate that no plane-constant volume strain occurs at this diffuse plate boundary (Zazo et al. 1999). Lateral E-W expulsion/extrusion of the different crustal wedges bounded by the aforementioned conjugate set of strike-slip faults at both sides of the Strait edge would provide a plausible scenario. This scenario is particularly relevant in the Atlantic sector of the Strait, where WNW compression has been deduced (González Lastras et al. 1991; Galindo Zaldivar et al., 1993) from paleostress analysis on Late Miocene and Early Pliocene sediments.

During the Miocene (Vejer-Barbate: Atlantic littoral) and Pliocene (Algeciras Bay: Mediterranean littoral) N-S trending marine grabens formed on both sides of the Gibraltar Strait (previously emerged). These sedimentary troughs subsided in response to an E-W extension at the uppermost crustal levels driven by crustal lateral extrusion (Goy et al., 1995; Zazo et al. 1999). During the Plio-Pleistocene, Late Neogene marine deposits were uplifted and deformed in the present-day transpressive setting (Fig. 1). In the following, the subsequent Quaternary marine sedimentation was mainly restricted to the littoral areas of the Gibraltar Strait. Recent continental Quaternary sediments are well developed only in river valleys and in the fluvio-lacustrine tectonic depression of La Janda Basin (Figs. 1 and 2).

Seismic activity in the studied area

Seismicity of the axial zone of the Gibraltar Strait area (6º50'W-5º14'E / 35º50'N-36º25'N) has been described by Goy et al. (1995) and Silva et al. (2006). Only sixty six earthquakes are catalogued for the period 1750-1993 AD in this area, demonstrating a relatively low seismic activity. But, there is no historical seismic information prior to the year 1750. The archeological remains of the ancient Roman city of Baelo Claudia indicate the occurrence of severe earthquake damage from the late 1st Century AD to the late 3rd Century AD. These Roman events fall in the time-span of remote earthquakes, which probably occurred in the Gulf of Cádiz – Cape of San Vicente area between 33 AD and 382 AD (Martínez Solares & Mezcua, 2002).

Seismic data illustrate the spatial relationships between the recorded epicenters and the main Quaternary faults of the coastal zone of the Gibraltar Strait (Fig. 1). Offshore, NE-SW and N-S trending faults have been extrapolated from the onshore faults. These correspond to similarly running faults in the Bolonia Bay as deduced from high-resolution seismic profiling (Hübscher et al. 2007). Intermediate to depth (14- 60 km) moderate events (3.1-4.2 mb) have been recorded in the Atlantic sector of the Gibraltar Strait in close relationship with the NE-SW trending strike-slip fault system. This observation lead Goy et al. (1995) to catalogue this conjugate strike-slip fault system as seismic source during the late Quaternary. However, about the 95% of the instrumental seismicity of the studied zone is commonly shallow (< 10 km), weak (mb $\leq$ 3.0) and closely linked to the system of N-S trending normal faults segmenting the Betic nappes in the Gibraltar Strait region (Fig. 1). These faults are nicely represented within the Plio-Quaternary grabens of Barbate and Algeciras Bays (Goy et al 1995; Silva et al. 2006), but also in the studied zone segmenting the Cabo de Gracia and San Bartolome ranges, adjacent to the ancient Roman city of Baelo Claudia (Fig. 2).

Therefore, instrumental records demonstrate that common ongoing seismic activity at shallower crustal levels is especially linked to the set of N-S normal faults (Fig. 1), but classified as an area of low earthquake hazard (Makris & Egloff 1993). However, Silva et al. (2005) related the archeoseismic damage recorded at Baelo Claudia with the offshore activity of the NE-SW Cabo de Gracia strike-slip fault (Fig. 1.1) But, all known local historic events never exceeded VI MSK maximum intensity (Goy et al. 1995) in the Gibraltar Strait area and major offshore events produced in the Gulf of Cadiz area (i.e., 1755 Lisbon Earthquake) only reached maximum intensities of VI-VII MSK (Martínez Solares et al. 1979) or V-VI EMS (Martínez Solares & Mezcua 2002) in this zone. Moreover, relevant strong earthquakes have been recorded in the adjacent sector of the Alboran Sea East to the strait zone (Fig. 1). These events recorded maximum magnitudes of 7.2 Ms and onshore intensities of VI-VII MSK in the Malaga zone (Baraza et al. 1992), but no intensity data are available for the studied zone. This same situation occurs for the strongest historic events (VIII-X MSK), occurred in this Mediterranean sector in 1494 and 1680 AD (Martínez Solares & Mezcua 2002). In addition, the catalogued presumably strong events occurred during the Roman period (33 AD and 382 AD) in the Gulf of Cadiz – Cape of San Vicente zone are poorly documented and do not offer macroseismic intensity data for the Gibraltar Strait region (Martínez Solares & Mezcua 2002). Therefore the available seismic data does not support strong seismic damage in the Gibraltar Strait region, which is in disagreement with the archaeoseismological evidence in Baelo Claudia studied in this work.

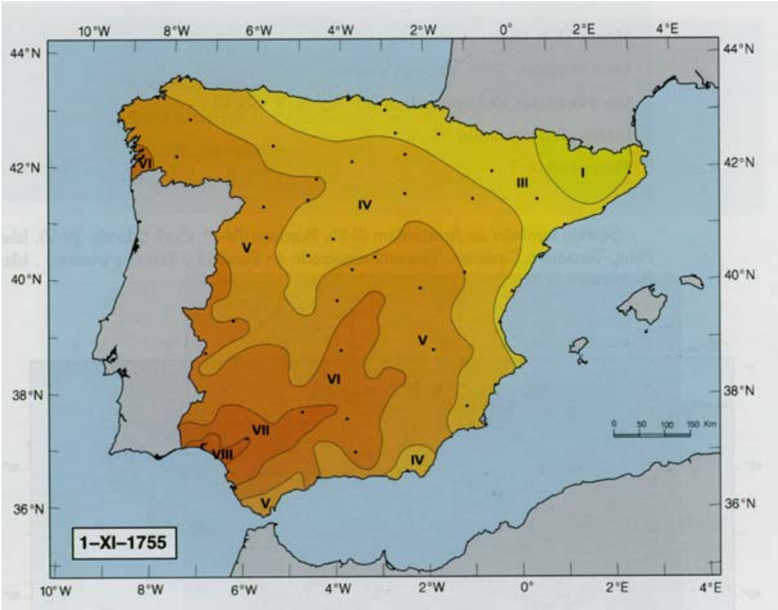

Fig. 2. Isoseismal Map of the 1755 AD Lisbon Earthquake-Tsunami event in Spain. EMS-98 intensities (from Martínez Solares and López Arroyo, 2004).

Stop 2

The Cabo de Gracia Fault (CdGF).

K. Reicherter, P.G. Silva, J.L. Goy, C. Zazo, M.A. Rodríguez Pascua, R. Pérez López, J.L. Giner-Robles and C. Grüztner

Introduction

Around the Bolonia Bay, the most extensive outcrops are the pervasively folded and tectonized Almarchal and Facinas formations (Fig. 3) of the Betic Flysch Zone in the Campo de Gibraltar. The Cretaceous to Miocene rocks form a clayey substratum in the ancient city of Baelo Claudia. These soft materials are framed horseshoe-like to the E and W by the rigid sandstones of the Aljibe formation, which are also folded and steeply dipping (almost vertical, partly overturned). Goy et al. (1995) and Silva et al. (2005, 2006) offered several paleoseismic indicators around the ancient roman city focusing in the Cabo de Gracia and Carrizales Faults, located between 5 and 10 km away east of Baelo Claudia (Fig. 2.1). Both vertical faults have a NE-SW orientation with sinistral strike-slip and minor normal displacement affecting Late Pleistocene or Pleistocene deposits. The Cabo de Gracia Fault displaces Late Pleistocene OIS 5 (Oxigen Isotopic Stage) marine deposits and the overlying dunes exhibit liquefaction structures of apparent coseismic nature (Goy et al. 1994; Silva et al. 2005). But this outcrop is actually buried and only it is possible to observe the traces and fault mirrors affecting the Aljibe sandstone bedrock at the end of the southern promontory of the Sierra de la Plata downslope the lighthouse (Figs. 3 and 4).

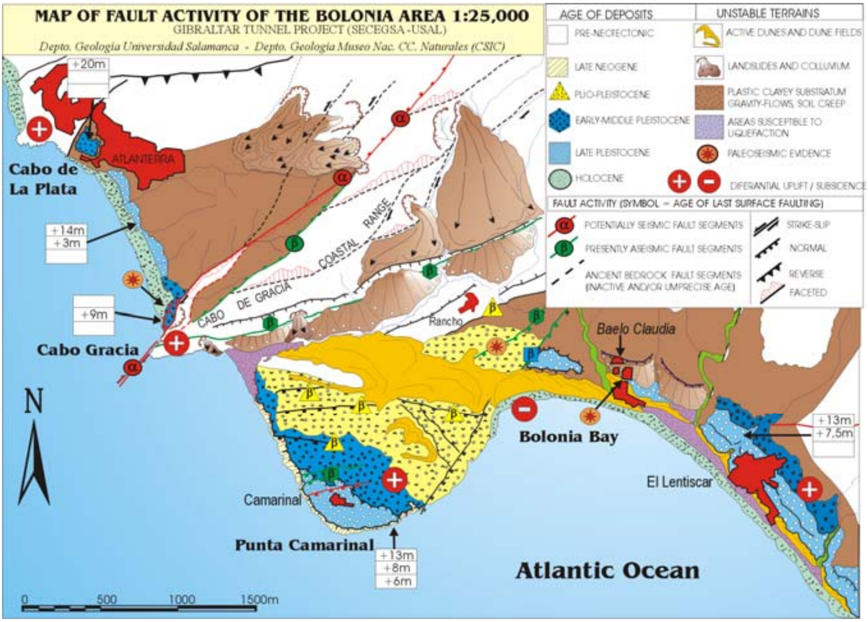

Fig. 3: Pilot Fault Activity Map of the Bolonia area produced for the Gibraltar Tunnel Project (Goy et al., 1995; Silva et al., 2006).

The Cabo de Gracia Fault zone at the promontory bedrock

The CdGF Fault primarily worked as an internal low-angle reverse fault related to the Mio-Pliocene structuration of the Sierra de La Plata (González Lastras et al., 1991). The fault-trace runs over the outer western limb of the major recumbent fold of the zone: the Bolonia Anticline (Balnayá et al., 1995). This fault has a total length of 8,65 km, and dies-out after its deflected adaptation to the E-W pericline termination of the Bolonia Anticline in its convergence with the La Janda NW-SE southern lineament (Figure1.1). Within the mapped zone in figure 2.1 the fault trace acts as an internal thrust of the Aljibe nappe, affecting different generations of fold axes generated during previous shortening phases. Towards the littoral the firmer Aljibe Sandstones override the basal plastic materials of the "Bolonia Unit" (Silva et al., 2006). The Principal Displacement Zone (PDZ) of the fault, of about 400 to 650 m wide, has a complex braided pattern. It comprises ancient reactivated betic thrust planes and folded mechanical contacts (within the Aljibe Sandstones) linked by newly generated NNE-SSW to N-S fault segments (Fig. 3). As a whole, the PDZ of the fault promotes the NE-SW trending stepped horst-like topography defining the Cabo Gracia Promontory Range (faceted range front-faults, and bedrock fault scarps) at the southern end of the Sierra de La Plata (Fig. 3).

Fig. 4: Fault Plane of the Cabo de Gracia fault affecting to the Aljibe sandstones bedrock at the southern promontory of Cabo de Gracia.

In detail, the Western flank of the Promontory Range is defined by a modest range front fault (<5m high) generated along the CdG Fault trace (Fig. 2.1). Drainage accommodates to this fault line and piedmont deposits are rare and/or limited to small-undissected colluvial wedges coating the fault plane. It essentially affects to the Aljibe bedrock materials, and consequently it is difficult to give any realistic age for the last episode of faulting, after its Pliocene structuration (Fig. 4). Striations measurements on exposed fault planes affecting the bedrock indicate a dominant right lateral strike-slip kinematics under NE-SW compresional stress-field for these older segments within the fault zone.

The Cabo de Gracia Fault zone at the Altanterra Beach

Only at the eastern end of the Atlanterra beach were documented deformations of the CdGF on Late Quaternary some years ago (Goy et al., 1994; 1995). Deformations occurred along a discrete NNW-SSE bend of the fault, late Pleistocene marine and eolian sands are deformed. These materials can be ascribed to the OIS 5 (ca. 128 – 95 ka BP) as reported by Zazo et al. (1998). They are involved in a spur-ridge of 9m of elevation topped by a more recent alluvial gravel-level that displays antiform-like upwarped geometry and seal the deformation. This spur ridge has a positive flower internal structure, defined by NNE-SSW reverse faults with an upwards fan-like arrangement (Fig. 5) and displaying soft-sediment deformation structures near the spur-ridge top affecting to the upper dune deposits (Silva et al., 2006). These soft-sedimentary deformations are closely related to the fault traces along which water escaped generating this deformational assemblage (Goy et al., 1994, 1995).

A relatively thin alluvial gravel level (down to 1.5m thick) is the unique deposit actually burying the described deformations. Therefore, no relevant sedimentary overburden processes can be invoked, and on the contrary they were characterized as earthquake-induced liquefaction features as initially reported by Goy et al. (1994). On the basis of liquefaction literature Silva et al. (2006) suggested that a moderate event (M 5 – 5.5) on the fault trace could generate these secondary deformations.

At present coastal erosion and gully incision removed most of the ancient outcrop and these soft-sediment deformations can not be observed.

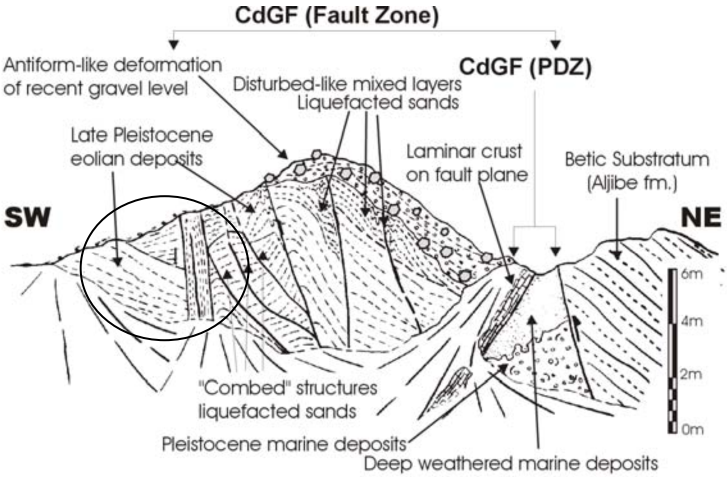

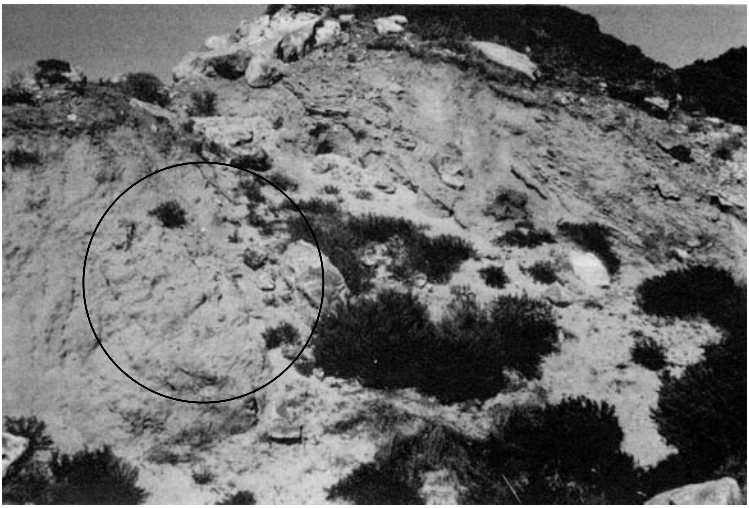

Fig. 5: Upper Geological cross-section showing the spur-ridge internal structure and soft-sediment deformation structures of Late Pleistocene deposits (OIS 5) on the coastal segment of the Cabo de Gracia Fault (from Silva et al., 2006). Lower: Original photography of the outcrop in 1992. Note banded liquefaction structures and minor faults in the encircled area (from Goy et al., 1995)

Faulting geometry and general arrangement of deformations allowed to assess the restraining nature of the intervening fault bend, the transpressive nature of the deformation, and consequently the "reversed" right-lateral kinematics of this NE-SW fault segment during the Late Pleistocene (Fig. 3). Similar reversal of the uplifting-subsiding trends of the crustal blocks separated by the CdGF can be deduced from the spatial-height analysis of the OIS 5 raised marine deposits developed by Zazo et al. (1998). Nowadays, coastal sectors separated by the CdGF, record an accumulated relative vertical offset of at least 5±0.5m since the deposit of the OISS 5c sediments (95 ka BP), indicating a relative uplift of the eastern overriding block of the fault which is in keeping with the present topography. On the contrary, the comparison of differential uplift recorded between the OISS 5e (128 ka BP) and 5c (95 ka BP), indicate a radical opposite behavior previous to the OISS 5c with a relevant uplift of ca. 6m of the present western downthrown block of the fault (Fig. 3). The relatively short time interval in which faulting reversal is achieved (ca.33 ka BP) strongly suggests that recurrent coseismic uplift, rather than a continuous one, occurred along the trace of the CdGF (Silva et al., 2006).

Although no relevant instrumental seismicity is recorded at this area (Fig. 1), the recorded post-OISS 5e liquefaction structures and the regional spatial displacements of the last interglacial deposits (Zazo et al., 1998) suggest the potential seismic character of the CdGF as mapped by Silva et al. (2006). Last reactivation along this more recent coastal segment of the fault zone is certainly younger than ca. 128 ka BP, but from the available data it is still impossible to give a more precise age-bracketing.

Stop 4

Tsunami deposits along the coast between Zahara and Barbate

K. Reicherter, D. Vonberg & B. Koster

Introduction

On November 1st, 1755 at 9.40 a.m. one of the most remarkable and destructive earthquakes occurred in the East Atlantic Ocean off Portugal, leaving Lisbon and other cities completely destroyed. The tsunami triggered by the earthquake devastated the entire Atlantic coastline from central Portugal far down south to Morocco; also parts of the Atlantic archipelagos of Madeira, Azores and Canaries were affected (Bryant, 2007). A vast amount of literature has been published on the seismogenic sources and, economic and societal consequences of this earthquake (e.g. Bryant, 2007, Baptista et al., 1998), as well as reports on the wave action of the tsunami (see Kortekaas and Dawson, 2007) and, also the wide-spread and highly variable deposits of the tsunami (e.g., Dawson et al., 1995, Dabrio et al., 1998; Hindson et al., 1999; Luque et al., 2001, 2002; Alonso et al., 2003; Whelan and Kelletat, 2005; Gracia et al., 2006; Becker-Heidmann et al., 2007; Kortekaas and Dawson, 2007; Mhammdi et al., 2008).

The Gibraltar-Azores major fault and plate boundary between the African and the Eurasian plates has produced several tsunamis in historical times, e.g. in 218 BC/216 BC, 210 BC, 209 BC, 60 BC, 382 AD, 881 AD, 1531 AD, 1731 AD, 1969 AD (after Bryant, 2007). However, sedimentary evidence has been provided only for an event with an age of approx. 2300 y BP in the Valdelagrana area near Cádiz (Luque et al., 2002). These authors argued that the extend of the 2300 y BP tsunamite, the impact and the morphological changes along the coast are of a comparable intensity and magnitude of the Lisbon 1755 tsunami. Remains of the other tsunami events have not been found to date, which is important to note, because the age assessment of the layers we are going to describe in this study is relative and refers only to the youngest preserved tsunamites.

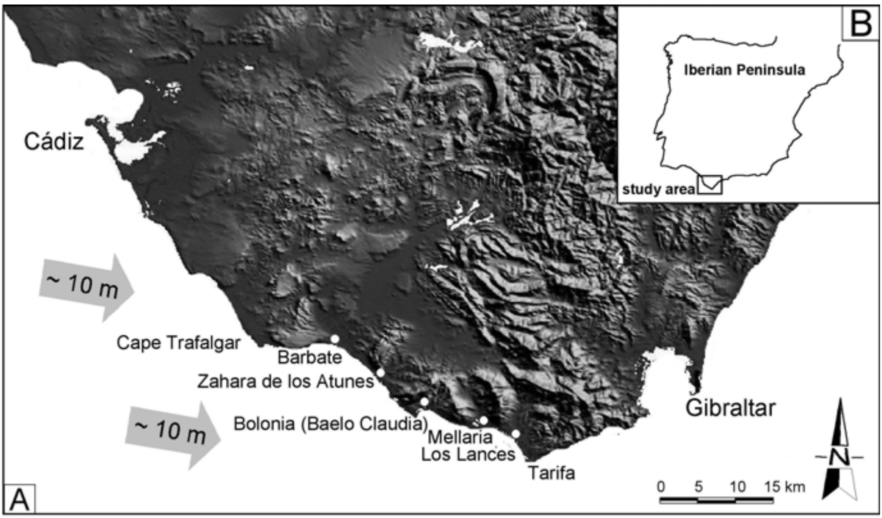

Fig.6: A. Topographic map of the excursion area in southern Spain and studied localities; arrows indicate direction of tsunami waves of the 1755 Lisbon event, numbers give vertical run-up (modified from Gracia et al. 2006). B. The study area in southern Spain.

We will not discuss the cause and source of the Lisbon 1755 event, but we need to keep in mind some observations during the event: in Lisbon harbour 18 individual waves have been described, probably secondary waves generated by reflections in the estuary setting of the Tejo river. Along the Algarve coast sedimentary evidence for three major waves has been found by Kortekaas and Dawson (2007), and was clearly distinguishable from storm deposits. The historically reported wave heights vary significantly along the coast: Lisbon 6-20 m; Cabo São Vicente 15-30 m; Algarve 9-13 m; Cádiz and Huelva 4-20 m; Tarifa 11 m; Gibraltar 2 m; Tangiers 10 m (data and references in Whelan and Kelletat, 2005). At Cape Trafalgar, boulder deposits have been described in a height of 19 m a.s.l. and attributed to the Lisbon 1755 event. The entire tombolo of the Cape Trafalgar was most probably completely washed over by the tsunami (Whelan and Kelletat, 2005). All these descriptions suggest that the coastline between Barbarte and Tarifa was hit by at least one historic tsunami with a considerable vertical run-up (ca. 10 m) and accompanied by far reaching horizontal ingressions in the marshlands (Fig.6). The mean tidal range in this area of the Gulf of Cádiz varies between 1.5 and 2.39 m, mean spring tidal level is 3.71 m (Gutiérrez-Mas et al., 2003). Rare winter storms have been observed with around 1.5 m wave height (Gracia et al., 2006).

Historical tsunamis along the Gulf of Cádiz

The Gulf of Cádiz and the Portuguese and Spanish coasts are a classical European site for tsunami deposits. Earlier works provide evidence for the 1755 Lisbon tsunami at the Valdelagrana spit bar near Cádiz, where wash-over fans have been recognized (Luque et al., 2002). Also, Luque et al. (2002) found evidence for an older, Roman tsunami (2.300 yr BP) in the same area. Whelan and Kelletat (2005) described larger boulder deposits at the Cape Trafalgar, and attributed those to the 1755 Lisbon tsunami (as we can visit on **Stop 5**). The same deposits were interpreted by Gracia et al. (2006) as tsunamites, and they described a run-up height (vertical run-up) of > 19 m in that area. Further south in the Bolonia Bay, Alonso et al. (2003) described wash-over deposits in the Arroyo de Alpariate with an age of 2.150-1.825 yr BP. Later, Becker-Heidmann et al. (2007) have dated huge sand deposits (at about 4 m above mean sea level) and interpreted those as probable tsunamigenic sediments. However, the charcoal yielded ages of 455 – 475 ±35 BP, and are approximately 200 years older than the Lisbon event. Possibly, the charcoal has been reworked during wave action. Other tsunami deposits in the Bolonia Bay were described by Gracia et al. (2006), which constitute “block fields”. These block fields have unfortunately not been dated. Near Tarifa, in the Marismas of the Río Jara, historical damage of buildings (bridges) and geomorphological and geological mapping of Gracia et al. (2006) evidenced as well deposits - here wash-over fans - of the Lisbon tsunami. Also, these deposits were not yet dated.

Marismas de Barbate

The marshlands of Barbate (Marismas de Barbate, Fig.7) have only little elevation of about 0 to 1 m above mean sea level and are flooded permanently by the tide. The salt marsh is intensely influenced by human activity and alteration (Muñoz-Pérez et al., 2002). In the meantime, a project for the restoration of this unique faunal and floral refuge closed down an open garbage dump was very successful. The plain flat area with tidal channels serves as an ideal tsunamite reservoir. Three cores were drilled with depths of > 5 m. Drill cores 7 and 8 were successful; a third site in the ancient garbage dump was stopped after 4 m, because of recent anthropogenic material in the core (plastics and glass shards), and failed. The cores in the liners were subjected to magnetic susceptibility measurements and grain size analyses.

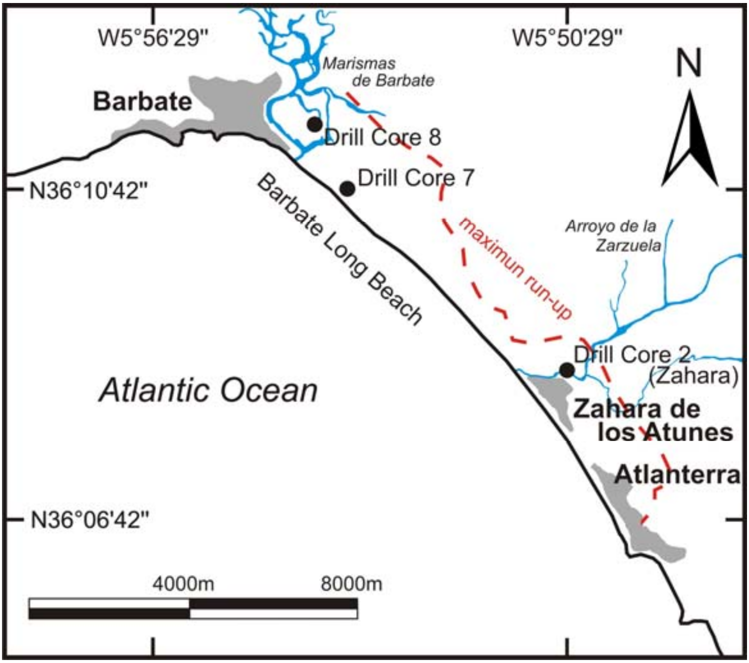

Fig. 7: Location map of the drilling in the Marismas de Barbate, including the beach sections (stippled box, see Figs. 6 and 7). For location see Fig.1. Red line indicates max. horizontal run-up based on topography and drill core evidence.

Three fining-up and thinning-up sequences are detected between 1.64 and 1.95 m in core 7 (Fig. 8a, legend in Fig. 8b), all with erosive bases. A variety of benthic and planktic foraminifera from different bathymetric depths have been found in the sieve residues. Also, coastal shallow-water fauna, like lamellibranches and gastropods are contained, partly broken. In summary, the sedimentary inventory of cores 7 and 8 provided evidence for tsunamigenic layers, in core 8 most probably two subsequent sedimentary events layers have been encountered. Age dating of charcoal and biogenic material is currently in progress.

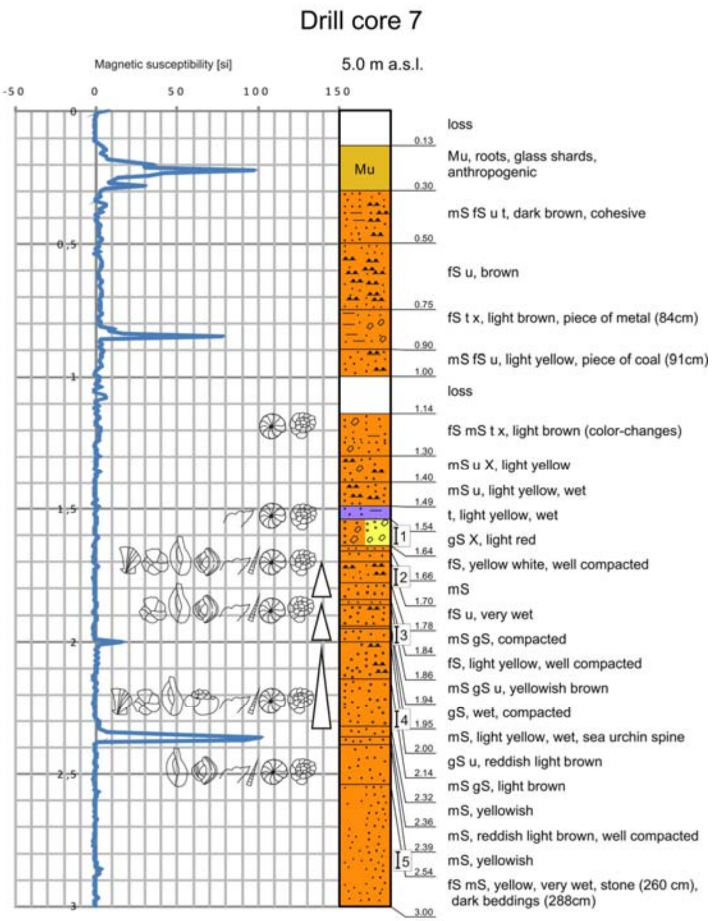

Fig.8: a) Litho-log of drill core 7 (location in Fig.7), numbers on the right side indicate sample intervals for grain size analysis and wash samples, the blue line is the measured magnetic susceptibility.

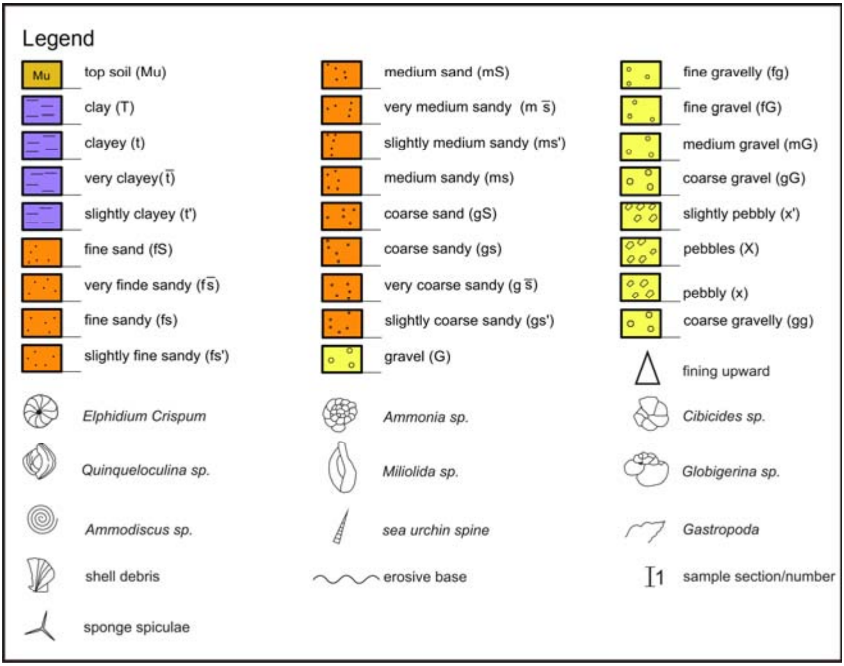

Fig.8: b) legend for the drill cores.

Tsunami deposits in the Beach section between Barbate and Zahara de los Atunes

The 5 km long rocky cliff has been mapped, leveled and sampled. We have surprisingly found only one sedimentary layer on top of the basement at the cliff, in varying altitudes between 1 and 4,5 m above mean sea level (Fig.9). The basement consists of Cretaceous to Eocene flysch deposits (mainly variegated marls and sandstones) or OIS 5 terraces (Tyrrhenian) of approx. 125 kyr (brownish calcarenitic sandstones). The dark sandy layer of about 1 m thickness constitutes a fining-up sequence with a coarse-grained base with conglomerates, shell debris and charcoal (Fig.10c). These deposits are channeled (Fig.10a), and clasts are imbricated (Fig.10b), paleo-flow direction is towards the Atlantic. As the beach sands are white to yellowish (Fig.9), and the layer is dark, organic- and clay mineral-rich, but sandy, with shell debris and well-rounded cobbles of the basement. Detailed litho-logs of the layers above the basement and samples at four localities along the coast have fining-up layers with varying thickness, the event layer usually consists of one fining-up cycle and is between 1.25 and 0.56 m thick. The base of the layer is made up of coarse-grained material and contains large shells (*Cardium* sp., *Glycimeris* sp., gastropods) and subangular to rounded sandstones of the basement and brownish calcarenites of the OIS 5 terraces.

Fig.9: Coastal cliff between Barbate and Zahara de los Atunes (see Fig. 1), dark layer on top of the Cretaceous-Eocene Betic substratum is a tsunami event and represents most probably back flow deposits, possibly that of 1755. Height of the cliff is about 4.5 m above mean sea level. Note the color difference between the modern beach (white) and the cliff top section (black).

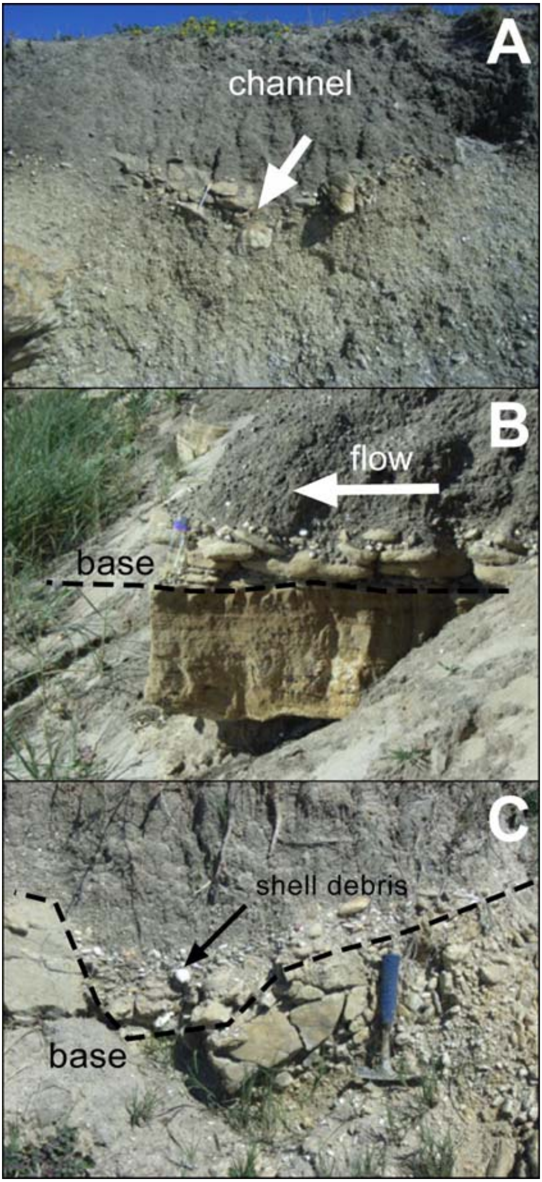

Fig. 10: Cliff section in detail of location in Figs. 7 and 9. A. channeled back flow with coarse-grained basal deposits. B: imbricated clasts in the back flow indicate paleocurrent towards the sea (left). C: shell debris and conglomerates in the back flow sediments.

To determine and compare the elevation of the tsunami deposits, line leveling was performed at four sections of the cliff. These profile show that the tsunami deposits are not at one level, but seem to fill and follow a paleorelief (a small channel), which resembles to today's topography. Anyhow, the thickness of the post-tsunami sediments (dune sands) is quite similar at the different sections. Local differences may result from earthworks in connection of the military road with support lines and water tubes close to the cliff.

Interpretation: we interpret this layer as a back flow deposit. Paleo-current directions endorse these observations and the evidence that only one layer is preserved. Presumably, former tsunamites were eroded due to multiple wave action and the cliff was "cleaned" to the basement by the waves. The tsunamite has reworked the dark clayey marshlands of Barbate and was deposited as a mixture of beach sands, boulders, shells and the clayey marsh deposits during the back flow of the last major wave. The Flandrian transgression had a maximum at about 7.000-6000 yr BP and reached altitudes of 1 m above the present sea level in the Gulf of Cádiz (Somoza et al., 1997; Zazo et al., 2008) and cannot therefore account for these deposits. The interpretation of the principal sediment-depositing mechanisms effective in tsunami surges is based on field observations of deposit geometry and internal sedimentary characteristics, which are clearly not related to a beach, neither to a lagoon. This is evidenced by the fact that lateral changes in characteristics of depositional facies are common and abrupt (channels) and show erosive bases, normal grading or fining-up. The tsunamite deposit is clast-supported, polymodal, basal boulder-bearing and composed mostly of well-rounded clasts and fewer angular clasts, partly imbricated pointing to paleo-flow direction towards the Atlantic. The clay to sand-sized, bioclastic (and Roman ceramic)-rich matrix is poorly sorted, implying that soft sediments eroded at the lower erosional surface contributed to the tsunami deposit, suggesting mixed sources of sediments (beach and marshes). Additionally, the faunal content in the wash samples is not typical for a lagoon, rarely ostracods are found. The majority of faunal components are shell debris, planktic and benthic foraminifera and reworked Tertiary and Cretaceous species of the basement. Dating of the suspect tsunamigenic layer is in progress, based on charcoal findings and closed bivalve shells (may indicate a sudden death due to an event, usually lamellibranchs disintegrate shortly after death into two shells).

Stop 4

The Hotel Flamenco Fault (Conil): Late Pliocene – Early Pleistocene faulting in the Gibraltar Strait.

P.G. Silva, J.L. Goy, C. Zazo, J. Lario, T. Bardají, M.A. Rodríguez Pascua, R. Pérez López, J.L. Giner-Robles and A. Cabero

Introduction

In the Atlantic sector of the Gibraltar Stratir NW-SE and NNE-SSW to NE-SW strike slip faults are common structures implied in the development of the landscape since Late Neogene times. The best outcrops are always located along the sea-cliffs carved on Miocene to Plio-Quaternary marine and littoral deposits of this area affected by NE-SW left lateral strike-slip faults. From East to west these faulted outcrops are, Barbate Cliffs, Caños de Meca (East Trafalgar), Conil, Torre del Puerco, San Fernando and Puerto de Santamaria (Benkhelil, 1977; Goy et al., 1995; Gracia et al., 1999, Silva et al., 2006).

From the End of the Miocene the nearly NNW-SSE compression between the African and Eurasian plates originated the tectonic uplift and emergence of this sector of the Betic Cordillera accompanied by a relevant secondary E-W extension. This last lead the development of relevant N-S trending grabens (Algeciras Bay and Vejer-Barbate troughs) filled by deltaic deposits feed by the first emerged reliefs to the North. Similar deltaic environments were common in the westernmost Atlantic sector of the Strait (up to the Cádiz Bay), giving place to thick Late Miocene-Pliocene detritic sedimentary sequences assembling fluvio-deltaic to nearshore bicocalstic littoral materials (Benot et al., 1993; Aguirre, 1995). The Upper Pliocene – Early Pleistocene sedimentary sequence culminates with a regressive episode of coarse-grained biocalstic deposits of fluvio-deltaic to estuarine-bay nature called “Roca Ostionera” in the whole Cadiz littoral sector (Benkhelil, 1977; Zazo and Goy, 1990; Benot et al., 1993). This deposit is rich in pectinic and ostrea littoral fauna with *Callista chione*, *Pecten jacobaens*, *Chlamys labnae* and *Pycnodonta cochelar* (Zazo and Goy, 1990). The following littoral deposits only record the well preserved set of Pleistocene marine terraces and related dune deposits, linked to the continuous Quaternary uplift of the Gibraltar Strait zone (Zazo and Goy, 1990; Goy et al., 1995; Zazo et al., 1998).

In the aforementioned outcrops the set of NE-SW strike-slip faults clearly affects to the "Roca Ostionera" deposits, leading the Early Pleistocene dating for faulting (Benkhelil, 1977). However the spatial-height analysis of Late Pleistocene marine terraces (Zazo et al., 1998) and some radiometric dating available for the Cadiz Bay sector (Gracia et al., 1999) corroborates the continuous activity of these faults during the Pleistocene.

The Hotel Flamenco sedimentary sequence

The sequence of deformed Late Neogene to Quaternary deposits outcropping in the NW-SE trending cliffs in the Conil beach are sketched in Fig. 11. The Late Neogene sedimentary sequence outcropping at the cliff is the following one:

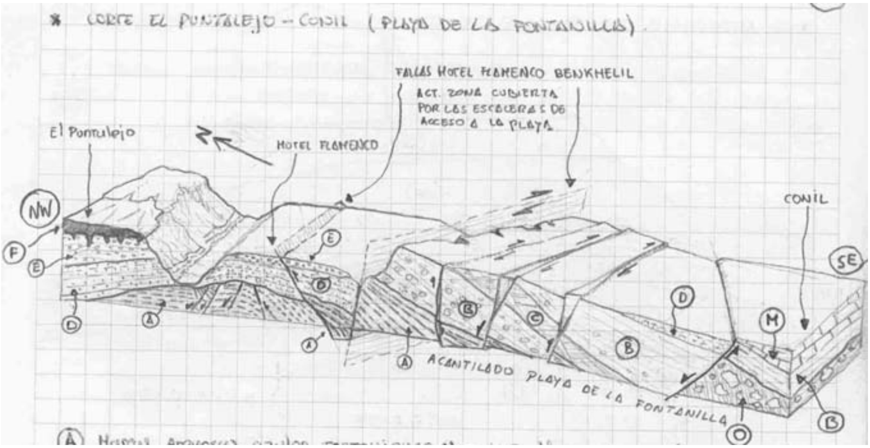

Fig. 11: Original field-sketch of P.G. Silva (1998) displaying the measured deformations and Late Neogene to Quaternary materials outcropping between La Fontanilla Beach (Hotel Flamenco Site) and the Conil village beach as viewed from the sea.

A. Upper Tortonian – Messinian Blue sandy marls with a maximum outcroping thickness of 0.8-0.9 m only visible during low-tide conditions at the Hotel Flamenco site. In this outcrop delineates a nice NE-SW periclinal termination also visible at the lowest-tide moments.

B. SE dipping siliciclastic sands affected by concentric boulder-like weathering with interbedded calcarenite levels (C). This thick sedimentary sequence represents a deltaic front and holds diagnostic microfauna (*G. acostaensis* and G. *plesiotomida*) of the Messinian (Benkhelil, 1977). The topmost of the sequence is sealed by an erosive level of bioclastic calcarenites (M) outcropping at the Conil village.

C. Bioclastic calcarenites with planar and through cross stratification. These outcrop at interbeded fine to 3-4 m thick levels in the deltaic front sequence (B) and represent subtidal littoral bars affected by festoon stratification and water escape structures (García de Domingo et al., 1990).

M. Bioclastic calcarenites with planar and through cross stratification with diagnostic microfauna (*G. menardi, G. sticula, G. bulloides, G. falconensis* and *G. riveroace*) representing the Messinian – Early Pliocene transit (Garcia de Domingo et al., 1990).

The Pliocene to Early Pleistocene sequence is represented by the Unit D.

D. Yellow bioclastic calcarenites with planar and through cross stratification. This unit is composed by 1,2 – 2,5 m thick strata with fining upwards sequences and fine laminated stratification representing littoral bars. This unit comprises the Early-Middle Pliocene and the Late Pliocene unit described by Aguirre (1995) for the Atlantic Pliocene materials of the Cadiz littoral. These units are separated by a characteristic level of bioturbation affected by characteristic *Thalassinoides* burrowing. The Late Pliocene unit displays levels of soft-sediment deformations (convolutes and pseudonodules) presumably originated by water escape process.

E. Roca Ostionera representing the establishment of regressive estuarine-bay environments in the zone from the Early Pleistocene. This deposit gives place to extensive marine platforms in the Cadiz littoral affected by intensive karstification after its uplift. Pleistocene red clayey-sands seal and fill all the karstic features (tubes, chimneys, pockets, etc.). At present the outcropping roca ostionera at the Hotel Flamenco zone is difficult to see due to urban development.

Finally the older materials ocutcroping along the Conil Cliff are the Lower Miocene olisthostromic unit (O) build up during the final phases of Betic nape emplacement. Its tectosedimenary development was correlative to the flysch unit of the El Aljibe Sandstones (García de Domingo et al., 1990). This unit only outcrop in the Conil Village and is constituted by a chaotic ensemble of blocks embedded by a plastic clayey matrix.

The Hotel Flamenco Fault and anticline

The whole described sequence is gently deformed by the NE-SW anticline described in the basal unit A (Blue sandy marls). Pliocene Calcarenites of unit D display gently dipping (12-18º) opposite NW and SE orientations. Internally the unit A is affected by a variety of N 112-120E and N150-157E normal and reverse faults depicting a complex horst and graben structure within the anticline core. This anticline deformation is probably linked to the activity of the WNW-ESE right-lateral strike-slip fault described by Benkhelil (1977). This fault is illustrated in the sketch of Fig. 12 describing the mechanical contact between the deltaic deposits of unit B and the Pliocene calcarenites of unit D west to the Hotel Flamenco. Today the outcrop described by Benkhelil (1977) is difficult to see due to vegetation and urban development. However the entire unit B is affected by large N 120-125E subvertical faults (Fig. 13) similar to that described by Benkhelil (1977). All these faults display clear right-lateral strike slip behaviour.

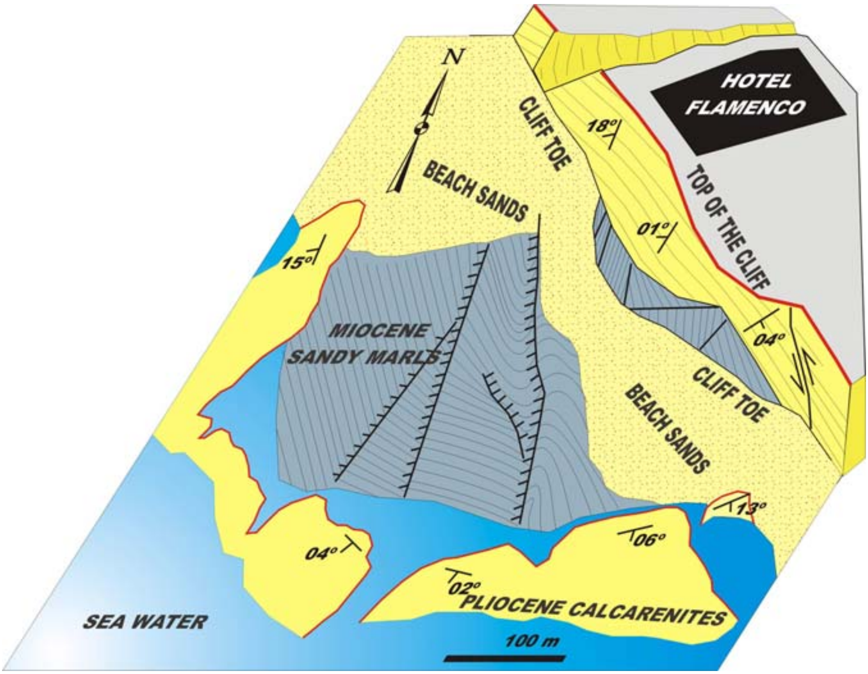

Fig. 12: Perspective view of the Hotel Flamenco zone, illustrating the plan-view arrangement of the periclinal termination of the anticline affecting to the Miocene and Plio-Pleistocene deposits.

In the eastern limb of the anticline structure some smaller N69-87 E reverse faults dipping 23 to 34º SE clearly affect the Late Pliocene calcarenites indicating the post-Pliocene activity of the faults (Fig. 13). Associated fault throws range from 0.64 to 1.4 meters diminishing upwards along the fault planes.

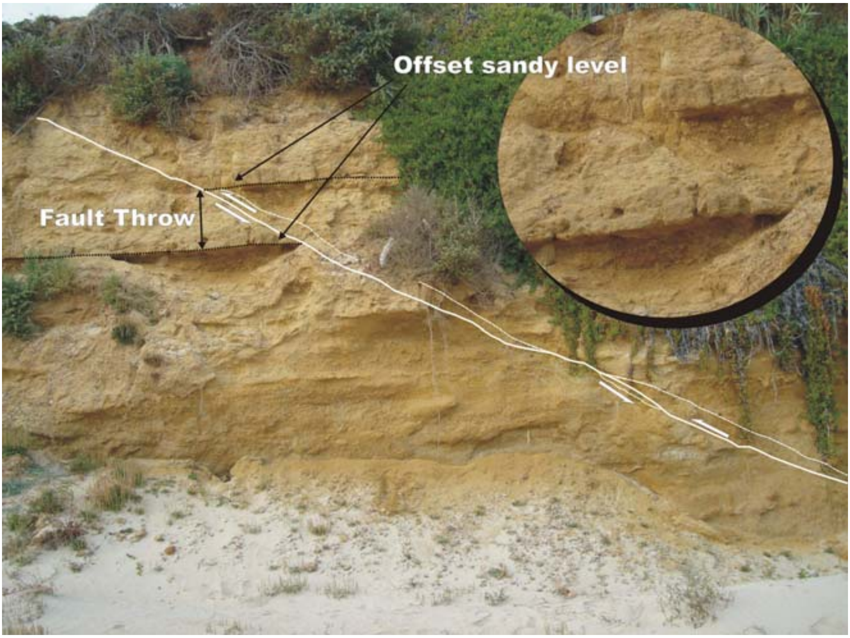

Fig. 13: Hotel Flamenco Fault affecting to the Late Pliocene calcarenites. Close-up view of offset sandy levels from which is possible the establishment of minimum fault-throw values.

Stop 5

Geomorphologic setting and 1755? tsunami deposits at Cape Trafalgar

A. Cabero , J. Lario , C. Zazo, J.L. Goy, C.J. Dabrio, F. Borja, E. Roquero, P.G. Silva, A. Garcia-Blazquez, T. Bardají, C. Hillaire-Marcel and N. Mercier

Introduction

Geomorphologic mapping of Quaternary units, stratigraphy and facies analyses, sedimentology, paleontology, and neotectonic studies in the Trafalgar area began in the early 1980's (Zazo, 1980). Later, dating methods (C-14, U-Th and OSL) provided a more accurate chronology of marine and terrestrial deposits that were published accordingly (Goy et al. 1995; Lario, 1996; Zazo, 1999, 2008a and b; Cabero 2009).

A summary of the coastal records of the 1755 tsunami waves along the Cadiz coast was presented by Gracia et al. (2006). At Trafalgar site, Whelan and Kelletat (2003, 2005) meticulously mapped and analyzed the tsunamigenic deposits, as well as Alonso et al. (2004).

Fig. 14: Tombolo of Cape Trafalgar (Ministerio de Medio Ambiente)

Geomorphologic setting and Quaternary deposits

Cape Trafalgar (36^{o} 10' N and 6^{o} W) is a double tombolo (Fig. 14), with two sand barriers that enclose a wide, shallow depression largely filled by silts and aeolian sands. The western barrier (Zahora beach) and the western flank of the rocky headland face the Atlantic swell and storms, and breaking wave heights reach up to 4 m during extreme storm events. In contrast, the eastern barrier (Playa del Varadero) faces a low energy, sheltered area where refracted storm waves hardly reach one meter (Gracia et al., 2006.). The mean tidal range is ~2m.

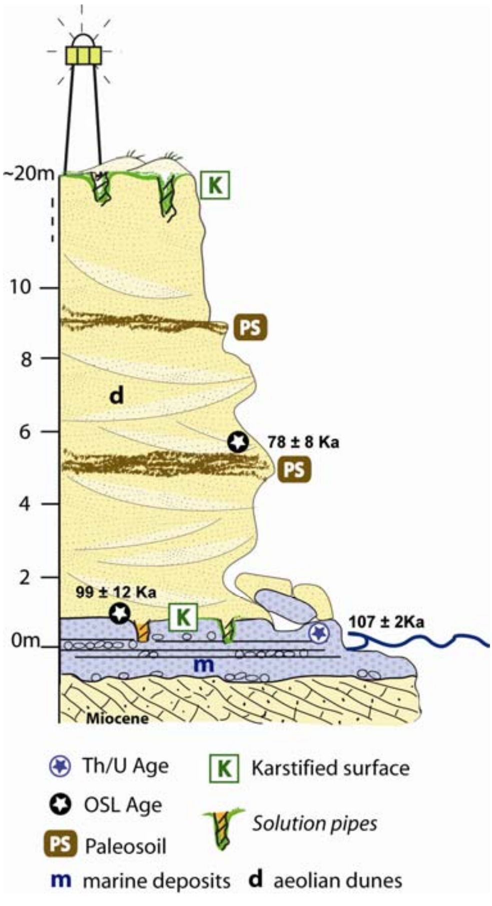

Fig. 15: Stratigraphic column of the Quaternary deposits at Cape Trafalgar (modified from Cabero, 2009)

The poorly cohesive headland of Trafalgar consists of Pleistocene cemented sediments that rest unconformable on a Messinian basement made up of biocalcarenites and silts that extends along the coast from Trafalgar to Barbate, some 10 km to the east. The up to 20 m thick sedimentary succession includes two major units in ascending stratigraphic order: marine and aeolian deposits well exposed in the lighthouse section (Fig. 15 and 16).

Fig. 16: Panorama of the Cape Trafalgar (**m**): M 5.5 marine deposits, (**d**) aeolian deposits

Marine deposits (**m** in Fig. 15 and 16) are cemented fossiliferous conglomerates of beach facies. Macrofauna remains include: *Ostrea*, *Glycymeris* and *Acanthocardia*. Unfortunately, intense calcification prevents more detailed, specific, determinations. Marine deposits are crisscrossed by two sets of joints with predominant N120^0-140^0 and N80^0 orientations. In Trafalgar site, the maximum elevation of this conglomerate is about 1.5-2 m, but the inner edge of the Pleistocene beach representing the transgressive maximum rises to 3.5 m a.s.l. (above mean high tide level) in Meca and 5m a.s.l. at El Elevador (near Barbate).

U-Th and OSL measurements of these deposits yielded ages (107+/-2.0 to78.3 +/-3.1 Ka U-Th ages, and 113+/-10 to 62+/-8 Ka OSL ages) pertaining to the Last interglacial period (MIS 5). Integrated facies analysis of marine and terrestrial deposits between Trafalgar and Barbate suggests that the beach deposits represent the second highstand of MIS 5 (MIS 5.5, ~120 Ka). The cemented marine deposits are topped by a karst surface (**K**, in Fig. 15) with solution pipes (Fig. 17) mostly devoid of the original calcarenitic filling (Fig. 18).

At Trafalgar, the karst surface is covered by weakly cemented bioclastic aeolian dunes accumulated under prevailing easterly winds. The surface can be followed further to the east, to Meca and Barbate, where it is overlaid by a red paleosoil.

Fig. 17: Cylindrical pipes on the conglomerate, with crust coating the inner wall of the pit. Fallen block.

Fig. 18: Cylindrical pipes with calcarenitic filling in the marine conglomerate. Present intertidal platform.

Rhizocretion horizons (**PS** in Fig. 14) interbedded in the aeolian sands are interpreted as paleosoils marking cessation of sand accumulation during wetter periods. A new karst surface, including cylindrical solution pipes more than one metre deep, tops the overlying cemented aeolian dunes. The inner walls of pipes are coated by calcrete with laminar crusts (Fig. 19 a, b, and c).

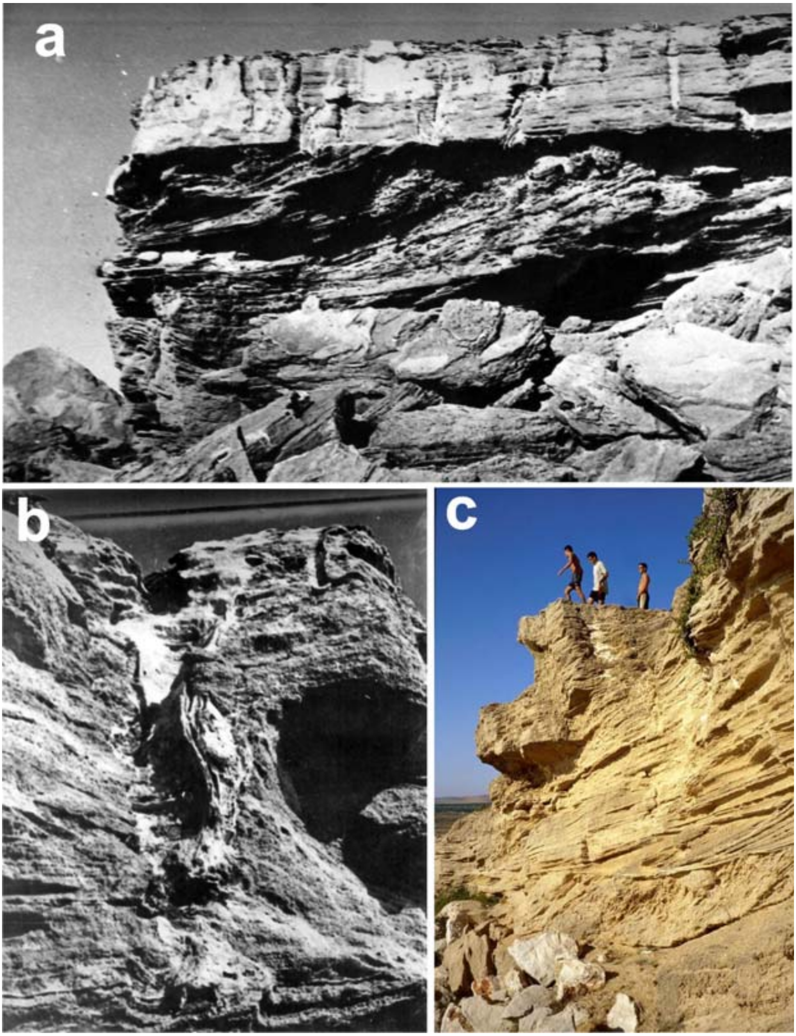

Fig. 19: a) Solution pipes on the top of aeolian deposits (year 1980, foto by C. Zazo); b) Solution pipes on the top of aeolian deposits (year 2002); c) Crust coating inner wall of the pit (year 1980, foto C. Zazo).

These karst features (rhizocretions inside the pits, cylindrical pipes and calcretes) are very much alike those described by Caron et al. (2009) in Late Pleistocene deposits of Crete and other sites along the Mediterranean coasts. According to these authors, the karst surface generated under a soil covering carbonate marine and aeolian sediments. The epikarst is related to solution by meteoric waters percolating downward through a vegetated soil cover. After this solution phase, "terra rossa" filled the pits under a wetter climate. Later formation of calcrete took place under more arid conditions favoured by waters that percolated preferentially the hollows between the host material and the red soil.

OSL data indicate that dune accumulation began during the last Interglacial (99+/-12 Ka) and extended during OISs 4, 3, and, probably, even during the early part of OIS2. In any case, more data are required to evaluate more precisely the time required to develop such epikarst surfaces.

The intertidal abrasion platform

At present the marine platform exhibits several erosive and bioconstructive features: *ring-like carving* in the marine conglomerate can be observed in the higher part of the platform (Fig. 17, 18 and 20). Whelland and Kelletat (2005) ascribed these features to a roman quarry for pillar sections and millstones, but Gracia et al (2003, 2006) suggested that the ring marks were carved during Middle Ages (11^{th}-12^{th} centuries), when a Muslin city "Becca" existed around one kilometre to the east of Trafalgar Cape. According to these authors, only small fisher settlements and related fisheries, but no major Roman cities, have been discovered in the area, but Amores (1978) describe the remains and structures of a large salt-fish factory in the cape and 500 m away.

In our opinion, at least some of the ring-marks correspond to the remains of the paleokarst developed on marine deposits. Partly eroded solution pipes, filled with calcarenites can be observed still. Wave-moved pebbles and small boulders came to rest inside the pipes, between the host rock and the calcarenitic filling, accelerating the radial enlargement of the rings (Fig. 17).

Other features relate to bioconstructional polygonal forms made by barnacles and vermetid gastropods (Fig. 21).

Fig. 20: Ring-like carving in marine conglomerate. Intertidal plataform.

Fig. 21: Bioconstruction of vermetids and barnacles developed in the Intertidal platform. At the end are visible large polygonal boulders.

Extreme Wave Events (EWE) at Cape Trafalgar

Around Cape Trafalgar it is possible to observe unusually large boulder deposits, some of theme imbricated. These deposits have been studied in detail by Whelan and Kelletat (2003, 2005) and Alonso et al. (2004), assigning always a tsunamigenic origin related with the 1755 Lisbon earthquake.

The deposits described by these authors are (Fig. 22):

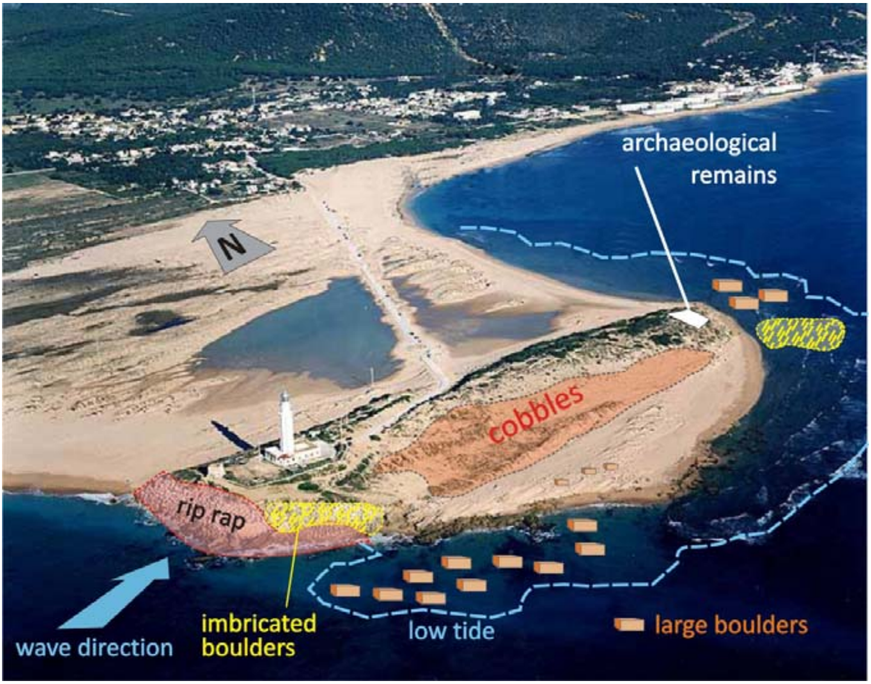

Fig. 22: Features of EWE deposits around Cape Trafalgar (data from Whelan and Kelletat, 2003, 2005; 50 by Alonso et al., 2004; aerial picture from MMA).

- large boulders located on the intertidal platform: There are a large amount (80 by Whelan and Kelletat, 2003, 2005; 50 by Alonso et al. , 2004) of large boulders between 10 to 100 tons, that lie on the marine platform located to the south and east of the cape. Most of the boulders are part of the marine conglomerate that constitutes the platform. There is no mark of recent movement of the boulders, but the presence of bioconstructions of vermetids and barnacles can difficult to observe it (Fig. 21).

- imbricated boulders (Fig. 23): Near 400 imbricated blocks between 1 to 10 tons have been recorded between high tide water and 5 m above (op.cit.), most located at the south, but near hundred of these at the east side of the cape. Most of the imbricated boulders were aligned perpendicular to the direction of transport (Whelan and Kelletat, 2003).

Fig. 23: Imbricated boulders around Cape Trafalgar

- cobbles and boulders on the cape platform: well rounded cobbles, and some boulders, mainly composed by tertiary sandstones and eolianite, can be observed almost to 16 m height. It is important to note that there is no remains of the marine conglomerate here, and it is difficult to understand where are located small remains or fragments of the marine conglomerate produced by the fragmentation of the large boulders detached from the platform.

All these deposits have been associated with the 1755 Lisbon earthquake by the cited authors based mainly on three assumptions: actual storms are not big enough to move this type of boulders, the boulders looks to young and the only strong event that produce a 19 m height wave have been the 1755 AD tsunami.

The study of the instrumental record of extreme marine conditions in the area show that maximum wave heights recorded during storms range from 5.25 to 7.80 m but the amplitude rises to 6.22 to 9.19 m when a 225 yr recurrence interval is considered. Maximum measured tidal ranges (astronomical plus meteorological/barometric) reach 3.86 to 4.30 m. These data support the idea that sea level during storms (water/wind set up) can rise high enough to reach some sites that have been usually considered out of the storms influence (Lario et al., 2009). Also during the last years have been possible to verify that in the area have been established hurracaine conditions (2005 Hurricaine Vince, 2009 Hurracaine Klaus) that were never recorded before.

Also, the historic document do not report any especial damage in this area after the 1755 AD tsunami and the wave height in this point have been not calculated (Campos, 1991). Whelan and Kelletat (2003) present a table with the run up height of the 1755 AD tsunami and assume 19 m in this area based on the record in Cadiz city. Recently Blanc (2008) reviewed original documents about this event and conclude that have been an historical mistake assuming this height and propose a more realistic values about 5 to 6 m height of the tsunami wave, but never more that 10 m, as also shown on the proposed modelling of the tsunami in this area. This also seem to happen with the 10 to 11 m wave height assumed by several authors in Tarifa, based in the Campos (1991) data, but a carefully reading of the data show that *"water surpass the Paloma Island"*. Morphology of Paloma Island show a vertical cliff around all the island that work as a defence wall and, as happen in Cadiz *"the sea broke furiously on the town walls, not that it topped over them"* (see Blanc, 2008). If a 10 to 11 m wave arrived to Tarifa there should be severe damages in village, but the study of the historical documents of this city only cited small damages due to the earthquake but not the tsunami (Terán, 2005).

Moreover, the 1757 nautical chart (Fig. 24) and the present one (Fig. 25) show an historical shallow sand accumulation (5 m depth) to the W and SW of Cape Trafalgar, just on the way of the 1755 tsunami wave direction reached the coast. Energy of the wave will be dissipated once reach these *bajios* (shoals) and arrived to the cape with low energy.

The Cape Trafalgar is affected by strong erosion as show the 1980 pictures (Fig. 18). The majority of solution pipes developed on marine and aeolian deposits have disappeared recently and remains of the old cliff have been incorporated to the platform. The anthropic action in the cape is also present almost since the roman times (and 9th century tower building, new light-house, road building, 1977 extended archaeological excavations…) and could modificate some natural features.

From these data is difficult to assign all the features to a single event, as the 1755 AD tsunami. Moreover, the review of the historical data do no support that the 1755 AD tsunami reach this area strong enough to produce the described features. Data support the occurrence of one or more Extreme Wave Events (EWE) in this area, but it is difficult to assign the origin and the age of these events. If a EWE reached the coast in the last 300 year, the waves have to come from the south or south-eastern, while the bathymetry of the area since then do not allow reaching the waves to the coast with high energy. Present presence of boulders around Cape Trafalgar seems to be a conjunction of EWE´s, natural erosion of the cliff and antrophic influence.

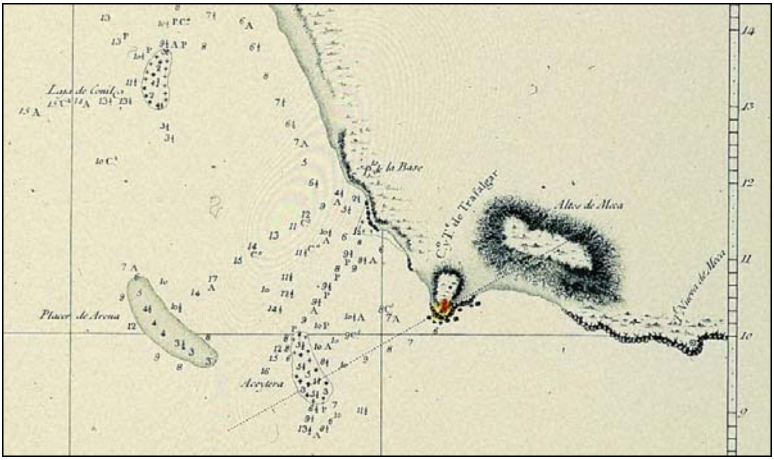

Fig. 24: Fragment of the 1787 nautical chart near Cape Trafalgar (Temiño, 1787). Note the presence of two main sands accumulations using historically as a sand quarry: Placer de Arena and Aceytera, just facing Cape Trafalgar. Depth is in spanish *brazas* (1 braza = 1.67 m).

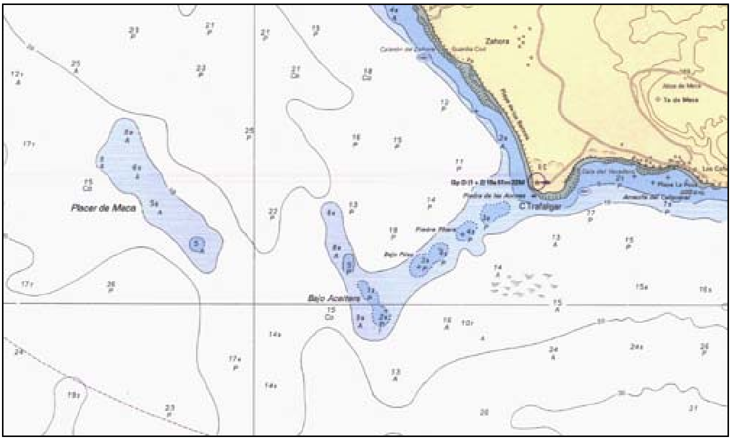

Fig. 25: 2001 nautical chart from the IHM. Placer de Meca and Bajo Aceitera still presents. Depth in meters.

Stop 6

Tsunami deposits at Torre de Castilnovo, Conil de la Frontera

J. Lario, L. Luque, C. Zazo, J.L. Goy, C.J. Dabrio, A. Cabero, T. Bardaji and P.G. Silva

Introduction

The 1755 Lisbon earthquake generated a tsunami that flooded Southwest Iberian Peninsula and Morocco coasts. The coast of Conil de la Frontera (Cádiz) was one of the most affected by these waves in the Spanish littoral. There are abundant information about historical record, damages, and landscape transformation related with this catastrophic event. Based on these data it has been possible to deduce a maximum height of the wave (run-up) of approximately 8 m over high tide level. This height implies a tsunami magnitude 3 empirically attributed to an 8 to 8.5 magnitude earthquake. This is coherent with the Lisbon earthquake inferred magnitude. Geomorphological study in the area shows the existence of two washover fans about 300 m long that were originated after overwashing beach dunes and flooding high marshland and floodplain in the backshore. Sedimentological and palaeontological analysis on sediments come out from drill cores revealed the presence of several interbedded layers attributed to sedimentary events of smaller magnitude such as storm-waves. All of these evidences allow us to conclude that washover fan sediments were deposited by the tsunami of November 1755. These deposits constitute one of the scarce records of tsunami deposits in the Spanish peninsular coasts.

The Conilete deposits

The coast of Conil de la Frontera is located in the Atlantic coast of the province of Cadiz, between the Roche and Trafalgar capes. It is a rectilinear coast, about 15 km in length, and oriented nor-northwest to south-southeastern that presents a large beach and a dune complex well developed that can reach 10 m.a.s.l. The dominant winds in the zone come from the East and from the West. It is a mesomareal coast, with a tidal range about 2.4 m of average and a maximum of 4 m (IGN, 1991). The dominant superficial currents follow a direction north-western to south-eastern.

Luque et al. (2004) reviewed all the historical information compiled in some reports (Real Academia de la Historia, 1756; Historical Reports in Biblioteca

Nacional (Anonymous, 1756) and unpublished documents deposited in the Conil church). From these documents have been possible to reconstruct the maximum flooding extension of the 1755 Lisbon tsunami (Fig. 26), and also that tsunami wave reached the coast at 9:30 AM.

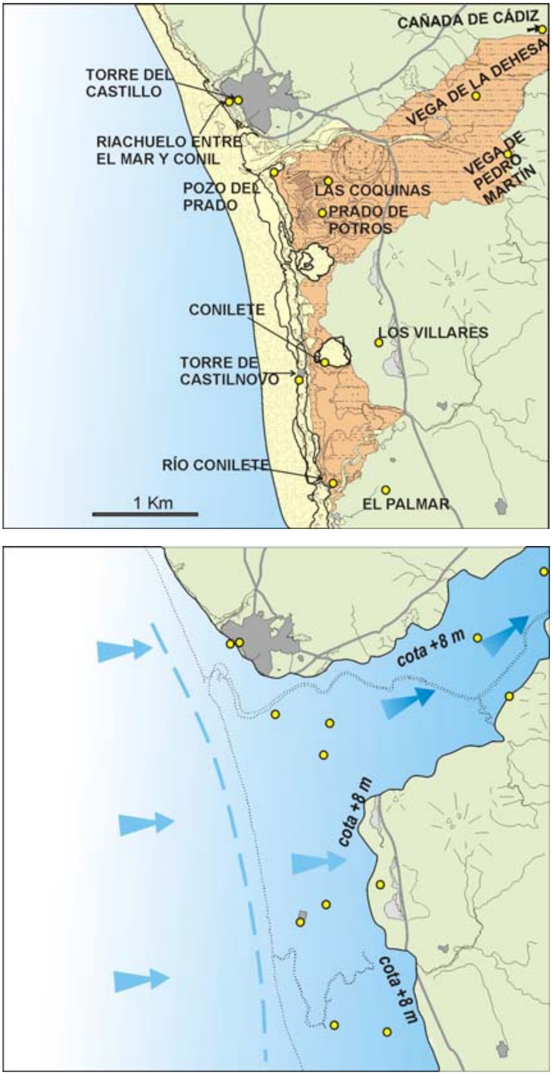

Fig. 26: Location of sites cited in the historical documents and reconstruction of the maximum flooding (8-8.5 m above high tide level) (from Luque et al., 2004).

First the sea water retreat and later almost two waves reached the coast breaking heavily. Flooding reached 8.25 kms to the hinterland and a height up to 8 to 8.5 m above high tide level. Sea-water was brown because contained large amount of sediments, mainly sands, stone fragments and plants remains. The waves destroyed wood and stone houses, move ships to the hinterland and drown cattle's. The small fishermen village of Conilete was totally ruined (Fig. 27).

Fig. 27: Remains of the Conilete fishermen village, destroyed during the 1755 tsunami.

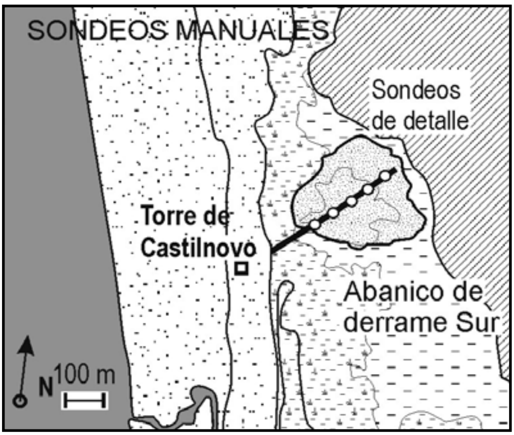

From the aerial picture have been recognized near Torre de Castilnovo two washover fans that cover the area flooding during the tsunami. The largest one (Fig. 28) is 300 m in length and includes fragments of walls, bricks and tiles from the Conilete village.

Fig. 28: Washover fan in Torre de Castilnovo.

Characteristics of these deposits were analysed from manual and mechanic cores (Luque, 2002; Luque et al., 2004). Most of these cores recorded similar sequence (Fig. 29):

a. Basal unit is founded between 2-1 m depth. Is composed mainly by clays with hydromorphism features with presence of organic matter and nodules of oxides and carbonates. Scarce presence or microfossils, only represented by benthonic foraminifers (*Haynesina* and *Ammonia*) and ostracods (species *Loxoconcha elliptica*, *Cyprideis torosa* and generic *Leptocythere*). Presence of macrofossil is also scarce but has been founded bivalves as *Cerastoderma edule* and gastropods as *Hydrobia.* The most significant feature of this deposit is the intrebbeded millimetric layers of fine to very fine sands, well selected and with more layers (14 maximum) and thicker (0.1 to 4 m) close to the sandy aeolian ridge. Microfauna is usually reworked (planctonic foraminifers). These sands are interbbeded at the top of the clay portion. Cores to the south, near to Conilete river, present an alternance of organic muddy sands with presence of gypsum and vegetal remains, with occurrence of freshwater to marine ostracods. Environmental interpretation of this clay level with sand layers correspond with the filing of high marsh with bad drainage in which the storm episodes sediment sands from the beach ridge. Toward the south a *laguna* that change from fresh water to salty water was established, including some desiccation episodes.

b. Second sedimentary unit reach 0.5 m depth and is characterized by the presence of brown clays and sandy clays, without microfossils and scarce organic matter. Contain carbonate nodules and sometime land gastropoda (Helix). To the south this level incorporates more sand. It corresponds to a continental environment such as alluvial plain.

c. Sedimentary unit at the top of cores is usually 0.5-0.4 m thick and thinner toward the hinterland. It is composed mainly by brown sandy silts and sand with millimetric nodules of carbonates, some times including marine shells fragments and some land gastropoda. This unit corresponds to a large washover fans. Five cores was done near the Castilnovo tower to investigate these washover fans. The results show that the sediments are similar to the underlying ones, but sandy fraction (mainly quartz and bioclast) is higher at the top while clay fraction increases at the bottom. Microfossils consist mainly in scarce presence of foraminifera. Increase in grain size and the shape of the washover fans point to an increase in the environment energy, as well as a sediment source, from the west to the east.

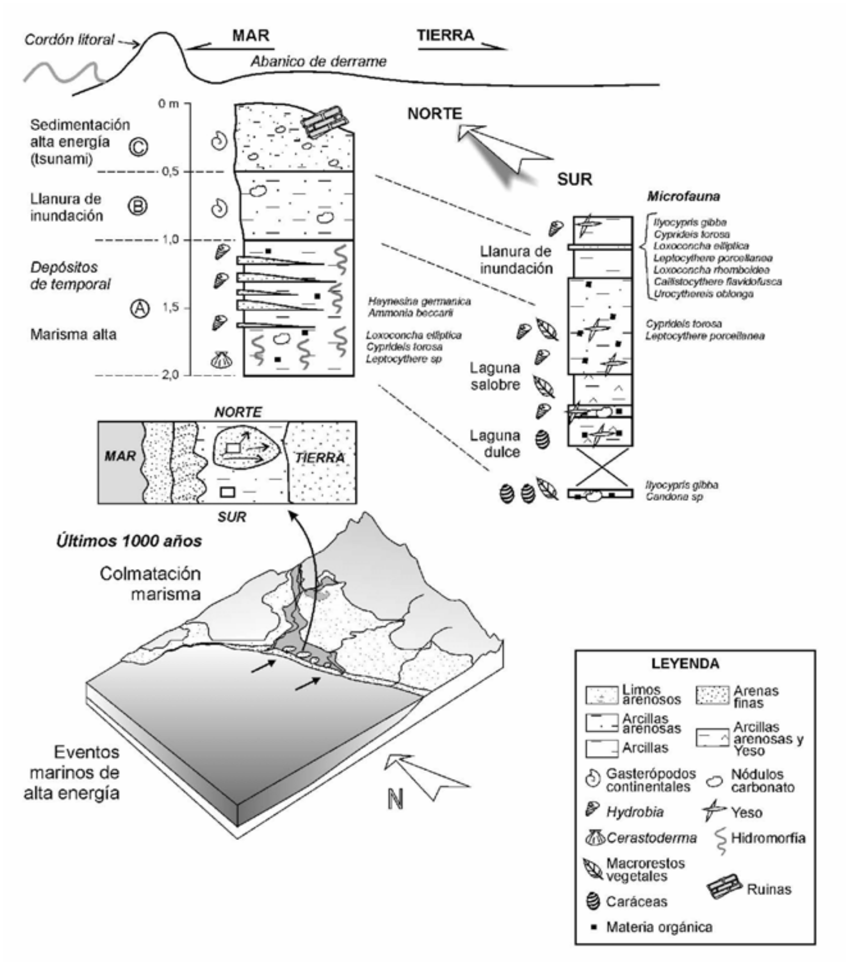

Fig. 29: Synthetic column of the sequence founded in washover fans near Torre de Castilnovo (from Luque et al., 2004).

Cores studied (Luque, 2002; Luque et al., 2004) show the presence of a high marsh environment with sporadic flooding by storms, that was filled gradually and transformed into alluvial plain. This transitional environment have been associated to the sedimentary filling of the Conil backshore zone developed dating the present Interglacial, and the input of tidal water by Salado and Conilete rivers. The sandy layers (up to 14) near the beach ridge that disappear to the hinterland correspond to a breaching of the beach ridge due to extreme storm episodes.

Related to the washover fans the cores show a top sandy layer thinner toward the hinterland. The thickness (0.55 m) and extension (300 m length) differentiate this layer from the underlying ones (0.06 m thick and 100 m length). There is absence of fauna, but include fragments of buildings of the Conilete village, that was destroyed during the 1755 tsunami generated by the Lisbon earthquake (op.cit.). Usually this type of deposits is associated with an erosional base and presence of marine fauna in sediments (Dawson, 2000; Goff et al., 2001; Morton et al., 2007). These anomalies will be explained by the fact that this area has been used for agriculture and the absence of microfauna in the actual beach ridge (Luque et al., 2004).

With the data apported by the effects of the tsunami generated by the Lisbon 1755 earthquake in this area, it is possible to check the palaeoseismic information about this event. The studies that related seismic information with the effects of tsunami events are based mainly in the wave elevation. This altitude defines the magnitude of the tsunami itself and, even depends of numerous local factors, it is reflect of the energy liberated during the sea floor displacement (Iida, 1963; Catalán et al., 1979). One of the most applied scale is the proposed by Iida, with values between -2 (waves smaller than 30 cm) and +5 (waves surpassing 32 m) after applied the formula m=$\log_2$Hr (Hr is the maximum altitude of run-up in the coast between 10 to 250 kms from the tsunami origin (Iida, 1963). With the maxima height of the wave (8 m) it is possible estimate a tsunami magnitude of 3 (Fig. 30), that correspond to an earthquake of 8 to 8.5 magnitude (Luque et al., 2004). These data are coherent with the magnitude proposed for the 1755 Lisbon earthquake.

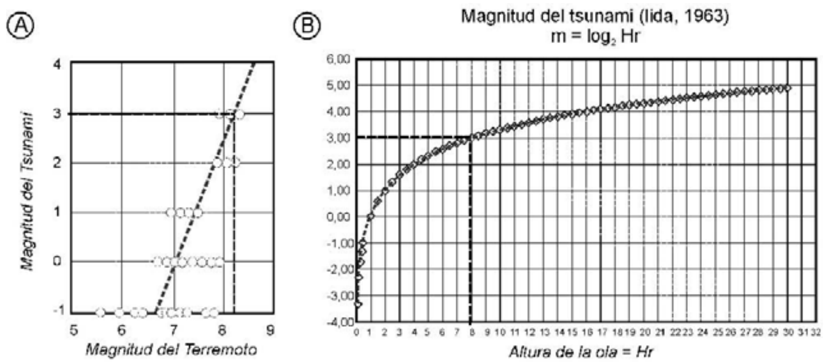

Fig. 30: Relation between the height of the wave in Conil and the magnitude of the tsunami and 1755 Lisbon earthquake (Luque et al., 2004).

References

Aguirre, J. 1995. Implicaciones paleoambientales y paleogeográficas de dos discontinuidades estratigráficas en los depósitos pliocénicos de Cádiz (SW de España). Rev. Soc. Geol. España, 8 (3), 161-174.

Akil, M., Chalouan, A., Istiquam, H., El Fahssi, A. & Mamad, A. 1995, Les formations quaternaires de la Rive Sud du Detroit de Gibraltar: Stratigraphie et déformation. In: Esteras, M. (ed.) El Enlace Fijo del Estrecho de Gibraltar, SECEG, Madrid, Vol. 2, 71-79.

Alonso Villalobos, C., Gracia, F.J., Ménanteau, L., Ojeda, R., Benavente, J. & Martínez, J.A. 2003. Paléogeographie de l'anse de Bolonia (Tarifa, Espagne) à l'époque romaine. In: The Mediterranean World Environment and History. Elsevier S.A.S. Amsterdam, 407-417.

Alonso, C., Gracia, F.J., Del Río, L., Anfuso, G., Benavente, J. & Martinez, J.A. 2004. Registro morfosedimentario de eventos históricos de alta energía en el litoral atlántico del Estrecho de Gibraltar (Trafalgar-Tarifa). - In: Benito, G. & Díez Herrero, A. (eds.): Contribuciones recientes sobre Geomorfología: 263-271. SEG-CSIC, Madrid.

Amores, F. 1978. Una nueva factoría romana de salazones en Trafalgar (Cádiz). Habis, 9, 441-454.

Anónimo. 1756. Relación verídica del terremoto de 1755. Biblioteca Nacional, R/34.612.

Balnayá, J.C., Esteras, M. García-Dueñas, V. & Izquierdo, J. 1995, Superposición de estructuras neógenas en las unidades alóctonas del Campo de Gibraltar (Arco de Gibraltar). In: M. Esteras, (ed.), El Enlace Fijo del Estrecho de Gibraltar, SECEG, Madrid, Vol. 2, 3-7.

Baptista, M.A., Heitor, S., Miranda, J.M., Miranda, P. & Mendes-Victor, L. 1998. The 1755 Lisbon tsunami; evaluation of the tsunami parameters. Journal of Geodynamics, 25, 143–157.

Becker-Heidmann, P., Reicherter, K. & Silva, P.G. 2007. ^{14}C dated charcoal and sediment drilling cores as first evidence of Holocene tsunamis at the Southern Spanish coast. Radiocarbon, 49, 2, 827-835.

Benkhelil, J. 1977. Etude néotectonique de la terminaison occidentale des Cordillères Bètiques (Espagne). Thèse d'Etat, Université de Nice, France. 180 pp.

Benot, C., Díaz, M.G., Mayoral, E., Parra, A. & Rodríguez Vidal, J. 1993. Nuevas aportaciones para la determinación del límite Neógeno-Cuaternario en la Bahía de Cádiz. In: El Cuaternario de España y Portugal. ITGE-AEQUA, Madrid. Vol. 1, 243-250.

Blanc, P.L. 2008. The tsunami in Cadiz on 1 November 1755: A critical analysis of reports by Antonio de Ulloa and by Louis Godin. C. R. Geoscience, 340, 251–261.

Bryant, E., 2007. Tsunami - The Underrated Hazard. Springer, 2nd edition, 330 pp.

Cabero, A. 2009. Registro costero de los cambios eustáticos y climáticos durante los interglaciares recientes cuaternarios: S y SE Peninsular, Islas Baleares, Canarias y Cabo Verde. Tesis Doctoral, Universidad de Salamanca, 452 pp.

Caron, V., Bernier, P. & Mahieux, G. 2009. Record of Late Pleistocene (Oxygen Isotopic Stage 5) climate changes during episodes of karst development on the Northern coast of Crete: Sequence stratigraphic implications. Palaeogeography, Palaeoclimatology, Palaeoecology, 277, 246–264

Catalán, M.; Boloix, M. & Valenzuela, J. 1979. Propagación de maremotos en la región de Azores-Gibraltar. Actas de la IIIª Asamblea Nacional de Geodesia y Geofísica. (Instituto y Observatorio de la Marina, San Fernando, 1979), IGN, 419-438. Madrid.

Dabrio, C.J., Goy, J.L. & Zazo, C. 1998. The record of the tsunami produced by the 1755 Lisbon earthquake in Valdelagrana spit (Gulf of Cádiz, southern Spain). Geogaceta, 23, 31-34.

Dawson, A.G. 2000. Tsunami deposits. Pure and Applied Geophysics, 157, 875-897.

Dawson, A.G., Hindson, R., Andrade, C., Freitas, C., Parish, R. & Bateman, M. 1995. Tsunami sedimentation associated with the Lisbon earthquake of 1 November AD 1755: Boca do Rio, Algarve, Portugal. The Holocene, 5, 209–215.

Esteras, M., Izquierdo, J., Sandoval, N.G. & Bahmad, A. 2000. Evolución morfológica y estratigráfica Plio-Cuaternaria del Umbral de Camarinal (Estrecho de Gibraltar) basada en sondeos marinos. Revista de la Sociedad Geológica de España, 13 (3-4), 539-550.

Galindo-Zaldívar, J., González-Lodeiro, F. & Jabaloy, A. 1993. Stress and palaeostress in the Betic-Rif cordilleras (Miocene to the present). Tectonophysics, 227, 105-126.

García de Domingo, A., González Lastras, J., Hernaiz, P.P., Zazo, C. & Goy, J.L. 1990. Cartografía geológica y memoria de la hoja 12-47 (Vejer de la Frontera). Mapa Geológico de España, Escala 1:50.000. Plan MAGNA, 2ª Serie. IGME, Madrid, Spain.

Goff, J.; Chagué-Goff, C. & Nichol, S. 2001. Paleotsunami deposits: a New Zealand perspective. Sedimentary Geology, 143, 1-6.

González Lastras, J., García de Domingo, A., Hernaiz, P.P., Zazo, C. & Goy, J.L. 1991. Cartografía geológica y memoria de la hoja 13-47 (Tarifa). Mapa Geológico de España, Escala 1:50.000. Plan MAGNA, 2ª Serie. IGME, Madrid, Spain.

Goy, J.L., Zazo, C., Silva, P.G., Lario, J., Bardají, T. & Somoza, L. 1995. Evaluación geomorfológica del comportamiento neotectónico del Estrecho de Gibraltar durante el Cuaternario. In: Esteras, M. (ed), El Enlace Fijo del Estrecho de Gibraltar, SECEGSA, Madrid. Vol., 2. 51-69.

Goy, J.L., Zazo, Mörner, N.A., C. Hoyos, M., Somoza, L., Lario, J., Bardají, T., Silva, P.G. & Dabrio, J.C. 1994, Pop up-like deformation of a Roman floor and liquefaction structures in SW Spain as possible paleoseismic indicators. Bulletin of the INQUA Neotectonics Comisión, 17, 42-44.

Gracia, F.J., Alonso, C., Benavente, J., Anfuso, G. & Del-Río, L. 2006. The different coastal records of the 1755 Tsunami waves along the Atlantic Spanish Coast. In: Scheffers, A. and Kelletat, D. (ed.). Z. Geomorph. N.F., Suppl. Vol. 146, 195-220.

Gracia, F.J., Rodríguez Vidal, J., Benavente, J., Cáceres, L. & López Aguayo, F. 1999. Tectónica Cuaternaria en la Bahia de Cádiz. In: Pallí, L., Roqué, C. (eds), Avances en el estudio del Cuaternario español. AEQUA-UdG, Girona, España, 67-74.

Gutiérrez-Mas, J.M., Moral, J.P., Sánchez, A., Dominguez, S. & Muñoz-Perez, J.J. 2003. Multicycle sediments on the continental shelf of Cadiz (SW Spain). Estuarine, Coastal and Shelf Science, 56, 667-677.

Herraiz, M., De Vicente, G., Lindo-Ñaupari, R., Giner, J., Simón, J.L., González-Casado, J.M., Vadillo, O., Rodríguez-Pascua, M.A., Cicuéndez, J.I., Casas, A., Cabañas, L., Rincón, P., Cortés, A.L., Ramírez, M. & Lucini, M. 2000. The recent (upper Miocene to Quaternary) and present tectonic stress distributions in the Iberian Peninsula. Tectonics, 19, 762-786.

Hindson, R., Andrade, C. & Parish, R. 1999. A microfaunal and sedimentary record of environment change within the late Holocene sediments of Boca do Rio (Algarve, Portugal). Geol. Mijnbouw, 77, 311-321.

Hübscher, C., Betzler, C. Reicherter, K. & Lüdmann, T. 2007. The Meteor M69/1 cruise report, CARBMED, unpublished report, University of Hamburg.

Iida, K. 1963. Magnitude, energy and generation and mechanisms of tsunamis and a catalog of earthquakes associated with tsunami. Abstract del 10th Pacific Science Congress Symposium, International Union on Geodesy and Geophysics Monograph, 24, 7-18.

Jiménez-Munt, I., Fernández, M., Torne, M. & Bird, P. 2001. The transition from linear to diffuse plate boundary in the Azores – Gibraltar Region: results from a thin sheet model. Earth and Planetary Science letters, 192, 175-189.

Jolivet, L., Frizon de Lamotte, D., Horváth, F., Mascle, A. & Sérrane, M. 1999. The Mediterranean Basins: Tertiary Extension within the Alpine Orogen - an introduction. In: Durand, B., Jolivet, L., Horváth, F. & Sérrane, M. (eds): The Mediterranean Basins: Tertiary Extension within the Alpine Orogen, Geological Society of London Special Publication, 156, 1-14.

Kortekaas, S. & Dawson, A.G. 2007. Distinguishing tsunami and storm deposits: An example from Martinhal, SW Portugal. Sedimentology, 200, 208-221.

Lario J., Luque L., Zazo C., Goy J. L., Spencer C., Cabero A., Dabrio C., Borja F., Civis J., González-Delgado J. A., Borja C. & Alonso-Azcárate, J. 2009. Tsunami vs. Storm surge deposits: a review of the sedimentological and geomorphological records of extreme wave events (EWE) during the Holocene in the Gulf of Cadiz, Spain. Z. Geomorph. (in press).

Lario, J. 1996. Último y Presente Interglacial en el Área de conexión atlántico-Mediterráneo (Sur de España). Variaciones del nivel del mar, paleoclima y paleoambientes. Tesis Doctoral, Fac. Ciencias Geológicas, Universidad Complutense de Madrid., 269 pp.

Leblanc, D., 1990. Tectonic adaptation of the external zones around the curved core of an orogen: the Gibraltar Arc. Journal of Structural Geology, 12, 1013-1018.

Luque, L. 2002. Cambios en los paleoambientes costeros del sur de la Península Ibérica (España) durante el Holoceno. Tesis Doctoral, Universidad Complutense de Madrid, 376 pp.

Luque, L., Lario, J., Civis, J., Silva, P.G., Goy, J.L., Zazo, C. & Dabrio, C.J. 2002. Sedimentary record of a tsunami during Roman times, Bay of Cadiz, Spain. Journal of Quaternary Science, 17, 623-631.

Luque, L., Lario, J., Zazo, C., Goy, J. L., Dabrio, C. J. & Silva, P. G. 2001. Tsunami deposits as palaeoseismic indicators: examples from the Spanish coast. Acta Geológica Hispanica, 36, 197-211.

Luque, L.; Zazo, C.; Lario, J.; Goy, J.L.; Civis, J.; González-Hernández, F.M.; Silva, P.G. & Dabrio, C.J. 2004. El efecto del tsunami de 1755 en el litoral de Conil de la Frontera (Cádiz). Zona Arqueológica, 4. Miscelánea en Homenaje a Emiliano Aguirre. V-I, Geología, 72-82.

Martínez Solares, J.M. & López Arroyo, A. J. 2004. The great historical 1755 Lisbon Earthquake: Effects and damage in Spain. J. Seismology, 8, 275-294.

Martínez Solares, J.M. & Mezcua, J. 2002. Catálogo Sísmico de la Península Ibérica (880 AC – 1900). Monografía nº 18, Instituto Geográfico Nacional (IGN). Madrid, Spain. pp.

Martínez Solares, J.M., López Arroyo, A. & Mezcua, J. 1979. Isoseismal map of the 1755 Lisbon Earthquake obtained from Spanish data. Tectonophysics 53, 301-313.

Menanteau, L., Vanney, J.R. & Zazo, C. 1983. Belo II : Belo et son environment (Detroit de Gibraltar), Etude physique d'un site antique. Pub. Casa de Velazquez, Serie Archeologie 4., Ed. Broccard, París.

Mhammdi, N., Medina, F., Kelletat, D., Ahmamou, M. & Aloussi, L. 2008. Large boulders along the Rabat coast (Morocco); possible emplacement by the November, 1st, 1755 A.D. Tsunami. Science of Tsunami Hazards, 27, 17-30.

Morton, R.A; Gelfenbaum, G. & Jaffe, B.E. 2007. Physical criteria for distinguishing sandy tsunami and storm deposits using modern examples. Sed. Geol., 200, 184-207.

Muñoz-Pérez, J.J., Fages, L., Asensio, B. & Caramé, N. 2002. Regeneration of Salt Marshes in Barbate (SW Spain): a project. Littoral 2002, The Changing Coast, 173-176; ed. EUROCOAST, Portugal; ISBN 972-8558-09-0.

Noomen, R., Ambrosious, B. & Wakker, K. 1993. Crustal motions in the mediterranean region determined from Laser ranging to Lageos. In: D.E. Smith & D.L. Truccotte (eds), Contribution of Space Geodesy to Geodynamics. AGU, Washington, USA. .Earth Dynamics, Geodynamics Series, 23, 331-346

R.A.H. 1756. Noticia individual que da la Academia de la Historia del Terremoto de 1º de noviembre de 1755 por orden del Rey Nuestro Señor a quien la dedica. Manuscrito, Real Academia de la Historia, Madrid: 367 pp.

Reicherter, K., & Becker-Heidmann, P. 2009. Tsunami Deposits in the Western Mediterranean: Remains of the 1522 Almería Earthquake? In: Reicherter, K., Michetti, A.M., Silva, P.G. (eds.). Paleoseismology: Historical and prehistorical records of earthquake ground effects for seismic hazard assessment. J. Geol. Soc. London, Spec. Publ., 316: 217-235.

Reicherter, K., Vonberg, D., Koster, B., Fernández-Steeger, T., Grützner, C. & Mathes-Schmidt, M. (2009). The sedimentary inventory of tsunamis along the southern Gulf of Cádiz (southwestern Spain): relation to the 1755 Lisbon event? Z. Geomorph. (in press).

Reicherter, K.R. & Peters, G. 2005. Neotectonic evolution of the Central Betic Cordilleras (southern Spain). Tectonophysics, 405, 191-212.

Sandoval, N.G., Sanz, J.L. & Izquierdo, F.J. 1996. Fisiografía y Geología del Umbral del Estrecho de Gibraltar, Geogaceta, 20 (2), 343-346.

Sanz de Galdeano, C. 1990. Geologic evolution of the Betic Cordilleras in the Western Mediterranean, Miocene to present. Tectonophysics, 172, 107-119.

Scheffers, A. & Kelletat, D. 2005. Tsunami relics of the coastal landscape of West Lisbon, Portugal. Sciene of Tsunami Hazards, 23, 3-16.

Silva, P.G., Goy, J.L., Zazo, C., T. Bardají, T., Lario, J., Somoza, L., De Luque, L. & González-Hernández, F.M. 2006. Neotectonic fault mapping at the Gibraltar Strait Tunel area, Bolonia Bay (South Spain). Engineering Geology, 84, 31-47.

Silva, P.G., Reicherter, K., Grützner, C., Bardají, T., Lario, J., Goy, J.L., Zazo, C. & Becker-Heidmann, P. 2009. Surface and subsurface paleoseismic records at the ancient Roman city of Baelo Claudia and the Bolonia Bay area, Cádiz (South Spain). In: Reicherter, K., Michetti, A.M. & Silva, P.G (eds.). Historical and Prehistorical Records of earthquake Ground effects for Seismic Hazard Assessment. J. Geol. Soc. London, Spec. Publ., 316, 93-121.

Somoza, F., Hernández-Molina, F.J., De Andres, J.R. & Rey, J. 1997. Continental shelf architecture and sea-level cycles: Late Quaternary high-resolution stratigraphy of the Gulf of Cádiz, Spain. Geo-Marine Letters, 17, 133-139.

Stich, D., Ammon, C.J. & Morales, J. 2003. Moment tensor solutions for small and moderate earthquakes in the Ibero-Maghreb region. Journal of Geophysical Research (Solid Earth), 108-B3, 2148.

Terán, J. 2005. El terremoto de Lisboa. Aljaranda: Revista de Estudios Tarifeños, 59, 38-42.

Tofiño, V. 1787. Carta esférica desde Punta Candor hasta Cabo de Trafalgar. Despacho Universal de la Marina.

Vázquez, J.T. & Vegas, R. 2000. Acomodación de la convergencia entre África y la Península Ibérica, Golfo de Cádiz, Mar de Alborán, a partir del análisis de terremotos. Geogaceta, 27, 171–174.

Weijermars, R. 1991. Geology and tectonics of the Betic Zone, SE Spain. Earth Science Reviews, 31, 153-236.

Whelan, F. & Kelletat, D. 2003. Analysis of Tsunami deposits at Cabo de Trafalgar, Spain, using GIS and GPS Technology. Essener Geographische Arbeiten, 35, 11-25.

Whelan, F. & Kelletat, D. 2005. Boulder deposits on the Southern Spanish Atlantic Coast: possible evidence for the 1755 AD Lisbon Tsunami?. The Science of Tsunami Hazards, 23: 25-38.

Zazo, C. 1980. El Cuaternario marino-continental y el límite Plio-Pleistoceno en el litoral de Cádiz. Tesis doctoral. Universidad Complutense de Madrid. Facultad de Geología.

Zazo, C. & Goy, J.L. 1990. Cartografía geomorfológica y memoria de la hoja 12-47 (Vejer de la Frontera). Mapa Geológico de España, Escala 1:50.000. Plan MAGNA, 2ª Serie. IGME, Madrid, Spain.

Zazo, C., Dabrio, C.J., Goy, J.L., Lario, J., Cabero, A., Silva, P.G., T. Bardají, T., Mercier, N., Borja, F. & Roquero, E. 2008b. The coastal archives of the last 15 ka in the Atlantic-Mediterranean Spanish linkage area: Sea level and climate changes. Quat. Int., 181, 72-87.

Zazo, C., Mercier, N., Lario, J., Roquero, E., Goy, J.L., Silva, P., Cabero, A., Borja, F., Dabrio, C.J., Bardají, T., Soler, V., García-Blázquez, A. & Luque, L. 2008a. Palaeoenvironmental evolution of the Barbate-Trafalgar coast (Cádiz) during the last ~140ka: tectonics, climate and sea-level interactions. Geomorphology, 100, 212-222.

Zazo, C., Silva, P.G., Goy, J.L., Hillaire-Marcel, C. Lario, J. Bardají, T. & González, A. 1999. Coastal uplift in continental collision plate boundaries: Data from the Last interglacial marine terraces of the Gibraltar Strait area (South Spain). Tectonophysics, 301, 95-119.

Notes

BAELO 2009

INQUA PALEOSEISMOLOGY

IGCP-567

EARTHQUAKE ARCHAEOLOGY

PALEOSEISMOLOGY

RWTH AACHEN UNIVERSITY

VNiVERSiDAD D SALAMANCA

UNED

Instituto Geológico y Minero de España

INQUA

IUGS UNESCO IGCP

AEQUA

JUNTA DE ANDALUCIA
CONSEJERIA DE CULTURA

CSIC

GOBIERNO DE ESPAÑA

MINISTERIO DE CIENCIA E INNOVACIÓN